



Institute of Biomechanics
Center of Biomedical Engineering
Kronesgasse 5-I
8010 Graz, Austria

DIPLOMA THESIS

Shear Properties of Passive Ventricular Porcine and Human Myocardium

to achieve the academic degree of
Diplom-Ingenieur

Author: Michael Kutschera

Supervisor: Gerhard Sommer, PhD

Head of Institute: Professor Gerhard A. Holzapfel, PhD

April 27, 2012

Contents

1	Introduction	1
1.1	Biomechanics of soft biological tissues - Definiton	1
1.2	Motivation	2
1.2.1	Aims	2
1.3	The heart	3
1.3.1	Anatomy of the heart - General organization	3
1.3.2	Structures of the myocardium	4
1.3.2.1	Anatomy at the microscopic level	5
1.3.2.1.1	Cardiac myocytes	5
1.3.2.2	Anatomy at the macroscopic level	8
1.3.2.2.1	Cardiac myofibers	9
1.3.2.2.2	Laminar sheets	9
1.3.2.2.3	Collagen in the human heart	11
1.3.3	Pathology in the human myocardium (cardiomyopathy)	12
1.3.3.1	Dilated cardiomyopathy	12
1.3.3.2	Hypertrophic cardiomyopathy	13
1.3.4	Anatomical differences between porcine and human hearts	14
1.4	Fundamentals of soft tissue biomechanics	15
1.4.1	Simple shear	15
1.5	State of the art - Conclusion	17
2	Materials & Methods	19
2.1	Materials	19
2.1.1	Specimen	19
2.1.1.1	Origin of hearts	19
2.1.1.1.1	Clinical Department of Transplant Surgery, LKH- University Clinic Graz	20
2.1.1.1.2	Institute of Pathology, Medical University of Graz	21
2.1.1.1.3	Slaughterhouse Marcher®	22
2.2	Methods	23
2.2.1	Equipment belonging to preparation and measurement of myocar- dial triaxial shear properties	23
2.2.1.1	Measurement utilities and instruments	23
2.2.1.2	Tools for specimen preparation	25

2.2.1.3	Other important used tools and utensils especially are: .	26
2.2.2	Chemical solutions for transport, storage and testing of porcine and human heart-tissue	27
2.2.2.1	<i>Phosphate buffered saline</i> (PBS)	27
2.2.2.1.1	<i>Ethylene glycol teraacetic acid</i> (EGTA)	28
2.2.2.2	Cardioplegic solutions (CPS)	28
2.2.2.2.1	Celsior®- cold storage solution	30
2.2.2.2.2	Custodiol®- cardioplegic solution	30
2.2.2.2.3	‘Conventional’ cardioplegic solution (CCPS, Landesapotheker Salzburg)	31
2.2.2.3	<i>Krebs-Ringer-solution</i>	31
2.2.2.4	<i>Formaldehyde</i>	32
2.2.2.5	Summary of different types of solutions according to their application	33
2.2.3	Preparation	34
2.2.3.1	Method of porcine heart dissection	34
2.2.3.2	Detailed specimen preparation	38
2.2.3.2.1	The FSN-coordinate system	39
2.2.3.2.2	Cubic specimen preparation - Cutting techniques	40
2.2.3.2.3	Six possible modes of simple shear	41
2.2.4	Experimental Setup: Triaxial shear testing device	42
2.2.4.1	Hardware configuration - MESSPHYSIK	42
2.2.4.2	Fixation of specimen into the triaxial shear apparatus	44
2.2.4.2.1	Modifications on platform-surfaces	44
2.2.4.3	Software - TestXPert II (Zwick & Roell)	46
2.2.4.3.1	Programmed test sequence	46
2.2.4.3.2	Modifications in the testing procedure	49
2.2.4.3.3	Modifications in the data-input interface	49
2.2.4.4	Testing protocol	50
2.2.4.4.1	Errors reported during testing	51
2.2.5	Data Analysis	51
2.2.5.1	Modified MATLAB®-GUI	51
2.2.5.1.1	The GUI and its functions	52
3	Results	55
3.1	Measurement data acquisition of porcine myocardial tissue	55
3.1.1	Results for the shear stress-strain relationship of specimens in Ringer solution	57
3.1.2	Results for relaxation testing concerning to modified Ringer solution	57

3.2	Mechanical data acquisition of human myocardial tissue	64
3.2.1	Tissue received from the Institute of Pathology	64
3.2.1.1	Results for the shear stress-strain relationship according to human samples from the Institute of Pathology	64
3.2.1.2	Results for relaxation testing	66
3.2.2	Tissue received from the Department of Transplant Surgery	73
3.2.2.1	Results for the stress-strain relationship according to human samples from the Clinical Dep. of Transplant Surgery	73
3.2.2.2	Results for relaxation testing	74
3.2.2.3	Determination of (unconfined) compression properties	74
4	Discussion	81
4.1	Data analysis of porcine tissue	81
4.2	Data analysis of human tissue	83
4.2.1	Comparison of mechanical properties: strain softening vs. myocyte activation	84
4.2.1.1	Effects caused by improper autolysis duration and activation	85
4.2.2	Unconfined compression behaviour of the human myocardium	86
4.2.3	Pathological aspects: gender, age, cardiac myopathy	87
5	Appendix	93
5.1	Measurement protocol on the basis of human myocardium	94
5.2	Dissection protocol for the Clinical Departments of Pathology and Transplant Surgery	98
5.3	Ethics applicant - Clinical Department of Transplant Surgery	100
5.3.1	Ethics comission humble	113
5.4	Ethics applicant - Clinical Department of Pathology	116
5.4.1	Ethics comission humble	130

List of Figures

1.1	Correlation of structure, mechanical stress and the function of tissues (adapted from Holzapfel, 2009)	1
1.2	Human heart diagram (Gray, 2008)	3
1.3	Diagram of different layers of the heart (Paulsen, 2006)	5
1.4	Eucaryotic cell (Humphrey, 2002a)	6
1.5	Cardiac myocyte (Walker and Spinale, 1999)	6
1.6	Three dimensional reconstruction of cardiac muscle cells in the region of an intercalated disc, a junctional complex between neighbouring cells (Gray, 2008)	7
1.7	Sliding filament model of muscle contraction (Cooper, 2000)	8
1.8	Representation of the myocardial structure where (A) correspond to the fibers and (B) show the laminar structure (Rohmer et al., 2007)	9
1.9	Visualization of the variation of the fibre direction through wall thickness: (a) the left ventricular free wall with a cutout (specimen) from the equator; (b) the microstructure from the cut out block (<i>endocardium</i> to <i>epicardium</i>); (c) the <i>transmural</i> changing of the fibre orientation; (d) the interconnection of collagen fibres between sheets (fibre axis \mathbf{f}_0 , sheet axis \mathbf{s}_0 and sheet-normal axis \mathbf{n}_0) and (e) a cube specimen with sides aligned to the principal material axis (Holzapfel and Ogden, 2009)	10
1.10	Visualization of the complex three-dimensional ventricular myocardium of a rat: A and B representate the schematic structure of the myocardium (myocyte autofluorescence); C and D (high intensity) show the distribution of collagen (Pope et al., 2008)	12
1.11	(A) Reduced left ventricular cavity in a heart with hypertrophic cardiomyopathy. (B) Masson's trichrome stained histological slice showing myocyte disarray (red) and fibrosis (green) (adapted from Ho, 2009)	14
1.12	(A) Cube specimen in FS- shear mode (F is the myocyte axis direction, S lies within the muscle layer transverse to F, and N is normal to the muscle layer). (B) Specimen in FS- shear mode in undeformed state (left) and in deformed state (right), which produce extension in fiber direction	16
2.1	Anterior view of a fresh porcine heart showing the right ventricle and atrium (left), the left chambers (right) and coronary arteries (LAD)	22
2.2	Experimental shear device (left) with controller towers (Z , Y , X), Personal Computer with software-package <i>TestXPert II</i> and heating bath (right)	23
2.3	Most common utilities and tools for myocardial specimen preparation	25
2.4	(A) 'Conventional' cardioplegic solution bottled by Landesapotheker Salzburg, (B) Celsior®-Cold storage cardioplegic solution and (C) commercial typical Ringer-solution by Fresenius-Kabi® (adapted from www.medprodukte.at)	27
2.5	Cardiac myocyte: showing ion concentration-gradients of potassium, sodium and calcium (Klabunde, 2011)	29
2.6	Inaccurate cut off of <i>atriums</i> due to the still visible valves of the heart; (1) left ventricle, (2) interventricular wall (<i>septum</i>) and (3) right ventricle	34
2.7	Carve along the LCA; (1) right ventricular free wall (RVFW), (2) <i>papillary</i> muscles and (3) part of the LCA (LAD, RIVA)	35
2.8	Excision of coronary arteries at the front wall (from a 93 year old female patient); (1) <i>ramus interventricularis anterior</i> (RIVA) and (2) <i>ramus circumflexus</i> (RCX)	36
2.9	The 'left heart': (1) represents the left ventricular free wall (LVFW), (2) the interventricular wall (IVW) and (3) visualizes a gentle cut at the <i>median</i>	36
2.10	Measurement of wall-thickness (A) and diameter (B)	37
2.11	Dissected organ parts: left ventricular free wall, interventricular wall (<i>septum</i>) and right ventricular free wall	37
2.12	(A) shows a 3D-model of human myocardium (RVFW, IVW, LVFW); (B) illustrates locations for the separation of myocardial tissue: the red marked area identifies the LVFW; (1) the black dashed lines border a typical received cotter at the front wall, which was received from various departments; (2) indicates possible slices for the investigation of triaxial shear properties, (3) represents possible slices dissection corresponding to biaxial tensile tests	38
2.13	Dissection of an appropriate piece out of the LVFW; (1) interventricular wall, (2) front wall, (3) dissected <i>transmural</i> base-apex segment showing the orientation of sheets at the equator (4 mm thick) at the free wall, (4) cubic sample with principal material axes in <i>NS-mode</i> (adapted from Dokos et al., 2002)	39
2.14	Preparation of a cubic specimen with axes aligned to the principal material axes; (A) represents the preparation at the left ventricular front wall of porcine myocardium, (B) denotes the equivalent for human tissue	40
2.15	Six possible modes of simple shear corresponding to the <i>FSN</i> coordinates, with surgical marker-labeled corners at the upper face (same as on the tissue) in order to identify orientations after testing. Shear deformation is commonly characterized by two coordinate axes; the first denotes the face that is translated by shear, and the second is the direction in which that face is shifted. Thus <i>NF</i> shear is represented by the translation of the <i>N</i> face in the <i>F</i> direction (adapted from Dokos et al., 2002)	41

2.16	(A) shows the triaxial shear apparatus with its lower platform moved relative in x and y direction; (B) indicates a fixed human cubic specimen in cardioplegic solution with additional potassium (20 mmol/l)	42
2.17	Block diagram showing the experimental setup for triaxial shear testing: laboratory immersion thermostat (controlled @ 37°C), Workstation (Software - Testing protocol, controlling for x , y and z - traverses), triaxial shear testing device with fixated cubic specimen, controller towers for traverses (left to right)	43
2.18	Sliding carriage: Upper platform (1) with fixated tissue specimen in NF -direction (2)	45
2.19	Fixation platforms before (A) and after (B) polishing using the water-abrasive method (embedded upper platform).	45
2.20	Part 1 of the testing sequence	46
2.21	Part 2 of the testing sequence with modification (A) and (B), which is explained in the following	47
2.22	Part 3 represents simple shear in x (M1) and y (M2) direction: <i>preconditioning</i> and <i>main cycles</i>	48
2.23	Part 4 visualizes step-testing (on the right), performed with 50% strain and the additional compression-testing (block (C))	48
2.24	Layout-Assistant for various parameter adjustments	50
2.25	Overview of the realized MATLAB® GUI	53
2.26	Plot of the original dataset of a typical stress-strain curve of a human myocardium in FN -mode at 30% shear displacement (blue) and again with shifted offset (red)	53
3.1	Ratio between shear stress and shear strain (main cycles, offset corrected) in NF and NS mode increasing from 10% to 50%.	58
3.2	Shear stress-strain relationship (offset corrected) in SF and SN mode increasing from 10% to 50% shear strain.	58
3.3	Main cycles (offset corrected) of the ratio of shear stress to shear strain in FS and FN mode increasing from 10% to 50%.	59
3.4	Averaging (mean value) of a set of six different porcine hearts at a maximum shear strain of 30 % in NF -mode (black bordered curve).	59
3.5	Averaging (mean value) of a set of six different porcine hearts at a maximum shear strain of 30 % in NS -mode (black bordered curve).	60
3.6	Averaging (mean value) of a set of six different porcine hearts at a maximum shear strain of 30 % in SF -mode (black bordered curve).	60
3.7	Averaging (mean value) of a set of six different porcine hearts at a maximum shear strain of 30 % in SN -mode (black bordered curve).	61
3.8	Averaging (mean value) of a set of six different porcine hearts at a maximum shear strain of 30 % in FS -mode (black bordered curve).	61
3.9	Averaging (mean value) of a set of six different porcine hearts at a maximum shear strain of 30 % in FN -mode (black bordered curve).	62
3.10	Mean curves for a set of six different porcine hearts at a maximum shear strain of 30 % in all modes of simple shear.	62
3.11	Relaxation test (porcine tissue) after a rapid displacement of 0.5 shear strain for 300 s in NF -direction (black curve) and NS -direction (blue curve).	63
3.12	Relaxation test (porcine tissue) after a rapid displacement of 0.5 shear strain for 300 s in SF -direction (black curve) and SN -direction (blue curve).	63
3.13	Relaxation test (porcine tissue) after a rapid displacement of 0.5 shear strain for 300 s in FS -direction (black curve) and FN -direction (blue curve).	63
3.14	(A) Myocardial piece (Clinical Department of Pathology) at the LVFW. Red outlined area in (B) retributes flinty calcium deposits at the base, (C) visualizes a prepared slice and (D) indicates a labeled cubic specimen for shear testing.	66
3.15	Shear stress-strain relationship (offset corrected and smoothed) in NF and NS mode increasing from 10% to 50% shear strain.	69
3.16	Shear stress-strain relationship (offset corrected and smoothed) in SF and SN mode increasing from 10% to 40% shear strain.	69
3.17	Shear stress-strain relationship (offset corrected and smoothed) in FS and FN mode increasing from 10% to 50% shear strain.	70
3.18	Averaging (mean value) of a set of three different human cubic specimens at a maximum shear strain of 30 % in NF -mode (red bordered curve) and NS -mode (black bordered curve).	70
3.19	Averaging (mean value) of a set of two different human cubic specimens at a maximum shear strain of 30 % in SF -mode (red bordered curve) and SN -mode (black bordered curve).	71
3.20	Averaging (mean value) of a set of two different human cubic specimens at a maximum shear strain of 30 % in FS -mode (red bordered curve) and FN -mode (black bordered curve).	71
3.21	Relaxation test (human tissue) after a rapid displacement to 0.5 shear strain for 300 s in NF -direction (black curve) and NS -direction (blue curve).	72
3.22	Relaxation test (human tissue) after a rapid displacement to 0.5 shear strain for 300 s in FS -direction (black curve) and FN -direction (blue curve).	72
3.23	(A) Received myocardial piece (Clinical Department of Transplant Surgery) from the left ventricular front wall (very adipose) with its labeled walls (B), (C) visualizes a prepared slice, (D) indicates a labeled cubic specimen for shear testing (fat deposits at myocardial sheets) and (E) shows a different received specimen with fibrin deposits (white outlined area) on its surface.	73
3.24	Shear stress-strain relationship (offset corrected) in NF and NS mode for Spec.#17 increasing from 10% to 50% shear strain.	75

3.25	Shear stress-strain relationship (offset corrected) in <i>SF</i> and <i>SN</i> mode for Spec.#18 increasing from 10% to 50% shear strain.	75
3.26	Shear stress-strain relationship (offset corrected) in <i>FS</i> and <i>FN</i> mode for Spec.#16 increasing from 10% to 50% shear strain ('strain softening').	76
3.27	Shear stress-strain relationship (smoothed and offset corrected) in <i>NF</i> and <i>NS</i> mode for Spec.#23 increasing from 10% to 50% shear strain at 17°C.	76
3.28	Shear stress-strain relationship (smoothed and offset corrected) in <i>SF</i> and <i>SN</i> mode for Spec.#24 increasing from 10% to 50% shear strain at 19°C.	77
3.29	Shear stress-strain relationship (smoothed and offset corrected) in <i>FS</i> and <i>FN</i> mode for Spec.#25 increasing from 10% to 50% shear strain at 15°C.	77
3.30	Relaxation test (human tissue) after a rapid displacement of 0.5 shear strain for 300 s in <i>NF</i> -direction (black curve) and <i>NS</i> -direction (blue curve) for Spec.#03.	78
3.31	Relaxation test (human tissue) after a rapid displacement of 0.5 shear strain for 300 s in <i>SF</i> -direction (black curve) and <i>SN</i> -direction (blue curve) for Spec.#18.	78
3.32	Compression test (human tissue) at 30% compression strain of HH #07 within CCPS at room temperature.	79
4.1	Mean curve of the shear stress-strain relationship in <i>NS</i> -shear mode (offset corrected) at 30 % shear strain of the RVFW (blue), IVW (green) and LVFW (red).	81

List of Tables

1.1	Wall-size (thickness) of the myocardium depending on species, pathology and location	13
2.1	Summary of different types of solutions where they were applied according to this thesis, denoted with (X), and species (porcine and human tissue), whereas ! reports effects which occurred during testing and are discussed in 4.2.1.1	33
3.1	Overview of relevant characteristics of suitable tested specimens according to measurement series on porcine tissue; Notations for locations and positions: <i>PH...</i> porcine heart, <i>LFW...</i> left ventricular free wall, <i>LV-FW...</i> left ventricular front wall, <i>end...</i> endocardial, <i>mid...</i> midwall, <i>epi...</i> epicardial, <i>equ...</i> equator; Notations due to solutions: <i>CCPS...</i> 'conventional cardioplegic solution', <i>Ringer...</i> modified Ringer solution with 15 mmolK ⁺ /l	56
3.2	Overview of relevant informations due to all received myocardial samples of human heart tissue; Origins: Departments of Pathology and Transplant Surgery; Notations: <i>HH...</i> human heart, <i>Ref. No...</i> reference number, <i>LFW...</i> left ventricular free wall, <i>IVW...</i> interventricular wall (septum) Notations due to solutions: <i>CCPS...</i> 'conventional cardioplegic solution'	65
3.3	Overview of relevant characteristics of tested specimens according to measurement series on human tissue (dissection location, specimen dimensions, solution for measurement at particular temperature) at v=1 mm/min.	67
4.1	Comparison of minimas and maximas of the shear stress-strain relationship of cubic specimens at the RVFW, IVFW and LVFW in NS-shear mode at 0.3 shear strain. <i>Notations: RVFW...</i> right ventricular free wall, <i>IVFW...</i> interventricular wall (septum), <i>LFW...</i> left ventricular free wall	82
4.2	Comparison of minimas and maximas of the shear stress-strain relationship of cubic specimens at the LVFW in all modes of simple shear at 0.3 shear strain for a representative shear stress-strain plot received from the Inst. of Pathology (left) and from the Dep. of Transplant (right). <i>Notations: Ratio...[$\frac{\%}{100}$]</i> ...inactivated tissue in relation to activated tissue	86

Abstract

Previous studies in the multidisciplinary field of heart research have shown that the pathology of the heart seems to have two major keys, not only cardiac electrophysiology, but also cardiac mechanics, which are strongly interlinked. The investigation of experimental data referring to the mechanical behaviour of myocardial tissue is of utmost importance for the understanding of structure and functions of human heart tissue. The main aim of the present diploma thesis, which is part of a major project (development of a finite element simulation model of the behaviour of healthy and diseased human myocardium) of the Institute of Biomechanics (Graz, University of Technology) was to take account into the shear properties of passive porcine and human ventricular myocardium, which are very rarely explored. Unfortunately today, there are no triaxial experimental data of human myocardium in the literature available. The use of autopsy material from all human subjects was approved by the Ethics Committee, Medical University Graz, Austria. In consequence, this work was motivated by the previous study on porcine tissue of Dokos et al. (2002) to emphasize the development of a standardized protocol for the triaxial examination of shear properties.

Further, this study deals with suitable preparation of cubic specimens ($4 \times 4 \times 4$ mm), with axis aligned within the principal material axis, to describe the assumed orthotropic character, in order to analyze the importance of different orientations, myocardial sheets respectively fibers and their contribution to the mechanical behaviour of the human heart. Another impact factor was to find suitable chemical solutions to ensure passive testing for both, porcine and human tissue, at body milieu ($T = 37^\circ\text{C}$).

A total of 14 porcine hearts and seven human hearts (only pieces of organs due to the high demand on human tissue) with collectively over 100 cubic specimens, were examined. Despite, the major differences in myocardial stiffness of those two species, the ventricular myocardium was observed to be nonlinear and viscoelastic, with its stiffness increasing as follows: N (normal direction) $< S$ (myocardial sheet direction) $< F$ (myocardial fiber direction).

Furthermore, this thesis emphasized new consolidated findings referring to proper inactivation of human myocardial tissue (suitable appliance of different cardioplegic solutions and their temperature dependencies) and the dependency of heart-age and the associated mechanical properties.

Zusammenfassung

Kardiovaskuläre Erkrankungen, im speziellen Erkrankungen des menschlichen Myokards, zählen mitunter zu der am häufigsten auftretenden Todesursache in Europa. Vorangegangene Studien haben gezeigt, dass neben den Untersuchungen der Elektrophysiologie, die biomechanischen Eigenschaften des ventrikulären Myokards eine wesentliche Rolle spielen. Diese Arbeit zielt darauf ab, die mechanischen Eigenschaften sowohl der Schweine als auch humanen Ventrikel und Septum, anhand von triaxialen Scherversuchen zu bestimmen. Durch Analyse der experimentell ermittelten Daten in Verbindung mit Daten aus biaxialen Zugversuchen und Miteinbeziehung der elektrophysiologischen Eigenschaften kann eine realistische Finite Elemente Methoden-Simulation, sowohl für den gesunden, als auch pathologischen Myokard, realisiert werden.

Für diese Testreihe soll ein Ansatz gefunden werden, der eine passive, quasi-statische Messung durch Einsatz einer kardioplegischen Lösung, angefangen beim Transport bis hin zur triaxialen Messung, reproduzierbar macht. Hinsichtlich der Präparation der kubischen Proben aus dem Myokard ($4 \times 4 \times 4$ mm), ist die Miteinbeziehung der Mikrostruktur (Myofibers und Sheets), wodurch insgesamt sechs verschiedene Schermoden entstehen, von äußerster Bedeutung um eine geeignete Aussage des biomechanischen Verhaltens treffen zu können. Zusätzlich zur Messung am Schweine-Ventrikel, sollen erstmalig Humanproben, einerseits vom Institut für Pathologie, als auch von der klinischen Abteilung für Transplantationschirurgie, für die Untersuchungen herangezogen werden und mit jenen Resultaten des Schweine-Myokards verglichen werden. Ein entsprechender Ethikantrag für die Untersuchung von humanen Proben wurde von der Ethikkommission der Medizinischen Universität Graz genehmigt.

Bei der Bestimmung der biomechanischen Eigenschaften, konnten die Ergebnisse der vorangegangenen Studie von Dokos et al. (2002) bestätigt werden, wobei die Schereigenschaften des Myokards als nichtlinear und viskoelastisch anzusehen sind und die mechanische Steifigkeit abhängig von der Orientierung der Mikrostrukturen wie folgt zunimmt: N (normal zur Orientierung der Sheets) $< S$ (in Richtung der Sheets) $< F$ (in Richtung der Myofibers).

Zusätzlich wurde die passive Messung und die damit verbundenen Kenntnisse bezüglich kardioplegischer Lösungen und deren Temperaturabhängigkeit für Untersuchungen der Schereigenschaften von humanem ventrikulärem Gewebe ermöglicht. Desweiteren konnte auch eine starke Abhängigkeit vom Alter des getesteten Myokards und dessen Änderung der mechanischen Festigkeit nachgewiesen werden.

Acknowledgment

I would like to express my gratitude to all those who gave me the possibility to complete this thesis.

I acknowledge the excellent supervision of Dipl.-Ing. Dr.techn. Gerhard SOMMER, thank you for supporting me during this thesis, we have even become friends.

I especially acknowledge the guidance of the well reputed Head of the Institute Univ.-Prof. Dipl.-Ing. Dr.techn. Gerhard A. HOLZAPFEL.

Furthermore, I want to thank Dr.med. Michaela SCHWARZ, Dr.med. Michael SACHERER and Aris VAFIADIS for providing human samples from the Clinical Department of Transplant Surgery (LKH-University Clinic Graz) and Ao.Univ.-Prof.Dr.med. Peter REGITNIG, as well as Christian VIERTLER, MD from the Institute of Pathology (Medical University, Graz) and for their professional advice during this thesis.

Ich bedanke mich beim DaRafaeloida, weil er mir den Weg zum Institut geebnet hat und mich immer wieder aus meinem Nest herausgeholt hat und jeden Blödsinn mitgemacht hat. Bei meinem Leidensgenossen RoliRolando der die langen Nächte gemeinsam mit mir im Labor ausgeharrt hat.

Und all meinen Freunden die mir immer eine große Stütze waren, ganz besonders dem Berndl, dem Andi, dem Berni, dem Sigi und meinem Nachbarn Martin, die während der langen Zeit immer wieder ein offenes Ohr hatten und vorallem auch Jenen, die ich die letzten Jahre aufgrund des teilweise schlechten Time-Managements meinerseits und der Entfernung leider oft vernachlässigt habe.

Ein herzlicher Dank gilt meinen Eltern, Mama und Manfred, meinen lieben Großeltern Oma Anneliese und Opa Giorgio (grazie mille), Oma Hilde und Opa Karli und natürlich der lieben Oma Grete und meinem kleinen Bruderherz, Thomas und alle anderen die ich jetzt nicht namentlich erwähnt habe, aber auch sicher nicht vergessen habe. Danke für Eure Unterstützung.

Michael Kutschera
Graz im April 2012

Dedication

Herzlichster Dank gebührt meinem kleinen Lischen, weil sie so lange durchgehalten hat, mich während dem Verfassen dieser Arbeit verköstigt hat und mich die ganzen Jahre über unterstützt hat. Weil Sie viel über sich ergehen hat lassen müssen und Ihr Herz einfach am rechten Fleck hat!

Ich liebe Dich und freue mich auf unsere hoch verdiente gemeinsame Zukunft!

Diese Arbeit widme ich Dir meine Maus.

1 Introduction

1.1 Biomechanics of soft biological tissues - Definiton

The notion ‘*biomechanics*’ is made up of two major key words: ‘*biology*’ and ‘*mechanics*’, which suggests that it explores the mechanical behaviour of biological systems. Further in modern biomechanics the functions of biological tissues are described due to the correlation of tissue structure and their mechanical properties (e.g. stress-strain relationship) (Holzapfel, 2009).

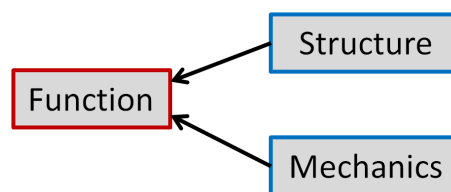


Figure 1.1: Correlation of structure, mechanical stress and the function of tissues (adapted from Holzapfel, 2009)

A change in the mechanical environment also causes a change in the structure, hence it influences the function of (soft biological) tissues (Fig. 1.1). J. D. Humphrey defined biomechanics of soft biological tissues as follows (Humphrey, 2002b):

‘Biomechanics is the development, extension and application of mechanics for the purposes of understanding better physiology and pathophysiology as well as the diagnosis and treatment of disease and injury.’

The term ‘*soft biological tissues*’ describes a primary group of tissue which binds, supports and protects our human body and structures such as organs (‘*soft connective tissue*’). The cells in this type of tissue are separated by extracellular material and may be distinguished from ‘*hard tissues*’ for their high flexibility and soft mechanical properties. They are complex fiber-reinforced structures and their mechanical properties are strongly influenced by the concentration and structural arrangement of constituents such as *collagen* and *elastin* (Holzapfel, 2000).

For applications in biomechanics, knowledge in mechanics, biology, mathematics and statistics are required.

1.2 Motivation

Cardiovascular related diseases (CVDs) are the most common cause of mortality not only in Europe, but all over the world claiming 17.3 million lives a year according to the WHO (World Health Organization, 2008 & 2010). By 2030, almost 23.6 million people will die from cardiovascular related diseases. Each year horrendous funds are spent to predict, prevent and heal those heart related diseases. Hence for better understanding this major cause of death, it can be recognized that there is an acute need for more fundamental research to be made on it. It has been shown that the pathology of the heart seems to have two major keys, not only cardiac electrophysiology, but also cardiac mechanics which are strongly interlinked. In the multidisciplinary field of heart research it is of utmost importance, for the description of phenomena like mechano-electrical feedback (*changes in myocyte lengths influences the duration of an action potential and the membrane potential*) or heart wall thickening during systole (LeGrice et al., 1995), to identify accurate myocardium material properties.

For better understanding the mechanical structure and behaviour of the human myocardium, biaxial tensile- and triaxial shear properties have to be determined. Demer and Yin (1983) and Yin et al. (1987) explored the myocardial mechanics based on biaxial tests, but however these tests are not enough to make an appropriate description. The tissue is not transversely isotropic as it was suggested at biaxial tests, this assumption was neglected in the more recent work by Dokos et al. (2002).

This Diploma thesis is part of a project of the Institute of Biomechanics (Graz, University of Technology) in cooperation with the Department of Transplant Surgery and the Institute of Pathology (Graz, Medical University) and is focused on ‘*triaxial shear properties of porcine and human ventricular myocardium*’ which are very rare explored. Unfortunately today, there is no triaxial experimental data of human myocardium and only one tissue-type (left ventricular free wall) of porcine myocardial tissue in the literature available. Moreover, there is no institution which has ever performed a combination of biaxial tensile and triaxial shear tests on any myocardial tissue.

1.2.1 Aims

The main aim of the whole project is to develop a finite element simulation model (FEM) of the behaviour of healthy and diseased human myocardium. This main objective is divided in different sub-aims:

- (a) Determination of passive *in vitro* mechanical properties of the human myocardium by means of biaxial tensile and triaxial shear testing. It is suggested that the myocardial tissue is dependent on the formulation of appropriate constitutive laws and identification of their material parameters (Dokos et al., 2002). In particular, important for better knowledge of the underlying fundamental ventricular mechanics are: (i) realistic descriptions of the 3D-geometry and structure of the myocardium including boundary

conditions, and (ii) constitutive equations that characterize the material properties of the myocardium (Holzapfel and Ogden, 2009).

- (b) Determination of the microstructure of the mechanically investigated myocardium by polarized light microscopic investigations of appropriately prepared histological slides.
- (c) Verification and/or modification of existing constitutive models using the determined experimental data.

1.3 The heart

1.3.1 Anatomy of the heart - General organization

The heart (*cor*), the main component of the cardiovascular system, is a hollow, fibromuscular organ whose organization is nearly the same in all animals (including all vertebrates). It helps to supply oxygen (O_2) and nutrients into the whole body and removes metabolic waste products and carbon dioxide (CO_2) by repeated, rhythmic contractions. In this thesis the human and porcine heart have to be considered, the understanding of the basic structure is relevant for the analysis of the data according to the realized experiments. A principal build up of a human heart is shown in Fig. 1.2, the porcine heart is very similar. The cardiac septum divides the heart into two halves ('left heart' and 'right heart'), and the halves are in turn divided into *atria* and *ventricle* by valves.

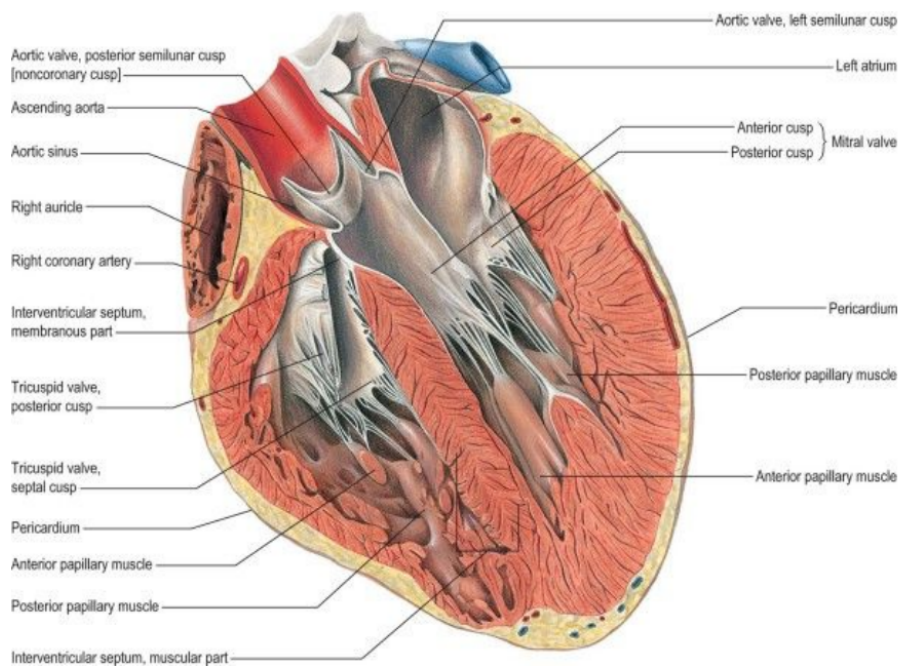


Figure 1.2: Human heart diagram (Gray, 2008)

The right atrium receives deoxygenated blood from *vena cavae inferior* and *superior* ('*diastole*'), via the *tricuspid* valve the blood is then pumped into the right ventricle where the pulmonary valve finally pumps the blood ('*systole*') through the pulmonary artery into the lungs (*pulmonary circulation*). In contrast the left *atrium* collects oxygenated *pulmonic* blood from the pulmonary veins ('*diastole*') and pumps it through the *mitral* valve into the left ventricle. A ventricular contraction ('*systole*') increases the pressure, which opens the *aortic* valve, enabling the outflow into the aortic sinuses and the ascending aorta, and thence to the entire systemic arterial tree, including the coronary arteries (Gray, 2008). The ejection phase of the left heart is shorter than that of the right, but fluctuations in pressure are much greater, which underlies the more massive build up than that of the right heart. A similar approach says that the resistance of the pulmonary circuit ('right heart') contains lower resistance, which causes the smaller tissue thickness requirement, respectively.

Coronary arteries are responsible for autoregulation to maintain the coronary blood flow at the myocardium. Epicardial coronary arteries, which can be seen on the surface of the myocardium play a major role in this thesis due to the inactivation of the specimens to make passive testing possible. (A detailed explanation is listed in chapter 2.2.2.)

At this point we have to consider of different orientations of the heart to specify the locations of specimen dissection. The pericardium is the outermost layer surrounding the heart and consists of fibrous connective tissue. The heart wall itself is a well organized structure composed out of three different layers:

- the innermost layer called endocardium consists of *epimysial* collagen, elastin and a layer of *endothelial* cells,
- the thick central layer is known as the myocardium consists of *cardiac myocytes* (contain only one or two *nuclei*),
- the outer layer called epicardium is a protective membrane and consists of *epimysial* collagen and elastin (Holzapfel and Ogden, 2009).

The majority of the heart is cardiac muscle tissue (myocardium), which is of utmost importance for this paper (Fig. 1.3).

1.3.2 Structures of the myocardium

The myocardium is known as the functional tissue of the heart wall and it is organized in a complex 3-dimensional complex structure (Rohmer et al., 2007). For preservation of the tissue architecture due to deformation and contractile motion of the heart wall, cardiac myofibers are embedded in an extracellular matrix. To make appropriate statements in biomechanics it is important to involve the internal constitution of a material which is indispensable for the response to applied loads. Therefore, a brief on histology to identify orientations, interconnections and microstructural components is thus fundamental for soft tissue biomechanics.

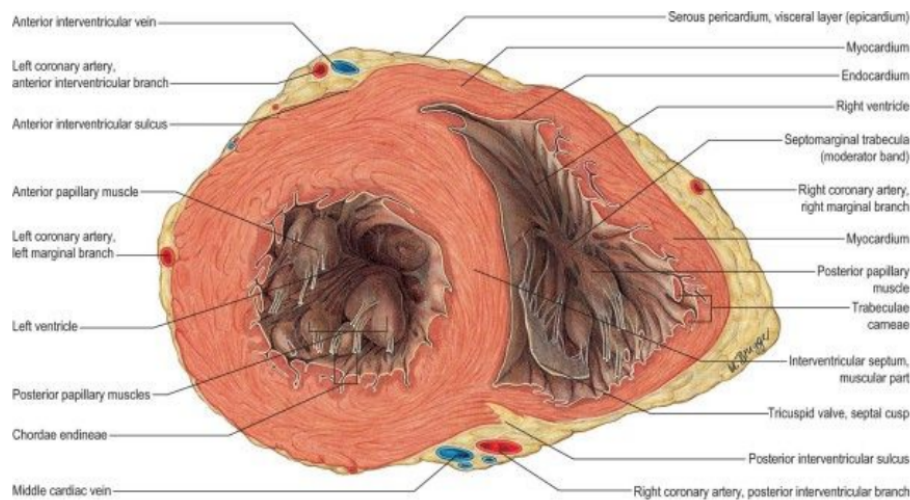


Figure 1.3: Diagram of different layers of the heart (Paulsen, 2006)

1.3.2.1 Anatomy at the microscopic level

A typical eucaryotic cell (from the biomechanical point of view) which consists of a variety of internal membranes and structures, called *organelles* and *cytoskeleton* is shown in Fig.1.4 (adapted from Humphrey, 2002b). The cytoskeleton, which constitutes the *interior* skeleton of the cell, consists of large proteins (protein filaments and associated proteins with multiple functions (McCulloch and Omens, 2006)) and gives the cell shape, structural integrity, the ability to move within the extracellular space and aids in cell division (Holzapfel, 2009). It contains cable-like *actin filaments*, rope-like *intermediate filaments*, hollow tube-like *microtubules* and *spectrin*. Actin filaments are differently organized depending on the location in the cell, for instance they are often organized in bundles so called *stress fibers*. Stress fibers connect the intermediate filaments to the extracellular matrix of a cell via transmembrane linker proteins (e.g., *integrins*). Intermediate filaments have the structural size between the actin filaments and the thick microtubules, hence the conceptual 'intermediate' and they can increase in density in response to applied increased mechanical stress. These three major types of filaments and collagen can mechanically be described owing the *persistence length* and the *contour length*. The persistence length specifies the maximum length over which a filament seems to be straight during thermal motion and is an indicator for stiffness of a cell. In contrast the contour length is the total length of a filament (A detailed explanation can be found in Garikipati and M. Arruda, 2008).

1.3.2.1.1 Cardiac myocytes

In this thesis the precise detailed explanation of heart muscle cells is of utmost importance. Cardiac myocytes (Fig. 1.5) are often branched and consist of one or two *nucleolus* which contain the genetic information known as the DNA, but there are many *mitochondria* which provide the energy for contraction.

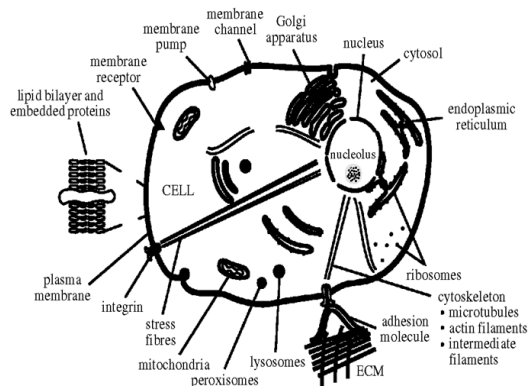


Figure 1.4: Eucaryotic cell (Humphrey, 2002a)

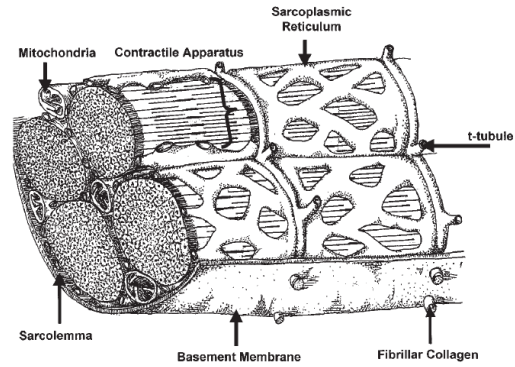


Figure 1.5: Cardiac myocyte (Walker and Spinale, 1999)

Heart muscle cells are built of an array of several hundred parallel myofibrils which can be seen as the functional units of the muscle. Each myofibril is composed out of several hundred *myosin* and *actin* filaments, which are large polymerized protein molecules. *Titin*, one of the largest proteins in the body, keeps the myosin and actin molecules side by side (Dorri, 2004). The proteins actin and myosin are very important for the biomechanical description as they provide the basis of the force-generating apparatus. The myofibrils are suspended inside the myocyte in an intracellular matrix called *sarcoplasm* which is composed out of different types of fluids. (A detailed explanation will exceed the scope of this thesis)

Surrounding this parallel array of myofibrils there is a plasma membrane called the *sarcolemma*, which defines the array of myofibrils as a single cell (Fig. 1.6). The sarcolemma is composed of a lipid bilayer containing *hydrophilic* heads and *hydrophobic* tails. Interwoven throughout the sarcolemma are integrins, which, with receptor transmembrane proteins, bind the myocyte to the extracellular matrix and basement membrane. It has been postulated that integrin engagement to the extra- and intracellular spaces is an essential component for the transduction of myocyte shortening into an overall ventricular ejection (Walker and Spinale, 1999). Furthermore, the sarcolemma forms two specialized regions of the myocyte, the *intercalated disks* and the *transverse tubular* system (Fig. 1.5). Intercalated disks are adhering structures which can be seen from the biomechanical point of view as a type of ‘glue’ that enable contractile force transmitted from one cardiac myocyte to another (Barallobre-Barreiro J., 2012). In contrast to skeletal muscle cells, the T-tubules in cardiac muscle tissue are larger and run along the Z-discs (Fig. 1.6). A force, which is generated by the motor protein *myosin* in thick filaments of cardiomyofibrils, is transmitted along the actin filaments to the Z-discs at the ends of the *sarcomere* and hence along adjacent myofibrils, until the force reaches the intercalated disks.

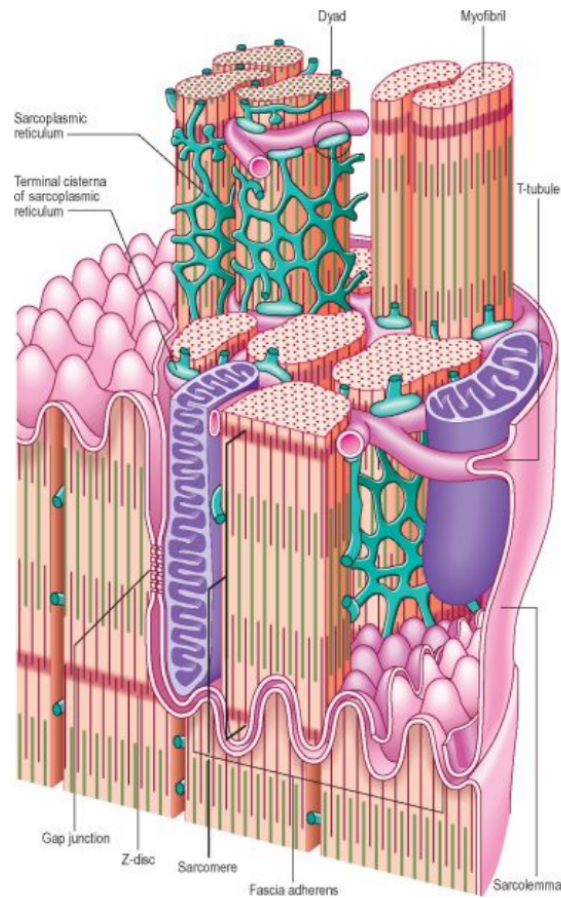


Figure 1.6: Three dimensional reconstruction of cardiac muscle cells in the region of an intercalated disc, a junctional complex between neighbouring cells (Gray, 2008).

The basement membrane separates the intra- and extracellular environment and plays an important role in anchoring the cytoskeleton. It is primarily composed of type IV collagen, the *glycoproteins laminin* and *fibronectin*, and *proteoglycans* providing an interface for myocyte adhesion and continuity with the extracellular matrix (Walker and Spinale, 1999). As in all cells a potential difference across the membrane arises from a trans-membrane ion gradient. The so called ‘action potential’ (about 300 msec) causes the *sarcoplasmic reticulum* to release large quantities of calcium ions (Ca^{2+}) that rapidly penetrate myofibrils and enter the cells. Ca^{2+} -ions activate the actin and myosin filaments and cause the contraction. It is suggested that the contraction is associated with a sliding mechanism (Fig. 1.7), where myosin heads can connect *crossbridges*. The energy which is needed for contraction is supplied by *adenosine triphosphate (ATP)*, which get degraded to *adenosine diphosphate (ADP)*.

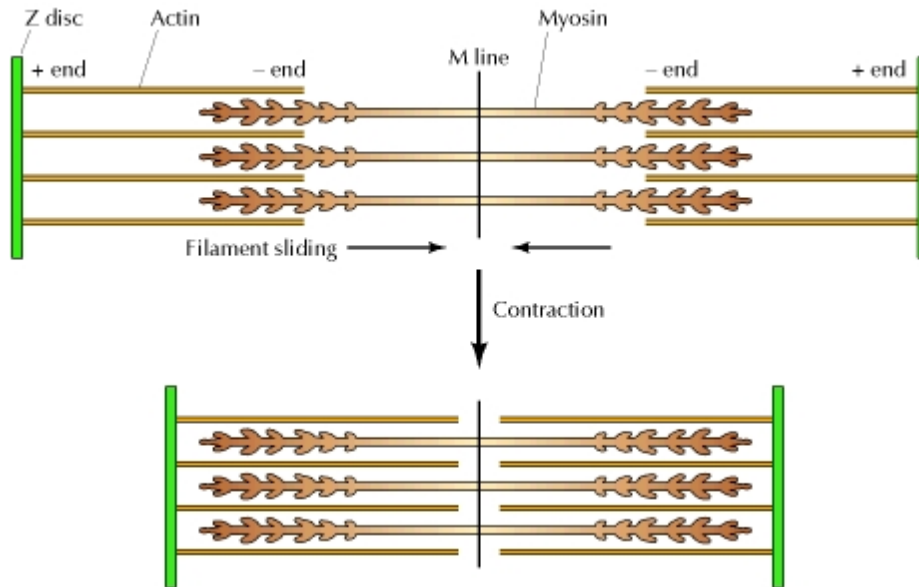


Figure 1.7: Sliding filament model of muscle contraction (Cooper, 2000)

In this thesis it is very important to prevent the contraction of the myocardial tissue due to the determination of passive mechanical properties (see also chapter 2.2.2). At this point we will now refer to the more macroscopic level to identify the laminar arrangement in the myocardium.

1.3.2.2 Anatomy at the macroscopic level

The exploration of myocardial structure has been carried on for several hundred years, but the work on relating structure to its function has been carried out mainly in the past several decades. In earlier decades, the study of myocardial structure-function relations was mostly focused on the fiber functions. Recently researchers (LeGrice et al. (1995), Costa et al. (2001), Dokos et al. (2002), Cheng et al. (2005), Gilbert et al. (2007), Rohmer et al. (2007), Pope et al. (2008), Holzapfel and Ogden (2009)) begun to explore the functional role of myocardial sheets (Dou, 2003).

There is still an ongoing debate concerning the structure of the heart (Gilbert et al., 2007), and, in particular, the nonlinear anisotropic cardiac microstructure. Gilbert et al. (2007) described the heart as a single muscle, coiled in a helical pattern, whereas the other approach, related to this thesis, considers the heart to be a continuum composed of laminar sheets.

The human heart is composed of a helical network of muscle fibers, organized to form sheets (about 70% of the volume) that are separated by a complex structure of cleavage planes (Rohmer et al., 2007). The remaining 30% consist of various interstitial components, whereas only two to five percent of the interstitial volume is occupied by collagen arranged in a spatial network between adjacent myofibres (Holzapfel and Ogden, 2009).

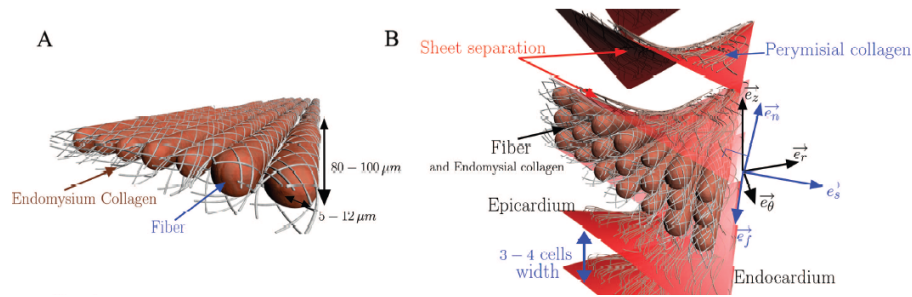


Figure 1.8: Representation of the myocardial structure where (A) correspond to the fibers and (B) show the laminar structure (Rohmer et al., 2007).

Furthermore, the passive myocardium tissue is an incompressible, orthotropic material having three mutually orthogonal planes with distinct material responses, as Dokos et al. (2002) have shown. Fig. 1.8 visualizes the interconnection between myofibers and cardiac sheets (established by Rohmer et al., 2007). According to the phenomena based on the myocardial laminar structure, it is important to take a closer look on cardiac myofibers and sheets.

1.3.2.2.1 Cardiac myofibers

Muscle fibers are composed of myocytes where each are 80-100 μm in length and have a cylindrical shape with a radius of 5-10 μm (Humphrey, 2002a). Histological studies have shown that the muscle fibre direction rotates from approximately $+50^\circ$ to $+70^\circ$ (sub-epicardial region) to nearly 0° in the mid-wall region to -50° to -70° (sub-endocardial region) (Fig. 1.9(b)) with respect to the circumferential direction of the left ventricle (Holzapfel and Ogden, 2009). The layers, in general, are not parallel to the vessel walls, as can be appreciated from Fig. 1.9. The fibers from apex to the base are a left-handed spiral from the *epicardium* to the *midwall*, have a planar circular geometry in the midwall, and are a right-handed spiral from the *midwall* to the *endocardium*. (short: Fibre orientation changes through wall thickness, which affects the anisotropic behaviour!) Furthermore, it has been observed that the number of cells along a radial line through the left ventricular free wall (LVFW) - when it was arrested and immobilized in systole - was up to about 50% higher than in the diastole-phase. Therefore, the fibres have to rearrange themselves during contraction of the ventricle. LeGrice et al. (1995) and Holzapfel and Ogden (2009) discovered that there are more investigations necessary, especially three-dimensional stress and strain measurements, to confirm the orthotropic material behaviour of the myocardial tissue, which is the main part of the current thesis.

1.3.2.2.2 Laminar sheets

LeGrice et al. (1995) obtained that the myocardium has a laminar organization, with myocytes arranged into branching sheets that are superposingly from apex to base, and twisted through the ventricular wall from endocardium to epicardium.

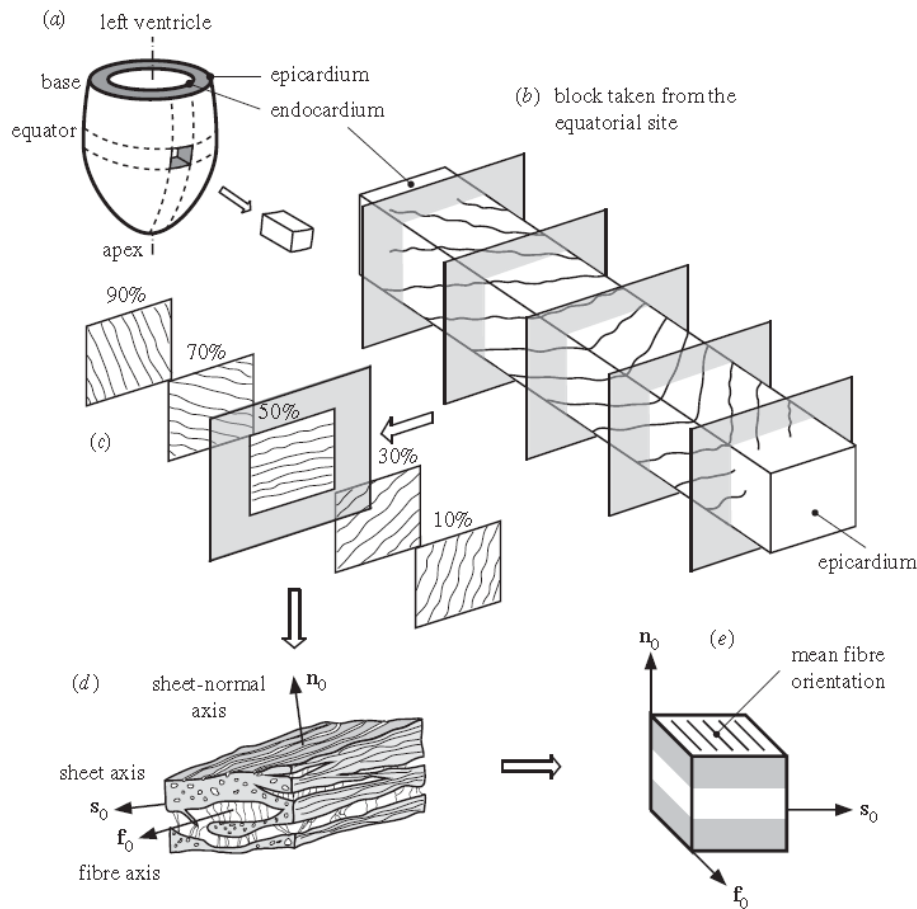


Figure 1.9: Visualization of the variation of the fibre direction through wall thickness: **(a)** the left ventricular free wall with a cutout (specimen) from the equator; **(b)** the microstructure from the cut out block (*endocardium* to *epicardium*); **(c)** the *transmural* changing of the fibre orientation; **(d)** the interconnection of collagen fibres between sheets (fibre axis \mathbf{f}_0 , sheet axis \mathbf{s}_0 and sheet-normal axis \mathbf{n}_0) and **(e)** a cube specimen with sides aligned to the principal material axis (Holzapfel and Ogden, 2009).

Sheets of myofibers are approximately three to four cells thick (Fig. 1.8 **(B)**) and are surrounded by connective tissue. Cardiac myofibers are embedded in a matrix of *endomysial* collagen, whereas myocardial sheets are surrounded by a meshwork of *perimysial* collagen. Fig. 1.9(d) represents the layered organization of myocytes and lateral connections, which are 120-150 nm long, between adjacent myocytes. The laminar structure is bounded by cleavage planes, that are responsible for some important mechanical properties of the myocardium. Dokos et al. (2002) have shown that for mid-wall locations, the orientation of muscle layers in the transmural plane is at about 45° to the base (see also chapter 2.2.3.2.1). Fig. 1.9(e) shows a cube specimen with sides aligned with the material axis.

The specimen which is visualized in NS-shear mode consists of the fibre axis \mathbf{f}_0 , which stands for the cardiac fibre direction, the sheet axis \mathbf{s}_0 , perpendicular to the fibre direction, and the sheet-normal axis \mathbf{n}_0 , which is defined to be orthogonal to the others.

In objective to this thesis, it is of utmost importance to consider of the sheet structure at the free wall (chapter 2.2.3.2.1) for optimal cube specimen preparation. According of the fact, that there are still unknown functions of the laminar structure, there is a need for further investigations.

1.3.2.2.3 Collagen in the human heart

Pope et al. (2008) defined the organization of the human myocardium as follows:

‘The organization and function of the myocardium is highly dependent on the cardiac extracellular matrix (ECM). ECM comprises fibrillar proteins such as collagen, elastin, and fibronectin, signaling molecules and enzymes, all surrounded by ground substance. Collagen is the predominant structural component of the ECM and has been classified into three components: epimysium (lies below the endothelium), surrounding the entire muscle, endomysium, surrounding and interconnecting individual myocytes and capillaries, and perimysium (consists of tendon-like extensions), surrounding and interconnecting groups of myocytes.’ (see also Fig. 1.8)

Collagen is known as the most abundant structural protein in higher vertebrates which occurs in more than 28 types (type I to XXVIII). Types I (most important for tensile strength), III, IV, V and VI collagen, which are most relevant for the human myocardium (*interstitium*), form large structural bundles and are synthesized by fibroblasts and smooth muscle cells (Holzapfel, 2009). The three-dimensional visualization (confocal microscopy) of perimysial collagen across the left ventricular wall have shown that it has a more complex network than has previously been realized. Laminar structure is evident throughout the subendocardium and midwall (mainly present in the form of sheets) but not the subepicardium, where perimysial collagen is composed of regular spaced cords. Fig. 1.10 C and D clearly show the distribution of collagen, which can be considered as an impact factor for the stiffness of the myocardial tissue.

Collagen fibers serve several functions: they supply scaffolds that support muscle cells and they operate as connections between cells and muscle bundles to maintain architecture while coordinating the delivery of force (generated by myocytes). Their tensile strength, which is proportional to fiber thickness (Weber, 1989), and resilience are important indicators of systolic and diastolic myocardial stiffness. Furthermore, they serve to resist myocardial deformation, maintain wall thickness and prevent ventricular aneurysms and ruptures (Weber, 1989).

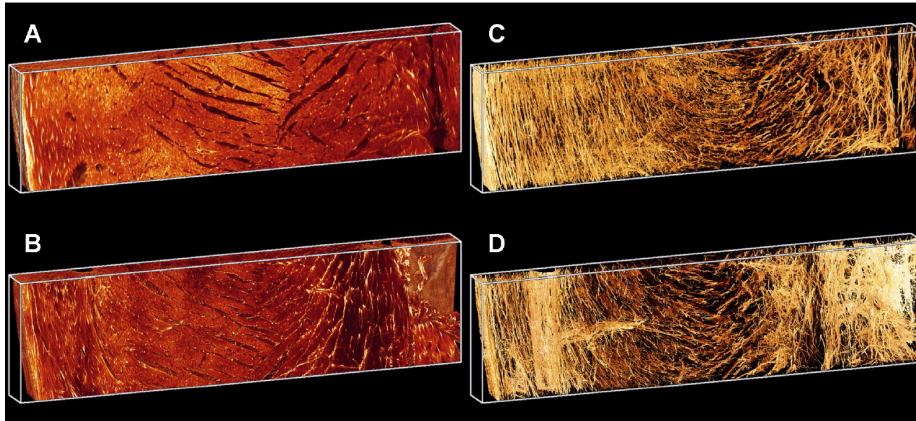


Figure 1.10: Visualization of the complex three-dimensional ventricular myocardium of a rat: **A** and **B** represent the schematic structure of the myocardium (myocyte autofluorescence); **C** and **D** (high intensity) show the distribution of collagen (Pope et al., 2008).

Cardiac *fibroblasts* are mainly responsible for the production of collagen type I and III as well as they produce the proteolytic enzyme *collagenase*, that is responsible for collagen degradation. This proposition may cause, when taking account into the mechanical behaviour, that a pathological change (e.g. *hypertrophic*- or *dilated cardiomyopathy*) in the fibrillar collagen matrix in the tissue strongly influences the stiffness of the human myocardium. Thus, the results of the triaxial shear tests interconnected with the knowledge of the heart-*anamnesis*, should infer the changes of the mechanical properties between the healthy and diseased human myocardium.

1.3.3 Pathology in the human myocardium (cardiomyopathy)

Cardiomyopathy always refers to diseases relating to the myocardium, which becomes enlarged, rigid, or thick. This study focuses on *hypertrophic* cardiomyopathy, *dilated* cardiomyopathy and *restrictive* cardiomyopathy and especially on the changes of the biomechanical properties associated with it. Tab. 1.1 represents the differences in wall-thickness according to species, location in the myocardium and pathology (cardiomyopathy).

1.3.3.1 Dilated cardiomyopathy

In dilated cardiomyopathy (DCM) the myocardium becomes weakened and enlarged, which causes a decreased heart function. The left or right systolic pump function is impaired which leads to chamber enlargement and hypertrophy, so called *remodeling* (Spinale, 2007). Weber (1989) declares this circumstance as the ‘stunned’ myocardium arising from a physical or biochemical abnormality of collagen tethers.

Table 1.1: Wall-size (thickness) of the myocardium depending on species, pathology and location

	Left ventricular [mm]	Septum [mm],	Right ventricular [mm]
Porcine heart (<i>no congenital heart defects</i>)	16 - 30	15 - 27	6 - 14
Human heart (<i>Healthy heart</i>)	13 - 15	13 - 16	3 - 5
Human heart (<i>Hypertrophic cardiomyopathy</i>)	> 15	> 16	> 5
Human heart (<i>Dilated cardiomyopathy</i>)	Expansion of chambers at constant wall-thickness		

Each of them may be responsible for the respective transformation in myocardial structure, including its thinning, impaired contractility and enlargement of the ventricular chamber. DCM is a form of non-ischemic cardiomyopathy, which can be caused by disorders of cardiac fibroblasts (see also chapter 1.3.3), accompanied by the degradation of the collagen fibers and the loss of their structural integrity. Beside of the abnormal thinning and spherical configuration of the ventricle, Weber (1989) observed in *post mortem* human hearts:

‘collagen tethers were markedly reduced in number; perimysial strands either were present but disrupted, or were absent’.

With respect to cube specimen preparation, it can be obtained that dilated cardiomyopathy barely influences the wall thickness (Tab. 1.1), but strongly influences the biomechanical properties, more specifically the myocardial stiffness.

1.3.3.2 Hypertrophic cardiomyopathy

Hypertrophic cardiomyopathy (HCM) results in remodeling, where both extracellular matrix and muscle cells increase in dimension. In addition, the physical transformation of collagen fibers is an adaptive process that facilitates the concentric growth of the myocardium and augments its generation of force while increasing diastolic stiffness. The increase in collagen concentration (*fibrosis*) and a structural and biochemical remodeling of the collagenous matrix of the left ventricular myocardium, occurs through e.g. ventricular pressure overload (Weber, 1989). Fig. 1.11 (A) shows the reduced cavity of a patient corresponding to hypertrophic cardiomyopathy, (B) indicates the increase in collagen.

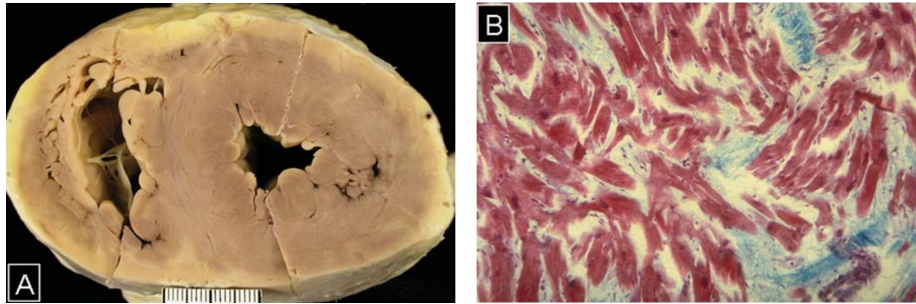


Figure 1.11: (A) Reduced left ventricular cavity in a heart with hypertrophic cardiomyopathy. (B) Masson's trichrome stained histological slice showing myocyte disarray (red) and fibrosis (green) (adapted from Ho, 2009).

Established hypertrophy has shown that *perimysial* strands increase and form new fibers, whereas *endomysial* strands which surround muscle fibers became entwined while forming an orthogonal grid of thin and thick collagen fibers. Weber (1989) concludes the greater the collagen accumulation, the more likely are patients to have symptomatic heart failure.

From a biomechanical view it can be said, that the collagen is that part which is most abundant for myocardial stiffness. Differences depending on collagen remodelling occurred by cardiac myopathy should be emphasized in this thesis.

1.3.4 Anatomical differences between porcine and human hearts

The structural building of porcine (*Sus scrofa domestica*) and human heart is considered to be nearly the same, as it is of interest for the present study. For the preparation of specimen, differences in wall-thickness of the free wall are abundant, listed in Tab. 1.1. In addition to the variations in wall-thickness, there have to be differences between those two species due to its location in the *thorax* and the orientation of the body (*unguligrade* stance, *orthograde* stance). The pig has a classic 'valentine heart shape', whereas humans have a 'trapezoidal silhouette'. The *apex* of porcine is formed entirely by the left ventricle (heart 'rests' on its apex), humans show that both left and right chambers have equal proportions, with the *interventricular* septum occupying an almost central position. Ventricular cavity in pig hearts due to their more massive build up of the myocardium is reduced. Furthermore, differences can be seen in trabeculation, the pig's ventricles possess coarser trabeculations than that in man. Those anatomical differences also result in different electrophysiological characteristics, the duration of the P-wave and PR-interval is much shorter than that in human, which may also explains the faster activation of the porcine ventricles (Crick et al., 1998).

Nevertheless, shear properties of porcine and human ventricular myocardium relate to each other, which should be indicated in this thesis.

1.4 Fundamentals of soft tissue biomechanics

Continuum biomechanics of soft biological tissues consist of three general areas of study, as Humphrey (2002b) declares:

‘(1) identification of fundamental concepts, postulates and principles; (2) formulation of constitutive relations that describe material behaviour; (3) and solution of initial-boundary-value problems of academic, industrial and clinical importance. Fortunately, soft tissues respect the basic concepts of mechanics such as stress, strain and entropic elasticity as well.’

This section presents theoretical postulates of soft tissue biomechanics referring only to the study cited here, otherwise it will exceed the scope. Previous studies of the noncontracting ventricular myocardium (see also chapter 1.2) have demonstrated *nonlinear, anisotropic, orthotropic* and *incompressible* mechanical behaviour. It can be assumed that the validation of passive ventricular myocardium material properties is limited by using uniaxial- and biaxial tensile loading protocols due to the three-dimensional build up of the human myocardium. Biaxial mechanical testing for example explores thin slices of myocardial tissue in which important structural features, like the the organization of the cardiac connective tissue matrix (chapter 1.3.2.1 and 1.3.2.2) and influences of the sheet layers, have been disrupted.

Shear deformation or relative sliding of myocardial layers with different material directions is thought to play an important role in the biomechanical function of the heart (Dokos et al., 2002). LeGrice et al. (1995) claimed that there is an evidence that this mechanism is responsible for the left ventricular ejection by contributing to subendocardial wall thickening during systole, as it is similar for wall thinning that occurs during passive ventricular filling, which is associated with reorientation or shearing of myocardial layers. Hence, the main objective of this thesis is the examination of the shear properties of passive ventricular myocardium of cubic specimens at the left ventricular free wall (LVFW) and interventricular septal wall (IVW) with axis aligned (1) with the myocyte direction, (2) transverse to the myocyte axis within a layer, and (3) normal to the layer.

1.4.1 Simple shear

Therefore, simple shear (deformation) has the mathematical representation:

$$x_1 = X_1 + \gamma X_2, \quad x_2 = X_2 \quad \text{and} \quad x_3 = X_3, \quad (1.1)$$

where (X_1, X_2, X_3) and (x_1, x_2, x_3) denote the Cartesian coordinates of a typical particle before and after deformation. $\gamma > 0$ is a dimensionless constant called the amount of shear (Horgan and Murphy, 2011). According to this study, Fig. 1.12 (A) shows a cubic specimen in FS-orientation, where F denotes the myocyte axis direction, S lies within the sheet layer (chapter 1.3.2.2.2) and N is normal to the sheet layer (chapter 2.2.3.2.1).

Simple shear can be interpreted as a two-dimensional rectangular specimen, whose dimensions are all of the same order and is deformed into a parallelogram (Fig. 1.12 (B)).

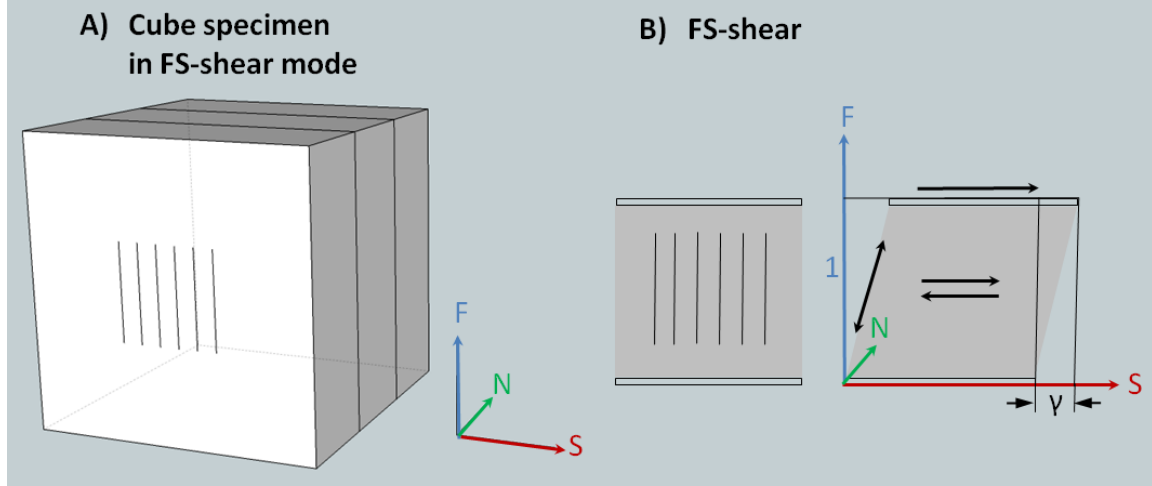


Figure 1.12: (A) Cube specimen in FS- shear mode (F is the myocyte axis direction, S lies within the muscle layer transverse to F, and N is normal to the muscle layer). (B) Specimen in FS- shear mode in undeformed state (left) and in deformed state (right), which produce extension in fiber direction.

For the specific orientation in FS- mode, Eq. 1.1 is given by Fig. 1.12 (B) as follows:

$$f = F, \quad s = S + \gamma F, \quad \text{and} \quad n = N \quad (1.2)$$

Owing to Eq. 1.2, the obtaining deformation gradient \mathbf{F} is given by

$$\mathbf{F} = \begin{bmatrix} 1 & 0 & 0 \\ \gamma & 1 & 0 \\ 0 & 0 & 1 \end{bmatrix} \quad (1.3)$$

Therefore, the right *Cauchy-Green* tensor $\mathbf{C} = \mathbf{F}^T \mathbf{F}$ can be written as

$$\mathbf{C} = \begin{bmatrix} 1 & \gamma & 0 \\ 0 & 1 & 0 \\ 0 & 0 & 1 \end{bmatrix} \begin{bmatrix} 1 & 0 & 0 \\ \gamma & 1 & 0 \\ 0 & 0 & 1 \end{bmatrix} = \begin{bmatrix} 1 + \gamma^2 & \gamma & 0 \\ \gamma & 1 & 0 \\ 0 & 0 & 1 \end{bmatrix} \quad (1.4)$$

The *Green-Lagrange* strain tensor \mathbf{E} is given by

$$\mathbf{E} = 0.5([\mathbf{C}] - [\mathbf{I}]), \quad (1.5)$$

where $[\mathbf{I}]$ denotes the unit matrix. Hence, the *Green-Lagrange* strain tensor \mathbf{E} can be derived due to Eq. 1.5 by

$$\mathbf{E} = 0.5 \left(\begin{bmatrix} 1 + \gamma^2 & \gamma & 0 \\ \gamma & 1 & 0 \\ 0 & 0 & 1 \end{bmatrix} - \begin{bmatrix} 1 & 0 & 0 \\ 0 & 1 & 0 \\ 0 & 0 & 1 \end{bmatrix} \right) = 0.5 \begin{bmatrix} \gamma^2 & \gamma & 0 \\ \gamma & 0 & 0 \\ 0 & 0 & 0 \end{bmatrix} = \begin{bmatrix} 0.5\gamma^2 & 0.5\gamma & 0 \\ 0.5\gamma & 0 & 0 \\ 0 & 0 & 0 \end{bmatrix} \quad (1.6)$$

The derivation of the *Green-Lagrange* strain tensor for the remaining modes can be interpreted due to chapter 2.2.3.2.1.

1.5 State of the art - Conclusion

As already mentioned in chapter 1.2 and 1.4, Dokos et al. (2002) disproved previous studies, in that case that the myocardial tissue is not *transversely* isotropic. This study could highlight the *anisotropic* and *orthotropic* mechanical behaviour of the tissue. The complex pattern of tensile and compressive loading and shear deformation of the myocardial tissue must be examined together to establish a suitable mathematical and finite element model.

Up to now, there are only very few data in the literature, according to myocardial triaxial shear deformation, available. Dokos et al. (2002) could report the outcome of a comprehensive experimental investigation of the shear properties of passive *porcine* ventricular myocardium, but however for the mechanical behaviour of *human* ventricular myocardium, this was only an approximation. To my knowledge, this thesis is the first where simple shear displacement is applied to *human* ventricular myocardium.

2 Materials & Methods

In order to obtain feasible high quality measurement results of passive porcine and human ventricular myocardium, the creation of a chronological procedure protocol (step-by-step) plays a major role. Hence, this chapter describes the operational sequence starting with the myocardial sample procurement, conditions at transport and storage of received specimens, therefore used chemical solutions and materials, and continues with the experimental setup including testing protocols for triaxial shear measurement, and ending with data analysis-tools (software).

2.1 Materials

2.1.1 Specimen

All myocardial specimens from **human** cadavers were either excised during autopsy within 30 h from death (*autolysis*) by the Institute of Pathology of the Medical University of Graz, or during sample preparation within four hours after failed heart transplantation (donor organ was not suitable, organ was placed at the disposal for scientific research) by the Clinical Department of Transplant Surgery, LKH-University Clinic Graz in collaboration with ZMF-Center for Medical Research. The use of autopsy material from all human subjects was approved by the Ethics Committee, Medical University Graz, Austria (for further details see chapter 5.3.1).

Porcine hearts were excised at the local abattoir Marcher®, further myocardial specimen preparation was performed at the Institute of Biomechanics.

2.1.1.1 Origin of hearts

In this chapter, different institutions for the myocardial specimen extraction regarding to species are listed.

2.1.1.1.1 Clinical Department of Transplant Surgery, LKH-University Clinic Graz

Four so-called *NON-FAILING* human hearts of brain death patients (donor-heart is not suitable for transplantation in terms of age, various diseases, alcohol, etc.) were arrested and inactivated during organ explantation by *in vivo* perfusion of 2000 ml cooled (4°C, specified domain-temperature) *Celsior*® -solution (cardioplegic solution, see also chapter 2.2.2.2 and 2.2.2.2.1) into the cannulated coronary arteries: *LAD* (*left anterior descending*) and *PDA* (*posterior descendet artery*). After successful explantation, the organ was inserted in 1000 ml cooled (4°C) *Custodiol*®-solution (chapter 2.2.2.2) with dissolved 2.1 g *BDM* (2, 3 *butanedione monoxime*, see also chapter 2.2.2.2.2), which is known to inhibit cross-bridge activity and prevents contracture of the heart muscle (Dokos et al., 2002). In order to the continuous research on human heart tissue, different specimen-parts for different institutions were excised, only small parts of the left ventricular free wall (*LFW*) and interventricular wall (*IVW*, *septum*) leading to this thesis could be delivered. Subsequent, the extracted myocardial samples were stored in cooled *Celsior*®-solution (to maintain cardioplegia, chapter 2.2.2.2) and transported via a refrigerator box to the Institute of Biomechanics, Graz University of Technology, to perform further steps in terms of specimen preparation according to this thesis.

Background information due to heart-transplant surgery

In order to be a suitable heart-donor, the patient should not be older than 60 years due to the fact that every exceeded decade result in negative effects relating to long-term survival of the recipient. The distinction between *FAILING*-heart (not suitable for transplant), whose ejection fraction (EF) is less than 50 %, and *NON-FAILING*-heart (generally suitable), which left ventricular function is more than 55 % of the normal LV-function (EF) of the appropriated age of the patient, is made by the diagnosis relating to echocardiography (cardiac ultrasound).

Furthermore, the list below represents influencing factors, relating to an optimal graft function:

- duration of cold ischemia
 - (less or complete circulatory failure)
- disorder of the organ according to warm ischemia
- age of donor
- number of rejections
- coronary graft sclerosis etc.

To sum up, either donor organs which have reached a certain age (> 60 a), or younger patients with various heart diseases, but still *NON-failing*, are left for scientific research belonging to this study.

For further informations relating to the excision and extraction of myocardial samples after explantation, see chapter 5.2.

Collaboration partners:

- (i) Michaela Schwarz, MD
(Assistant doctor, Clinical Department of Transplant Surgery, LKH-University Clinic Graz)
- (ii) Michael Sacherer, MD and colleagues
(Phd student, Clinical Department of Cardiology, LKH-University Clinic Graz; ZMF-Center for Medical Research, Graz)
- (iii) Aris Vafiadis
(Master student at the ZMF-Center for Medical Research, Graz)

2.1.1.1.2 Institute of Pathology, Medical University of Graz

Three human hearts were excised during autopsy within 30 h from death and dissected due to the regulations of the *ROKITANSKY*-method (for further informations see Bankl, 1998), which is known as the standard pathological procedure for heart dissection at the LKH-University Clinic Graz. The extracted samples of the *LFW* and *IVW* were directly stored in cooled ‘conventional’ cardioplegic solution (chapter 2.2.2.2.3) after they became available. Aligned slices of the tissue were prepared and fixed in 4% neutral-buffered *formaldehyde*-solution (pH \sim 7.4) by the Institute of Pathology, Medical University Graz, Austria for the histological exploration in terms of myocardial-pathology (e.g. cardiomyopathy) and structure-identification. Subsequent, the specimens were labeled (*TU MYO* 01/12 – *TU MYO* 03/12) belonging to the patient-anamnesis affiliation and transported via a refrigerating box to the Institute of Biomechanics.

In terms of the used dissection method (*ROKITANSKY*) of the clinical institute and the therefore resulting loss of myocardial tissue due to specified sectioning, it was important to define a detailed protocol-routine for possible areas of specimen extraction at the myocardial wall (see chapter 5.2) and more specifically at the front wall of the left ventricle.

Collaboration partners:

- (i) Peter Regitnig, MD
(Professor at the Institute of Pathology, Medical University Graz)
- (ii) Christian Viertler, MD
(Assistant doctor, Institute of Pathology, Medical University Graz)
- (iii) Augustin Donnerer
(Prosector, Institute of Pathology, Medical University Graz)

2.1.1.1.3 Slaughterhouse Marcher®

For realistic passive porcine myocardial data acquisition, it is of utmost importance that the acquired hearts are very fresh (still at body temperature $\sim 37^\circ\text{C}$) and in a good condition (not truncated by the veterinary), such an untreated porcine (*Sus scrofa domestica*) heart is visualized in Fig. 2.1. Therefore, 14 porcine hearts were immediately obtained after slaughtering at Marcher® corporation, Graz, in order to keep the duration of *autolysis* as low as possible.

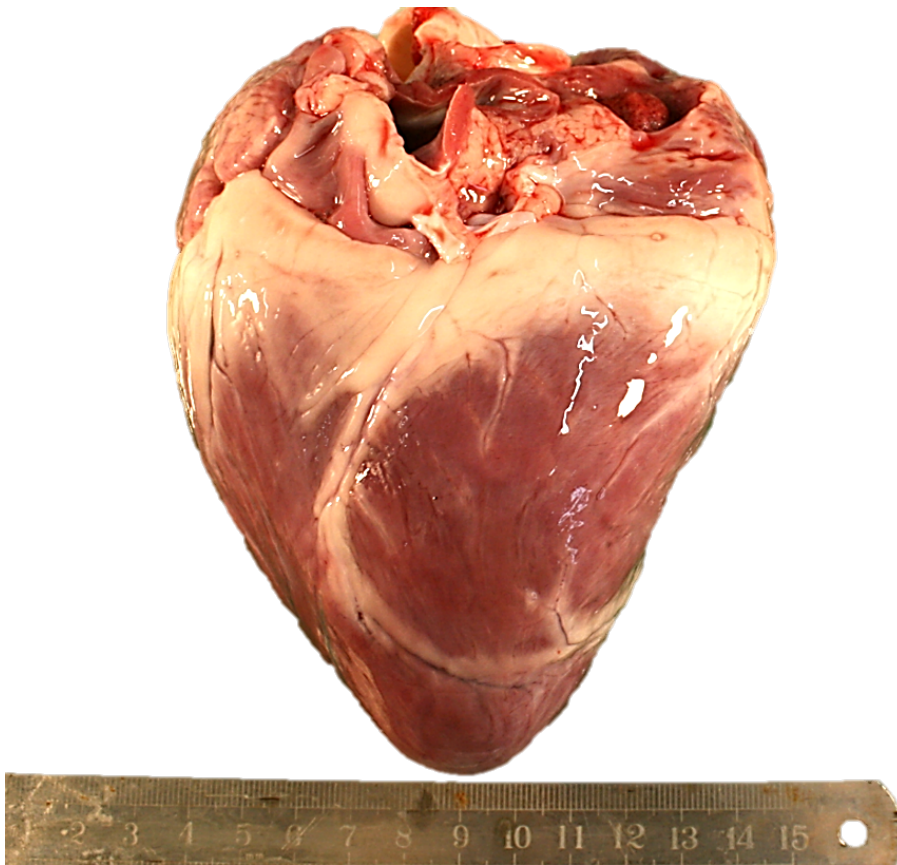


Figure 2.1: Anterior view of a fresh porcine heart showing the right ventricle and atrium (left), the left chambers (right) and coronary arteries (LAD)

Subsequent, the collected hearts were either: (1) immediately arrested using cooled (4°C) *cardioplegic solution*-perfusion into the coronary arteries (LAD, PDA) to prevent tissue activation and provide blood coagulation; or (2) stored in *phosphate buffered saline* (PBS; see also chapter 2.2.2.1) to prevent tissue drying and slow down phenomena like *tissue-necrosis* (cannot be used in terms of tissue-inactivation!). Samples, which were not investigated within the next 48 h were washed in the laboratory and immediately frozen (-18°C) without storing in PBS to stop advanced tissue necrosis and ‘frost’-damage referring to volume dilatation.

2.2 Methods

2.2.1 Equipment belonging to preparation and measurement of myocardial triaxial shear properties

The listing below represent an overview of instruments and tools, which are needed according for specimen preparation and measurement. An accurate description of the experimental setup and the used chemical solutions will be discussed in the following (see chapters 2.2.2 and 2.2.4).

2.2.1.1 Measurement utilities and instruments

Fig. 2.2 represents an overview of the relevant measuring instruments depending on the measurement of human and porcine shear properties. Detailed information referring to the experimental setup and testing protocol is elaborated in 2.2.4.

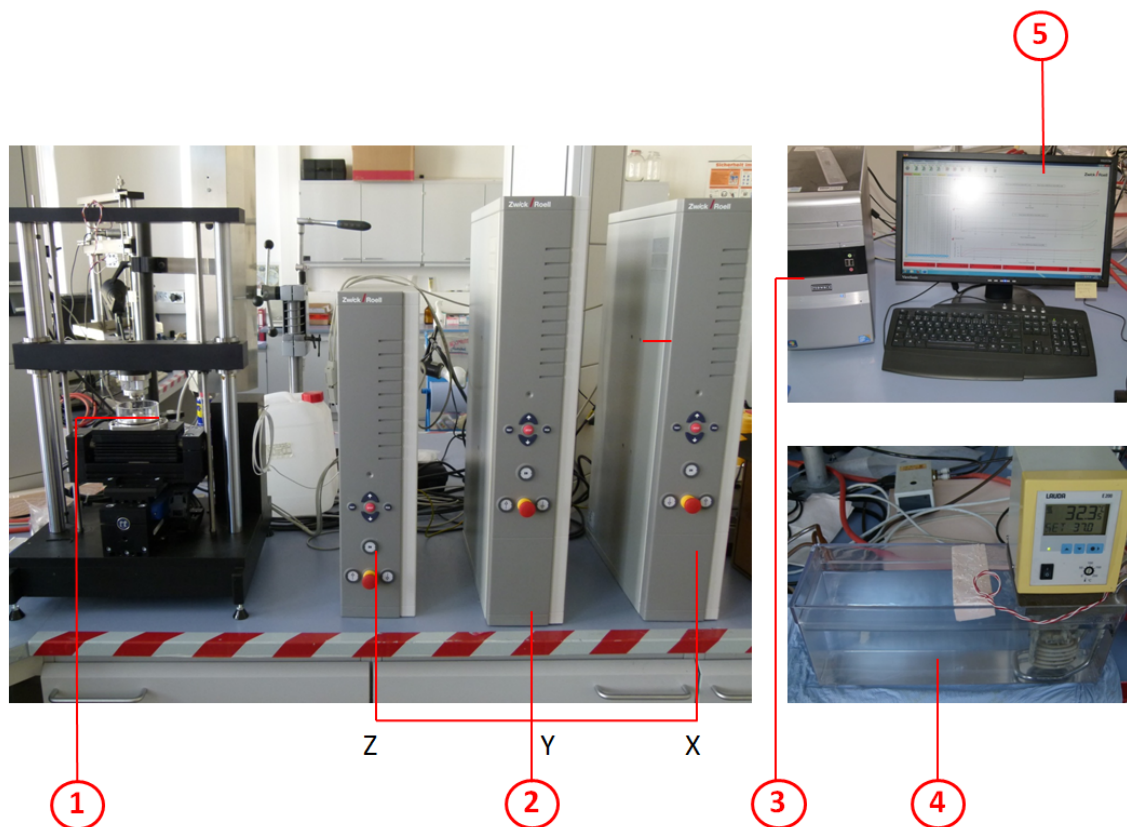


Figure 2.2: Experimental shear device (left) with controller towers (Z, Y, X), Personal Computer with software-package *TestXPert II* and heating bath (right)

The numbering of the listing below is depending on Fig. 2.2.

1. Experimental shear apparatus (hardware)
 - with triaxial loading cell, nominal force $N_{XYZ} = \pm 2 \text{ N}$;
MESSPHYSIK Laborgeräte GmbH, 8280 Fürstenfeld, Austria
2. Three controller towers connected to the triaxial shear device (hardware)
 - one for each axis: X -, Y -, and Z - traverse;
ZWICK / ROELL GmbH & Co. KG, 89079 Ulm, Germany
3. Personal Computer (hardware)
 - used as control monitor for the shear apparatus, enables controlling of the three directions via interface; Type: chiliGREEN, Intel(R) Core(TM) Quad CPU Q 8300 2.50 GHz, 3 GB RAM, Windows 7 Home Premium 32 Bit;
Quanmax AG, 4021 Linz, Austria
4. laboratory heating immersion thermostat with heating basin
 - for precise temperature regulation of chemical solutions (measuring at body conditions: $37,^{\circ}\text{C}$); Type: LAUDA Ecoline Staredition E200;
LAUDA GmbH & Co. KG, 97922 Lauda-Königshofen, Germany
5. *TestXPert II* - software program
 - used for programming of testing sequences, testing and data evaluation;
ZWICK / ROELL GmbH & Co. KG, 89079 Ulm, Germany
6. Videoextensometer (not shown in Fig.)
 - for precise measurement of specimen thickness consisting of CCD-camera 1/3" (Minitron), Objective (50 mm) and Software-interface;
Type: Videoextensometer ME 46-350;
MESSPHYSIK Laborgeräte GmbH, 8280 Fürstenfeld, Austria

2.2.1.2 Tools for specimen preparation

The picture (Fig. 2.3) below shows the most common tools according to myocardial cube specimen preparation, more specifically for cutting and admeasuring the samples.



Figure 2.3: Most common utilities and tools for myocardial specimen preparation

Declaration of utensils (Fig. 2.3) in order to perform the preparation of myocardial cube specimens:

- | | |
|---|---|
| 1. Allen key for upper torso fixation | 7. steel straight edge (metric scale) |
| 2. upper/lower bolt for specimen fixation | 8. glass slides for cube preparation |
| 3. plastic foil with mm-scale | 9. admeasuring inlay for magnifier (17) |
| 4. dissection blade (very sharp) | 10. surgical scissors |
| 5. triangular straight edge for thickness measurement | 11. apportioning vessel with ml-scale |
| 6. disposable scalpel (left) and surgical scalpel III (right) | 12. instant adhesive; Loctite Superkleber-Power Gel |

- | | |
|---|---|
| 13. aluminium capillary tube for omitting solutions | 16. tweezers |
| 14. medical syringe for dispensing | 17. magnifying glass with light and ad-measuring scale; 10 x / 38D / 40; Es-chenbach, Germany |
| 15. caliper rule | |

2.2.1.3 Other important used tools and utensils especially are:

- microscope Axio Scope A1; Zeiss
- camera DS 126 151; Canon
- desk lamp with magnifying glass
- cutting boards - rough and smooth (PVC)
- universal cutter with 45 °cutting-angle and precise width-adjustment; GRAEF
- container and basins for sample-storage
 - rigid plastic containers for storage of hearts
 - petri dishes for storage of small myocardial slices
 - laboratory tubes for cube specimen fixation into formaldehyde
- column thermometer to keep temperature at a constant level during the measuring process
- high precision libra with single-cell weighing system; KERN
- powder-free latex gloves; rotiprotect®-LATEX; ROTH
- surgical masks, BRAUN
- surgical goggles
- skin and surface-disinfection Cutasept F; Bode Chemie, Hamburg
- litter bin for biohazard materials (human waste products)

2.2.2 Chemical solutions for transport, storage and testing of porcine and human heart-tissue

At research of biomechanical shear properties of passive ventricular myocardium, knowledge, of influencing processes caused by different types of chemical solutions (highly application-oriented) for different species/origin and autolysis-time, is of utmost importance.

This chapter treats all used types of chemical solutions depending on their field of application (transport, storage, testing and fixation).



Figure 2.4: (A) ‘Conventional’ cardioplegic solution bottled by Landesapothek Salzburg, (B) Celsior®-Cold storage cardioplegic solution and (C) commercial typical Ringer-solution by Fresenius-Kabi® (adapted from www.medprodukte.at)

2.2.2.1 Phosphate buffered saline (PBS)

Phosphate buffered saline is known as a water-based salt solution and helps to maintain a constant pH ($\sim 7.2 - 7.4$), its osmolarity and ion concentration is based on the human body-milieu (*isotonic*). PBS is non-toxic to cells and often used with EDTA to disengage attached and clumped cells. To our applications, PBS was solely used for storage and experimental testing of porcine ventricular myocardium, because of the fact that it prevents tissue-drying and is also cheap and easy to produce (mixed at the Institute), but however it cannot be used for inactivation of tissue and is therefore unsuitable for experimental human heart analysis.

- Quantitative composition-formula of PBS at the Institute of Biomechanics, Graz University of Technology:
 - 1.44 g $\text{NaH}_2\text{PO}_4 + 2\text{H}_2\text{O}$
 - 0.24 g KH_2PO_4
 - 0.2 g KCl
 - 8 g NaCl
 - dissolved in (distilled) 1000 ml H_2O

2.2.2.1.1 Ethylene glycol teraacetic acid (EGTA)

EGTA (white powder) is a *polyamino carboxylic acid*, which was used as a chelating agent in PBS, that resemble the environment inside living cardiac cells, where calcium ions are usually at least 1000-times less concentrated than magnesium. Calcium is known as the most important intracellular component, small fluctuations may regulate many enzymes and contractions in cardiac myocytes (Bett and Rasmusson, 2002). Under certain conditions the amount of calcium may also lead to activation of cardiac myocytes. Hence, it must be reduced to a low level by using a calcium chelator which tightly binds free calcium. Cohen and Lederer (1988) reported that contractions of adult cardiac myocytes were rapidly abolished by adding EGTA.

Mixing the solution, EGTA was added to PBS (10 mg EGTA : 100 ml PBS) within the use of the high precision libra, in order for the passive determination of shear properties of porcine ventricular myocardium.

2.2.2.2 Cardioplegic solutions (CPS)

In order to accomplish *hypothermic cardioplegia* (*cardio-the heart and plegia-paralysis*), a cardioplegic solution ($\sim 2\text{l}$ at 4°C) was *in vivo* perfused into the coronary artery vasculature, which caused prompt arrest of cardiac electromechanical activity so that surgical procedures (heart-explant and passive mechanical testing) in a tranquilized and bloodless field could be applied. By the use of cardioplegic solution, the protection of cardiac myocytes from cell death during ischemia can be achieved by reducing myocardial metabolism due to the reduction in cardiac workload and hypothermia (Wikipedia.org, 2012).

Hypothermic cardioplegia

As already mentioned, *hypothermic cardioplegia* was induced by CPS during heart transplant in terms of inactivating the myocardial tissue so that no contractions and damage of myocytes could occur. Therefore, the high potassium (K^+) concentration in a CPS play a major role, when determining the membrane potential of a cardiac myocyte. The membrane potential is primarily determined by three factors: (1) the concentration of ions (K^+ , Na^+ and Ca^{2+}) in the intracellular and extracellular matrix, (2) the permeability of the membrane to those ions (potassium, sodium, calcium) and (3) the activity of electrogenic pumps

(Na^+/K^+ -ATPase, Ca^{2+} -ATPase and $\text{Na}^+/\text{Ca}^{2+}$ -exchanger) that maintain the ion concentration across the cell membrane.

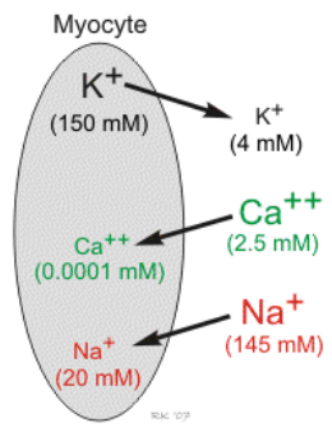


Figure 2.5: Cardiac myocyte: showing ion concentration-gradients of potassium, sodium and calcium (Klabunde, 2011)

Fig. 2.5 visualizes the chemical concentration gradients for potassium, sodium and calcium, where K^+ favors to diffuse out of the cell through selective permeable potassium-channels due to the much higher intracellular concentration than extracellular concentration and the opposite situation for Na^+ and Ca^{2+} . Hence, the cell becomes more negative, which leads to a separation of charges across the membrane and therefore a potential difference across the membrane. To prevent K^+ from diffusing out of the cell, it is necessary to apply a negative charge inside the cell, which can be derived due to the equilibrium potential (E_K ; Nernst potential) for potassium in Eq. 2.1 (Klabunde, 2011),

$$E_K = \frac{-61}{z} \log \frac{[\text{K}^+]_i}{[\text{K}^+]_o} = -96 \text{mV} \quad (2.1)$$

where $[\text{K}^+]_i = 150 \text{mM}$, $[\text{K}^+]_o = 4 \text{mM}$ and $z = 1$ (K^+ , monovalent).

Now, if the extracellular K^+ -concentration were increased from 4 to 40 mM, like it was done by the use of cardioplegic solution with additional potassium (see chapter 2.2.2.2.3), the concentration gradient, and therefore the membrane potential of potassium was reduced, according to the Nernst equation (Eq. 2.1). Hence, the highly ascended resting potential makes muscle fibers inexcitable to ordinary stimuli, thus the contraction of the tissue is inhibited.

A second important key component of cardioplegia is *hypothermia* (cold cardioplegia at $4^\circ - 8^\circ\text{C}$), which is employed by lower myocardial metabolism during periods of ischemia. It is generally approved that the oxygen consumption will drop by 50 % for every 10°C reduction in temperature (Wikipedia.org, 2012).

The following listed cardioplegic solutions differ only slightly in their potassium-fraction (9 mM - 16 mM), as they differ in their additional ingredients, which are mainly responsible to prevent damage of cardiac myocytes.

2.2.2.2.1 Celsior®- cold storage solution

Celsior® - cold storage solution (Fig. 2.4(B)) by genzyme is mainly used in the clinical sector for the cooled (*hypothermia*) *in vivo* perfusion of cardioplegic solution into the coronary arteries (2000 ml) before heart explantation at the donor and storage due to preparation for cardiac research.

• Ingredients

- Mannitol 60 mmol
- Lactobionic Acid 80 mmol
- Glutamic Acid 20 mmol
- Histidine 30 mmol (buffer)
- Calcium Chloride 0.25 mmol
- Potassium Chloride 15 mmol
- Magnesium Chloride 13 mmol
- Sodium Hydroxide 100 mmol
- Reduced Gluthathione 3 mmol
- Water for injection up to 1 litre

The solution ($\text{pH} \sim 7.3 \pm 0.2$ at 20°C) was used immediately after removal from refrigerated storage ($2^\circ - 4^\circ\text{C}$) for inactivating the received myocardial specimens (front wall of LV) of Transplant Surgery during transport and preparation of cubic samples (end product for testing). In order for the experimental investigation of shear properties of **passive** ventricular myocardium at body temperature (37°C), it has been shown that this solution is not suitable for meaningful test results (there is no data in the literature available for the behaviour of the solution at body temperature, which will be discussed in 4).

But, however referring to the additional ingredients beside potassium, the use of Celsior® and Custodiol® (see chapter 2.2.2.2.2) provided the most reliable appliance during transport and further preparation for human specimens according to cell necrosis, and if provided a remedial within the increase of potassium, it can also be used for testing issues.

- Main disadvantage: very expensive

2.2.2.2.2 Custodiol®- cardioplegic solution

Custodiol® by Dr. F. Köhler GmbH, which was used for cardiac preservation immediately after heart-explant at the ZMF, is very similar composed to Celsior® (but differ in potassium concentration: 9 mmol) and therefore does not show any disadvantages in comparison, as it was reported from Ackemann et al. (2002). During excision of myocardial specimens at ZMF-Center for Medical Research, Custodiol® was centrifuged with additional 2.1 g BDM and again perfused (*in vitro*) into the coronary vasculature (LAD and RCX). Following this, the excised specimen for the investigation of biaxial and triaxial mechanical properties was transported via cooled storage solution (Celsior®) to the Institute of Biomechanics, where further progress, preparation (cubic specimens, see chapter 2.2.3) and testing (chapter 2.2.4.4), have been made.

BDM - 2,3 butanedione monoxime

The main convenience of using different additives in cardioplegic solutions like *BDM* (2,3 butanedione monoxime), is to prolongate the duration of cardioplegia at simultaneous minimization of cell necrosis according to reperfusion. *BDM* is well known, as a nucleophile agent which suppresses cardiac muscle contraction by inhibiting myosin-light-chain reactions with actin. $\text{Na}^+/\text{Ca}^{2+}$ exchange is one of the major mechanisms for regulating intracellular Ca^{2+} concentration: In normal cardiac myocytes, Ca^{2+} is extruded to maintain an intracellular Ca^{2+} concentration which is $10^3 - 10^4$ times lower than that in the exterior milieu (Watanabe et al., 2001). Adams et al. (1998) assumed, that *BDM* reduces the primary Ca^{2+} influx into cardiac myocytes, which result in a direct interaction with contractile elements of the muscle cell.

To ensure, 'total' inactivation of myocardial tissue, *BDM* (2.1 g) was centrifuged with 1 l Custodiol® at ZMF, and immediately perfused into coronary arteries. During dissection and preparation of only certain parts of the human heart, the whole organ was inlaid in the mixed solution at 4 °C.

2.2.2.2.3 'Conventional' cardioplegic solution (CCPS, Landesapotheke Salzburg)

The cardioplegic solution mixed by Landesapotheke Salzburg (Fig. 2.4 (A)), the main used solution for testing human specimens (both Pathology and Transplant Surgery), was self-named as 'conventional' (CCPS) due to the lack of a proper name.

In insurance of suppressed inactivation of cubic human specimens, 20 mmol potassium were added in 1 l CCPS (overall: 35 mmolK⁺/l) according to the measurement of mechanical properties at body temperature (37 °C).

2.2.2.3 Krebs-Ringer-solution

Based on the afore mentioned (chapter 2.2.2.2.1) uncertainty of cardioplegic solution at body temperature due to inhibit muscle-contraction, an alternative was sought: *Krebs-Ringer-solution* is probably the most appropriate dilution ('blood-like without cells') in this case, but however assembly was not possible due to absent equipment at the Institute.

Nevertheless, the prescription is demonstrated below, by the reason that it can be of utmost importance for further research (composed of two major steps of assembly):

1. Stock solution 1000 ml:

- *NaCl* 138,4 g
- *KCl* 7.0 g
- *KH₂PO₄* 3.2 g
- *MgSO₄* 2.8 g or *MgSO₄7H₂O* 5.8 g
- *CaCl₂2H₂O* 7.4 g
- Milli Q H₂O 700 ml

2. Krebs-Ringer-solution 2000 ml:

- Stock solution 100 ml
- Milli Q H₂O 1900 ml
- NaHCO₃ 4.4 g
- Dextrose 4.2 g

ad 1.

Add soluble salines by dint of magnetic bar in the listed order, at last assign CaCl₂·2H₂O, and agitate until solution becomes transparent. Finally, add dissolved salines to 700 ml Milli Q H₂O, again agitate, and fill-up with more Milli Q H₂O to obtain one litre stock solution.

ad 2.

First pour 500 ml Milli Q H₂O in 'Erlenmeyerkolben' (2l), add 4.4 g NaHCO₃ and agitate until saline is dissolved. Do it the same way with 4.2 g Dextrose, add 100 ml Stock solution and fill up with Milli Q H₂O to get 2l in total. Finally, the solution has to be filtered.

Ringer solution with additional potassium

Therefore, a commercial Ringer solution by Fresenius Kabi (Fig. 2.4 (C)), which initially does not contain potassium, was modified with additional 20 mmolK⁺/l due to the inactivation of cardiac muscle cells. This infusion solution is the most common solution for the replacement of extracellular fluid due to isotonic and hypotonic dehydration and also used for short-term volume replacement.

Phenomena which occur due to the investigation of mechanical properties of the tissue by the use of modified ringer solution are discussed in 4.

2.2.2.4 Formaldehyde

Four percent *Formaldehyde* (CH₂O) was used as a fixative for tested specimens in order to establish histological slices for further observations (macroscopic analysis is insufficient). Hence, myocardial layers, sheet- and fibre directions, can easily be obtained due to staining with e.g. *masson's trichrome* by microscopic investigation.

2.2.2.5 Summary of different types of solutions according to their application

Table 2.1: Summary of different types of solutions where they were applied according to this thesis, denoted with (X), and species (porcine and human tissue), whereas ! reports effects which occurred during testing and are discussed in 4.2.1.1

	chem. solutions	Perfusion 2°-4°C	Storage ~ 4°C	Transport ~ 6°C	Preparation ~ 15°C	Testing 37°C	Fixation ~ 21°C
Porcine hearts	PBS		(X)	(X)	(X)	(X)	
	PBS:EGTA (100ml : 10mg)		(X)			(X)!	
	Ringer (mod.) (+20mmolK ⁺ /l)				(X)	(X)	
	CCPS	(X)	(X)	(X)	(X)	(X)	
	Formaldehyde (4%)						(X)
Human hearts	Celsior®	(X)	(X)	(X)	(X)	(X)!	
	Custodiol® (add.2.1gBDM/l)	(X)	(X)				
	CCPS	(X)	(X)	(X)	(X)	(X)	
	Ringer (mod.) (+20mmolK ⁺ /l)				(X)	(X)!	
	Formaldehyde (4%)						(X)

2.2.3 Preparation

The following section deals with dissection, preparation of specimens and conditions during preparation of specimens. The method of heart excision and dissection is only explained via porcine tissue with CPS, because of the fact that human hearts are already truncated (high demand, relating to different studies on human hearts), which makes a detailed description more difficult, but however porcine and human tissue show high similarities in their physiology and anatomy (chapter 1.3.4).

2.2.3.1 Method of porcine heart dissection

Immediately after perfusion of CPS into coronary arteries at the abattoir Marcher®, the cooled hearts (transported at $\sim 2^{\circ}\text{-}6^{\circ}\text{C}$) were cleaned (should be washed with the same solution which is used for testing, due to constant inactivation and pH -sensitivity of the tissue) from blood residues at the Institute of Biomechanics.

According to an accurate preparation (Dokos et al., 2002; see chapter 2.2.3), the heart must be dissected into both ventricles and septum. Hence, the first step deals with cutting off the unfeasible *atriums* and the *apex* (known as the thin bottom, where the heart rests in its *thorax*) with a special trimming blade (Fig. 2.3 (4); material: carbon steel; blade length: 130 mm; manufacturer: FEATHER CO., LTD), which ensured only small deformations of the tissue samples during dissection.

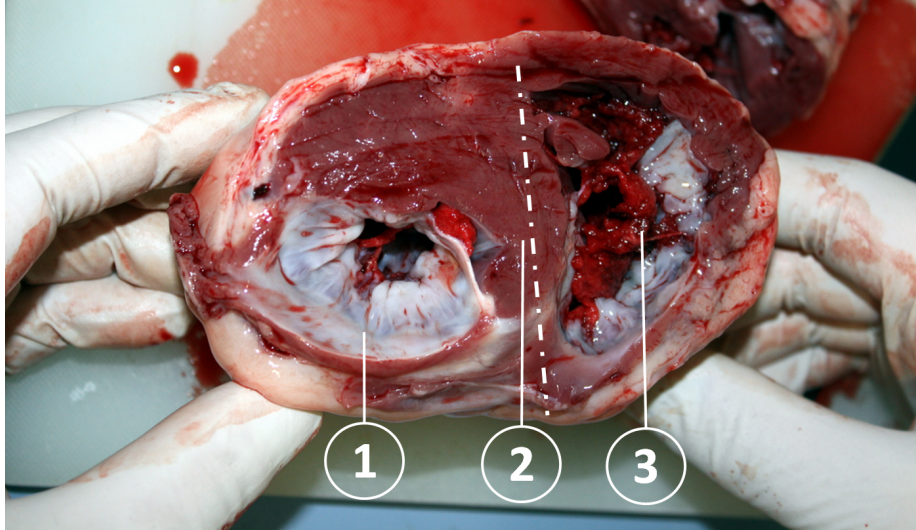


Figure 2.6: Inaccurate cut off of *atriums* due to the still visible valves of the heart; (1) left ventricle , (2) interventricular wall (*septum*) and (3) right ventricle

A precise cut off of *atriums* was necessary due to less possible regions of specimen extraction according to the need of homogeneous samples for biaxial tensile and triaxial shear tests.

Further, it was important not to cut away too much at once, which is visualized in Fig. 2.6, where the valves (*mitral* valve on the left and *tricuspid* valve on the right) are still visible.

At this point it might be useful to mark the *median* of the ventricles with a gentle cut due to easier latter specimen orientation (*basial*, *apexial* directions).

Accordingly, a long carve, using a surgical scissor (Fig. 2.3 (10)), next to the *arteria coronaria sinistra* (LCA) led the right ventricular free wall (RVFW) to fold aside. This is caused by preload (residual stress) of *papillary* muscles (Fig. 2.7).

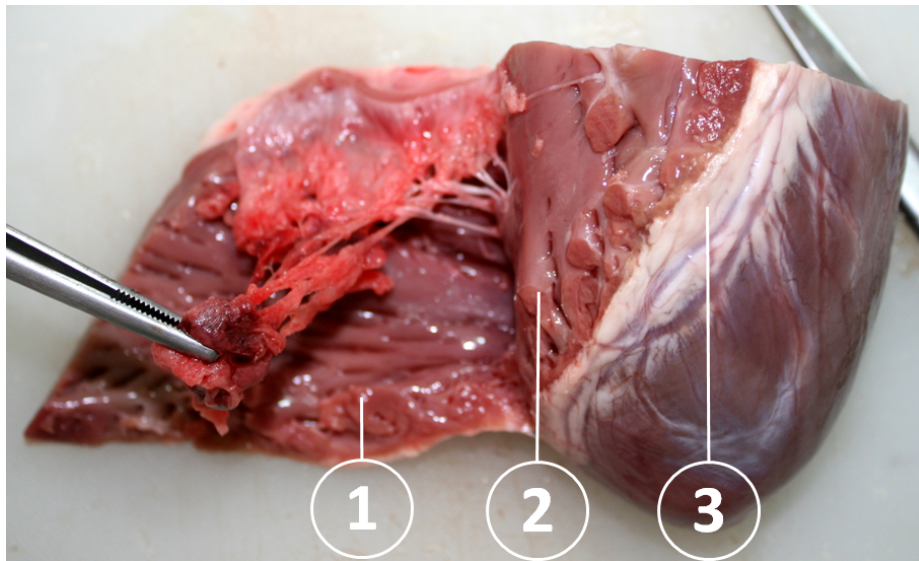


Figure 2.7: Carve along the LCA; (1) right ventricular free wall (RVFW), (2) *papillary* muscles and (3) part of the LCA (LAD, RIVA)

The next step is based on the human myocardium, any further steps rely again to porcine myocardium. Relating to structure investigation tests on human coronary arteries, a project by A. J. Schriefl (Inst. of Biomechanics), the excision of coronary arteries is shown by using a disposable scalpel with a sharp tip (Fig. 2.3 (6a)). Fig. 2.8 visualizes the dissection of the coronary arteries, *ramus interventricularis anterior* (RIVA, (1)) and *ramus circumflexus* (RCX, (2)).

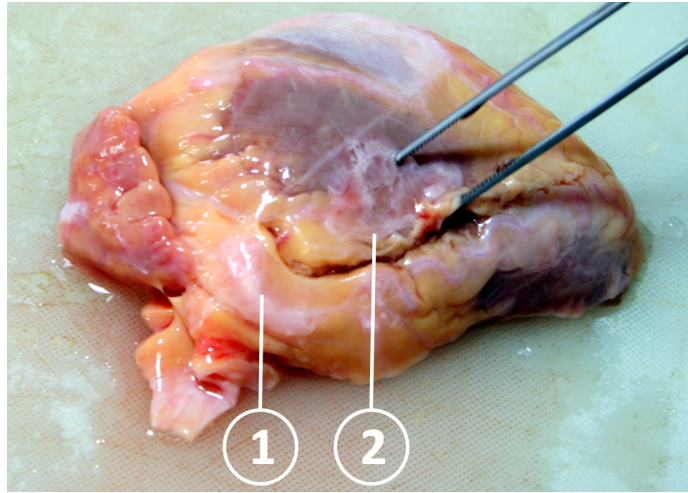


Figure 2.8: Excision of coronary arteries at the front wall (from a 93 year old female patient); (1) *ramus interventricularis anterior* (RIVA) and (2) *ramus circumflexus* (RCX)

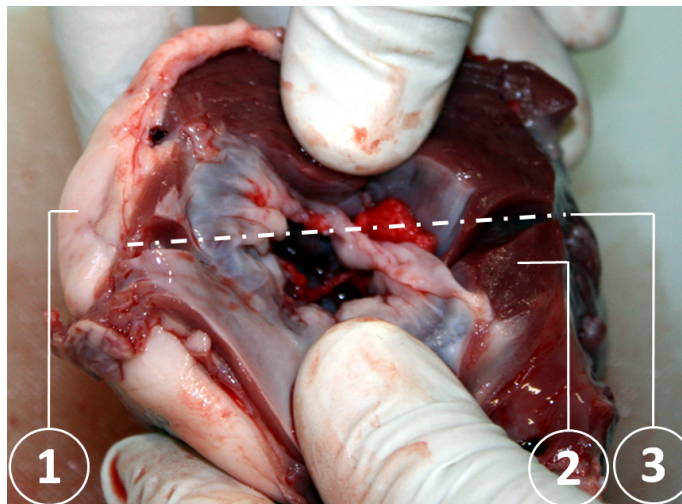


Figure 2.9: The 'left heart'; (1) represents the left ventricular free wall (LVFW), (2) the interventricular wall (IVW) and (3) visualizes a gentle cut at the *median*

Subsequent relating to porcine myocardium, the right ventricular free wall could be separated and immediately inlaid into cooled (4 °C, laboratory refrigerator) cardioplegic solution. The remaining 'left heart' with its gentle cut at the *median*, is shown in Fig. 2.9. The next step, the fragmentation of the LVFW and IVW, was done by performing a precise cut (in the direction: basal to apexial), again by use of the special trimming blade.

In terms of later considerations according to e.g. stiffness of the tissue, the measurement of wall-thickness (Fig. 2.10 (A)) and diameter (B) is of utmost importance.

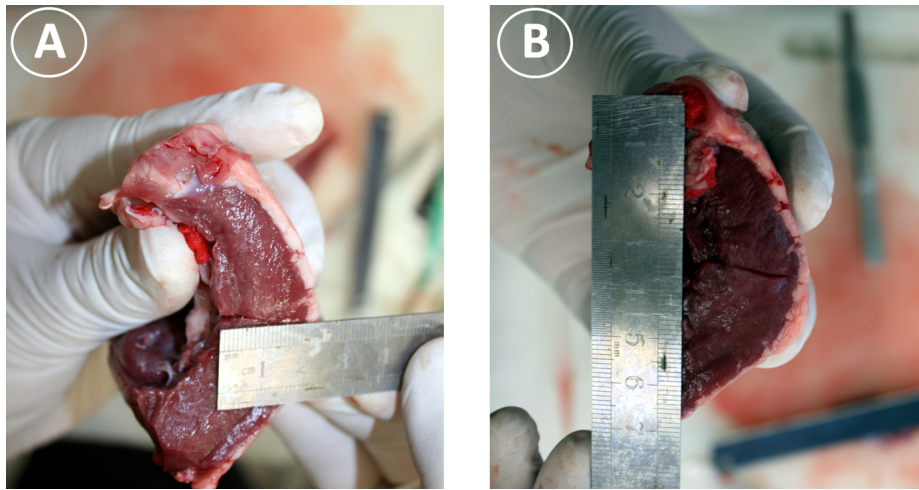


Figure 2.10: Measurement of wall-thickness (A) and diameter (B)

During dissection of organ parts, the tissue must constantly be moistened to prevent tissue-dehydration and cell-necrosis, as already mentioned in chapters 2.1.1.1.3 and 2.2.2.2.1. At least, in the same context, received organ parts, shown in Fig. 2.11, are immediately inlaid into PBS or CPS and kept cool at $\sim 4^{\circ}\text{C}$.



Figure 2.11: Dissected organ parts: left ventricular free wall, interventricular wall (septum) and right ventricular free wall

After successful dissection of the heart, it may be continued with the extraction of appropriate slices due to the preparation of cubic samples with sides aligned to the principal material axes. Therefore, Dokos et al. (2002) reported the outcome of the *FSN-coordinate system*, which is explained in the following text.

2.2.3.2 Detailed specimen preparation

In order to obtain suitable data for the shear properties of passive human ventricular myocardium, a definition of possible regions for the separation of specimens (slices), is very important (e.g. sheet-layers are relatively uniform and aligned at 45° to base, reported from Dokos et al., 2002) and should be nearly the same for all testing cycles. Appropriate areas of sample procurement (slices) are also highly dependent on the size of the available human myocardial tissue, provided from different institutes (high demand on human tissue!; see chapter 2.1.1.1).

Cubic specimens should have at least 3 mm edge length, the dissection of slices out of the RVFW due to the average of the thickness of human right ventricular walls (much thinner than porcines, see Tab. 1.1), is therefore not useful, only the LVFW and IVW of human tissues are of interest for the present study. Further, due to simultaneous comprehension of biaxial tensile and triaxial shear tests, whereby required slices must be separated in two different ways, and the small amount of human tissue, a precise sample excision protocol had to be developed (see Appendix 5.2).

Disassembly of the free wall into slices

Slices were either separated from *anterior* to *posterior* relating to biaxial tensile tests, *circumferential* to the surface of the LVFW (Fig. 2.12 (B) 3), or transverse to it from *epicardial* to *endocardial*, *perpendicular* to the free wall (Fig. 2.12 (B) 2), relating to the investigation of triaxial shear properties.

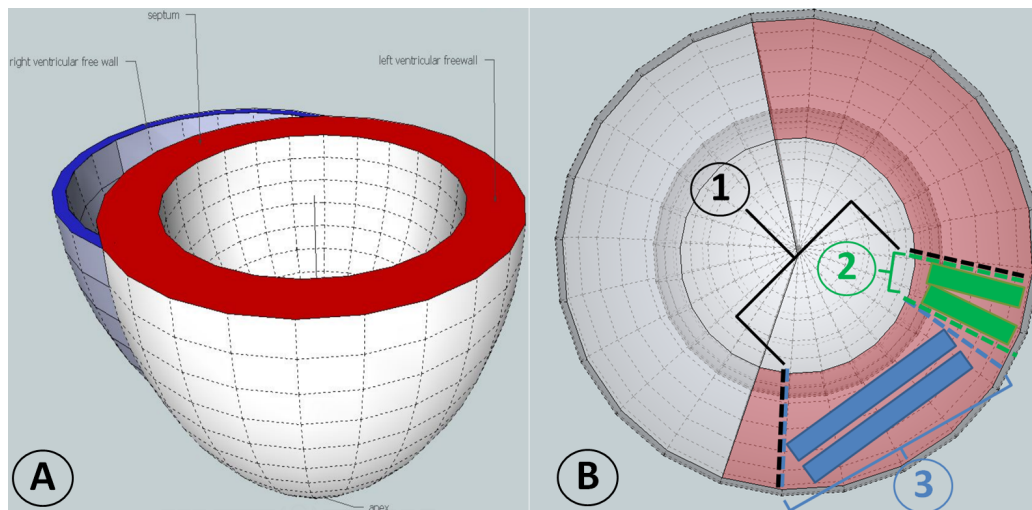


Figure 2.12: (A) shows a 3D-model of human myocardium (RVFW, IVW, LVFW); (B) illustrates locations for the separation of myocardial tissue: the red marked area identifies the LVFW; (1) the black dashed lines border a typical received cotter at the front wall, which was received from various departments; (2) indicates possible slices for the investigation of triaxial shear properties, (3) represents possible slices dissection corresponding to biaxial tensile tests

Based on the small size of the received tissue of the different departments and the very different modes of extraction, it can be recognized that the creation of such a model was indispensable. Further, slices for the two types of investigations are perpendicular to each other (difficult to dissect according to small amount of tissue), which can be explained by the fact that due to the preparation of cubic specimens ($4 \times 4 \times 4\text{mm}$; triaxial), the direction of myocardial sheets is most significant, and on the other hand, the direction of myofibers is initial for the preparation of cuboid samples ($25 \times 25 \times 3\text{mm}$; biaxial).

2.2.3.2.1 The FSN-coordinate system

As already afore mentioned, Dokos et al. (2002) defined a right-handed orthogonal set of axes at every material point within the ventricular wall on the basis of the local laminar architecture. Hence, Fig. 2.13 shows the defined axes relating to the *mean myofiber direction* (F), the direction *transverse to the fiber axis* (S) within the layer, and the direction *perpendicular to the layers* (N).

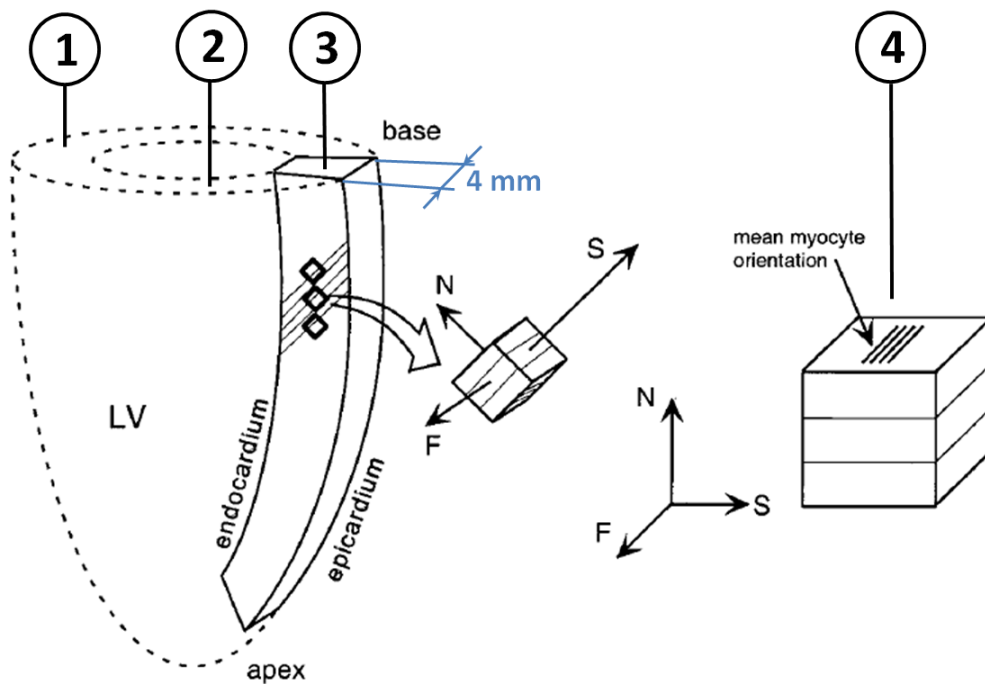


Figure 2.13: Dissection of an appropriate piece out of the LVFW; (1) interventricular wall, (2) front wall, (3) dissected *transmural* base-apex segment showing the orientation of sheets at the equator (4 mm thick) at the free wall, (4) cubic sample with principal material axes in *NS-mode* (adapted from Dokos et al., 2002)

2.2.3.2.2 Cubic specimen preparation - Cutting techniques

These *transmural* base-apex segments were first sliced with an electric universal cutter (material: titan blade; angle-variation up to 45° ; manufacturer: Gebr. GRAEF GmbH & Co. KG) to achieve *homogeneous* (smooth surface; which is of utmost importance for identification of sheet-layers), uniformly thick slices of ~ 4 mm (Fig. 2.13). Within the slices (Fig. 2.14; the dark dot on the upper section of the slice marks the basal direction), a region was selected in which sheet-layers were most uniform in orientation.

According to easier structure identification a desk light with magnifying glass was used and additionally a more precise magnifying glass lighter with scale. Auxiliary, cellulose paper and in some cases, *Evans blue dye* was used to highlight the laminar structure. Subsequent, the slices were incised parallel to sheets (Fig. 2.14 (A)), indicated through black lines) at an interspace of an edge-length of the cube to be prepared.

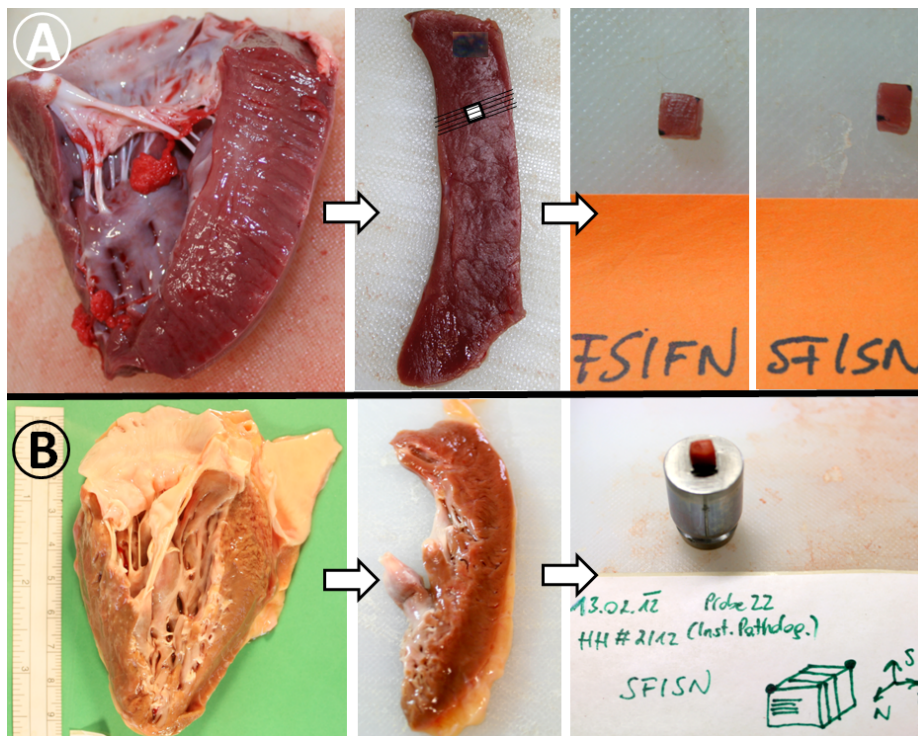


Figure 2.14: Preparation of a cubic specimen with axes aligned to the principal material axes; (A) represents the preparation at the left ventricular front wall of **porcine** myocardium, (B) denotes the equivalent for **human** tissue

Therefore, the special trimming blade, which is known to allow precise, thin incisions (inhibits deformations) without rupturing the tissue due to the small amount of the needed pressure, was used. Further, according to the much more *inhomogeneous* surface (rather suffers damage) of human tissue (Fig. 2.14 (B)), a cutting board with smooth surface was used instead of the more rough, same as forceps without serrated grippers.

The remaining columnar samples (4 mm width and 4 mm thick) were truncated at 4 mm to achieve cubic samples with the dimensions: $4 \times 4 \times 4$ mm.

2.2.3.2.3 Six possible modes of simple shear

To achieve an entire measurement series of an orthotropic material, three cubic specimens are necessary to cover all six possible modes of simple shear, which were cut from regions of the left ventricular wall with sides aligned with the principal axes (Fig. 2.15).

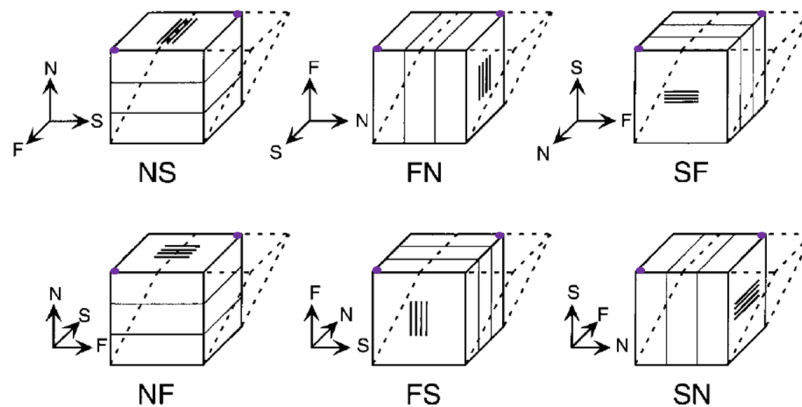


Figure 2.15: Six possible modes of simple shear corresponding to the *FSN* coordinates, with surgical marker-labeled corners at the upper face (same as on the tissue) in order to identify orientations after testing. Shear deformation is commonly characterized by two coordinate axes; the first denotes the face that is translated by shear, and the second is the direction in which that face is shifted. Thus *NF* shear is represented by the translation of the *N* face in the *F* direction (adapted from Dokos et al., 2002).

Depending on wall thickness and surface-structure of the sliced slice of the observed ventricle (compare Tab. 1.1), three adjacent cubic specimens (in best case) are dissected so that their edges were aligned with the laminae on the transmural face (*S*) and with two sides parallel to the *F* and *N* directions (Fig. 2.13).

In order to define sample orientation for later histological investigations, the prepared cubic specimens were labeled at two corners on the upper surface (for each mode) with a surgical marker, as Figures 2.14 (tissue) and 2.15 (theoretical) clearly show.

The measurement setup (hardware and software assembly) and requirements according to specimen fixation in order to perform appropriate investigations on shear properties of passive myocardium is explained in the following text.

2.2.4 Experimental Setup: Triaxial shear testing device

The (custom-built) triaxial shear testing device (short: TRIAX) was developed and built by the Institute of Biomechanics, Graz University of Technology, Austria in cooperation with the company MESSPHYSIK Materials Testing, Fürstenfeld, Austria. This device was optimized for testing highly deformable soft biological tissues using shear deformation.

2.2.4.1 Hardware configuration - MESSPHYSIK

The device consists of two main components; an upper platform movable in the z -direction and a lower platform containing a two-dimensional translation stage.

The operation principle is that the tissue specimens are affixed to both the upper and lower platforms using a thin layer of cyanoacrylate adhesive and bathed in a tempered solution (CPS, PBS) at $\sim 37^\circ\text{C}$ (Fig. 2.16). The lower platform is moved relative to the fixed upper platform using a biaxial translation stage. The system operates with a stroke resolution of $0.25\ \mu\text{m}$ in the x - and y -direction and of $0.04\ \mu\text{m}$ in the z -direction. The temperature-controlled tissue bath is available to simulate the physiological environment of the specimen. The device incorporates a 3-axis force-sensor that allows the three orthogonal forces in the directions x , y and z to be recorded. A capacity of $\pm 2\text{N}$ and a linearity error of 2% between 20mN and 2N of the force sensor are specified by the manufacturer. Furthermore, the cross-talk between the x - and y -axis of the force sensor is specified to be $<0.5\%$, whereas the crosstalk between the z - and x -/ y -axis is specified to be $<1\%$ by the manufacturer. Motor control and data acquisition are achieved using the software ‘TestExpert II’ Version 3.2 (Zwick/Roell GmbH & Co. KG, Ulm, Germany) on a Windows based personal computer.

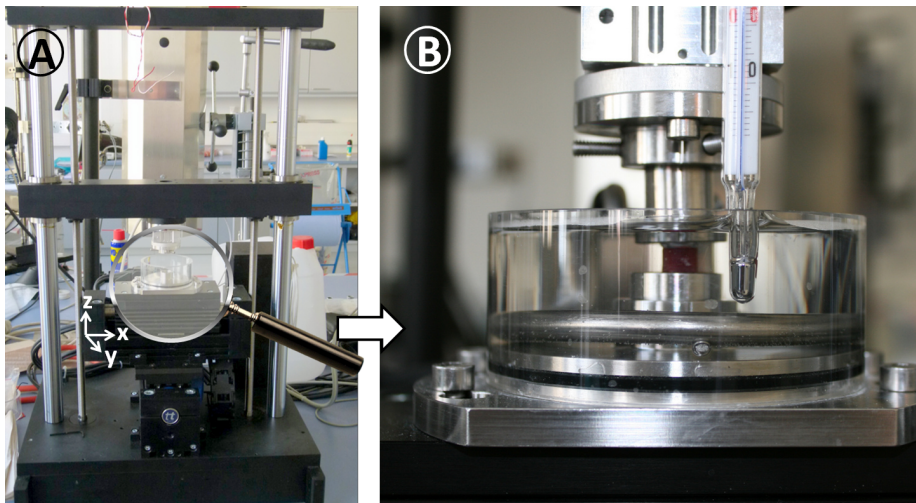


Figure 2.16: (A) shows the triaxial shear apparatus with its lower platform moved relative in x and y direction; (B) indicates a fixed human cubic specimen in cardioplegic solution with additional potassium (20 mmol/l)

Block diagram - Experimental Setup:

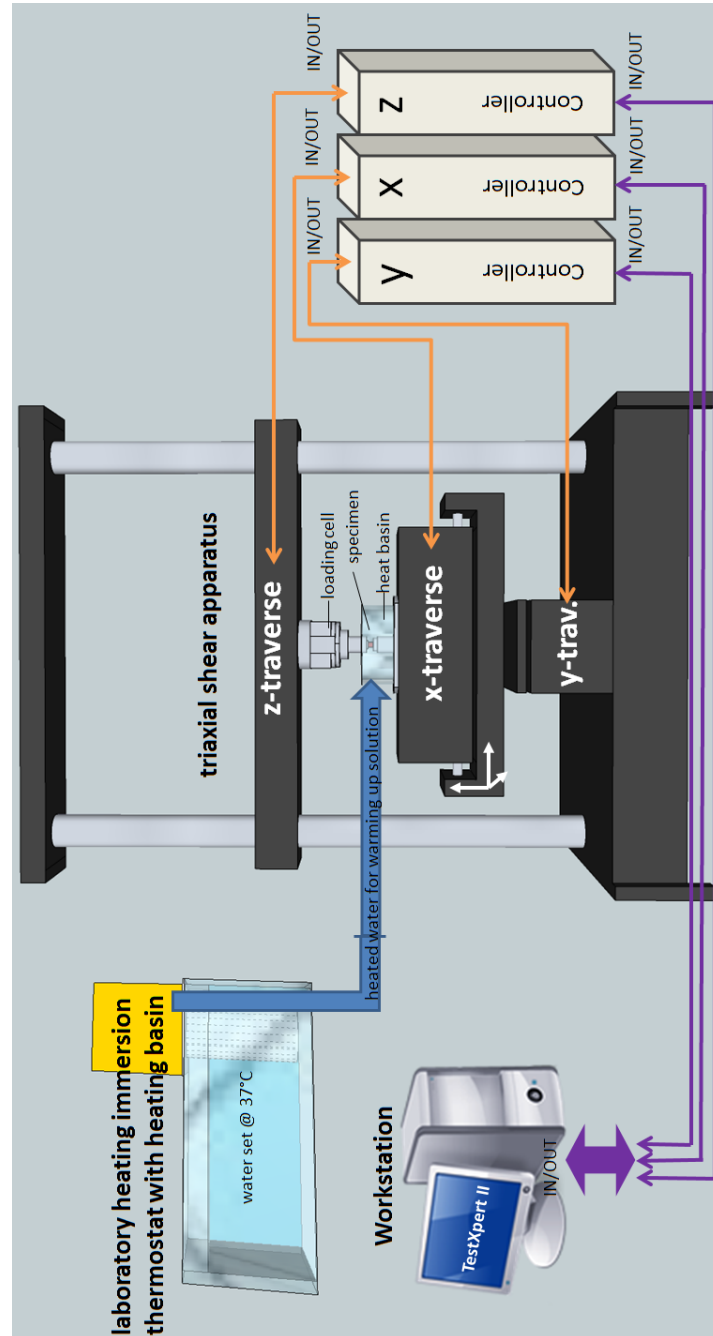


Figure 2.17: Block diagram showing the experimental setup for triaxial shear testing: laboratory immersion thermostat (controlled @ 37°C), Workstation (Software - Testing protocol, controlling for x, y and z - traverses), triaxial shear testing device with fixated cubic specimen, controller towers for traverses (left to right)

Figure 2.17 visualizes the experimental setup for the investigation of triaxial shear properties of passive myocardium with all its components. The three traverses are connected to three automatic controller towers, which can be served manual at the front side or via software.

2.2.4.2 Fixation of specimen into the triaxial shear apparatus

The prepared (on the upper face dot-labeled) cubic specimen are affixed into the TRIAX as follows:

1. moving up the sliding carriage, used for the fixation of the upper platform in order for simpler fixation handling
2. purify both platforms from fat by the use of a disinfection agent and again clean with deionized water
3. coat a thin, consistent layer of cyanoacrylate adhesive (Loctite® - Super Kleber - Power Gel) onto the face of the upper platform using a transparent plastic foil (drop of glue, applied within the foil results in the thin, consistent film of glue)
4. apply cubic specimen in direction of dot-labeled face onto the adhesive surface of the upper platform using forceps
5. detach potential cross connections between adhesive and tissue by the use of a scalpel
6. drying-duration for adhesive: 5 min
7. plugin upper platform using an allen key into the sliding carriage (indentation-frontal), illustrated in Fig. 2.18

Figure 2.18 shows a model for a fixated specimen at the upper platform in *NF*-shear-mode.

2.2.4.2.1 Modifications on platform-surfaces

As the consequence of chipping the faces of the platforms/specimenholders (Material: stainless steel) with a scalpel after each test (removing glue residues), the surfaces got too rough over time. To inhibit both, infiltration of adhesive into the tissue and detachment from platforms, the faces were carefully polished using the water-abrasive method within a very fine ('Korn' 1000-3000) abrasive paper. Due to inhibit edge rounding the upper platform was further embedded, illustrated in Fig. 2.19.

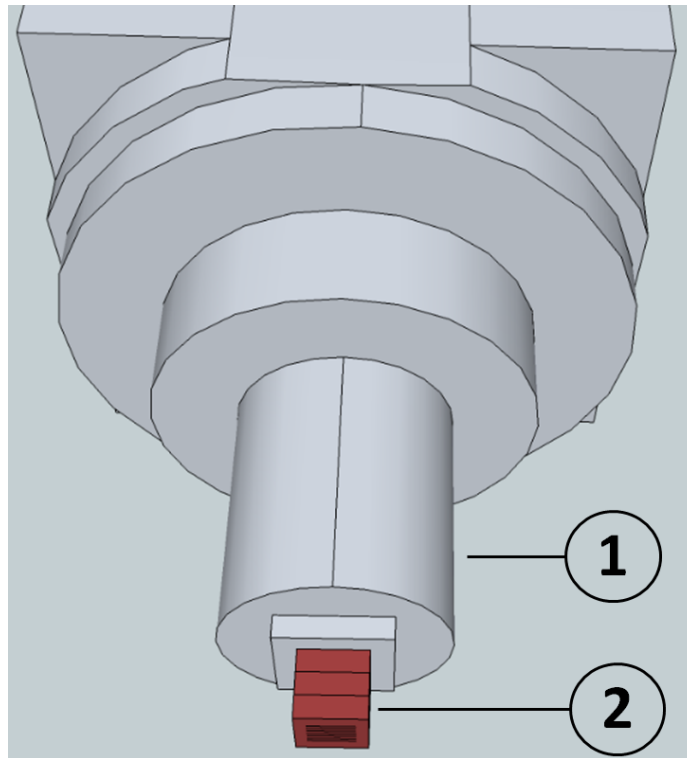


Figure 2.18: Sliding carriage: Upper platform (1) with fixated tissue specimen in *NF*-direction (2)

According to inhibit errors during measurement series and depending on the number of measured samples, the platforms have to be polished from time to time.

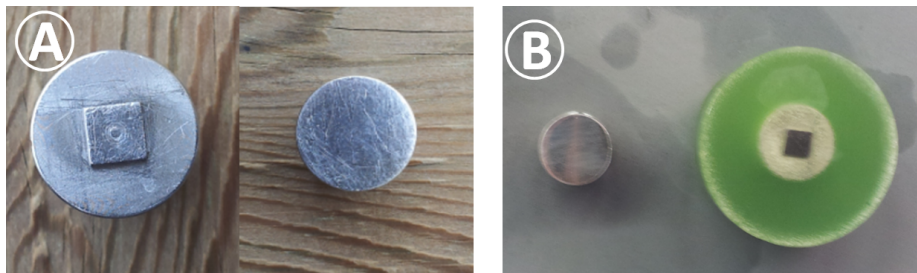


Figure 2.19: Fixation platforms before (A) and after (B) polishing using the water-abrasive method (embedded upper platform).

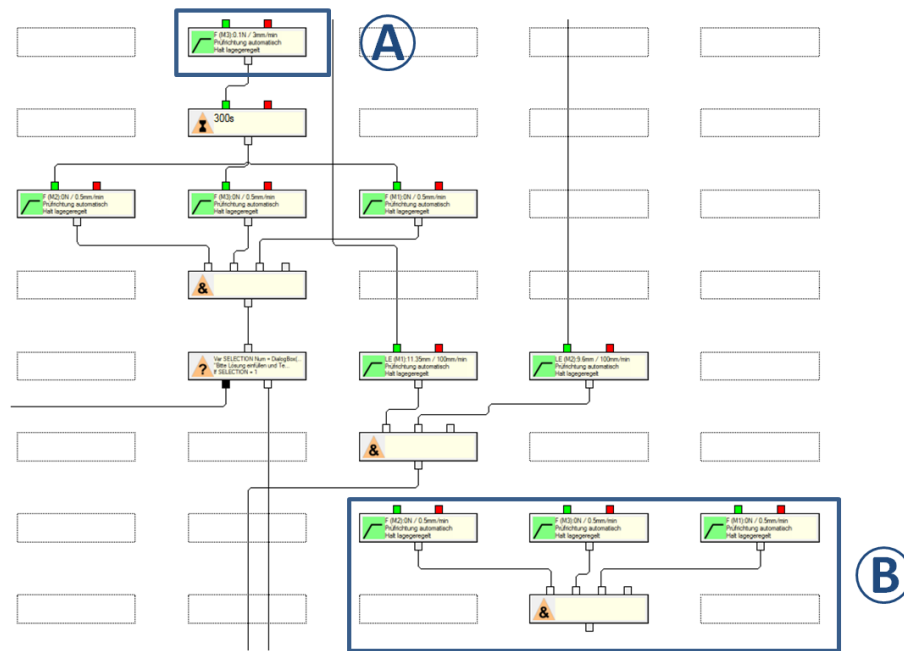


Figure 2.21: Part 2 of the testing sequence with modification (A) and (B), which is explained in the following

Part 2 (Fig. 2.21) waits for 300 s (until adhesive has cured), subsequent traverses are set to 'kraftgeregelt', which connotes that their movement is relating to the applied force, which is set to 0N (*tension free state*). Thus, measurement-startup at consumed forces unequally to zeros are inhibited.

The blocks in part 3 contain the elements for shear testing, where the applied shear strain depends on sample-thickness. As can be seen in Fig. 2.22, shear testing is separated in $x(M1)$ and $y(M2)$ direction and further in *preconditioning* and *main cycles*.

The remaining part 4, illustrated in Fig. 2.23, emphasizes relaxation testing ('step testing', see chapter 2.2.4.4) and the blocks for unconfined compression measurements.

Concerning to the input of required input parameters, it is referred to chapter 2.2.4.3.3 and Fig. 2.24.

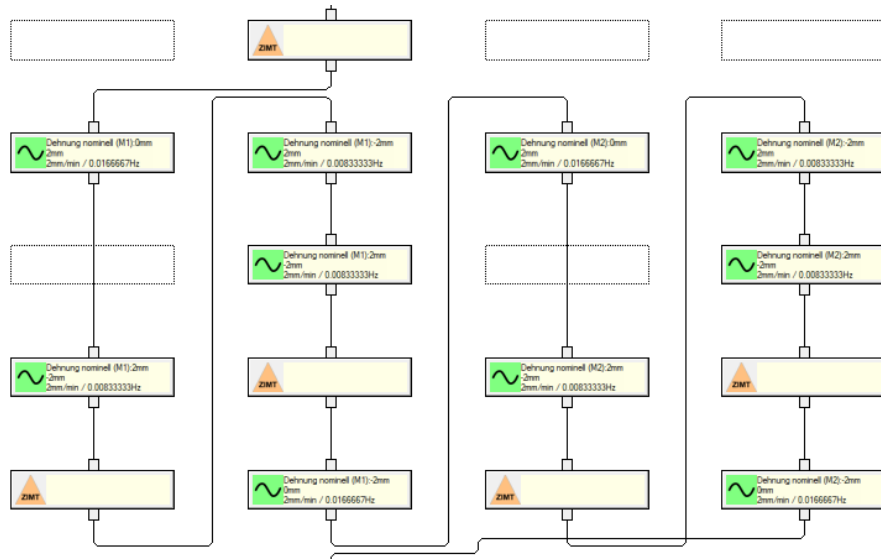


Figure 2.22: Part 3 represents simple shear in x(M1) and y(M2) direction: *preconditioning and main cycles*

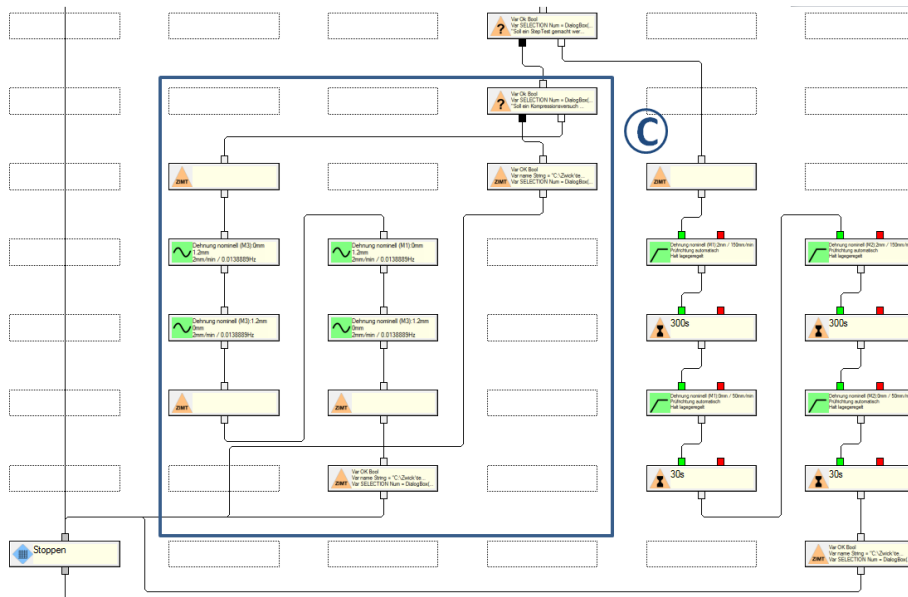


Figure 2.23: Part 4 visualizes step-testing (on the right), performed with 50% strain and the additional compression-testing (block (C))

2.2.4.3.2 Modifications in the testing procedure

- *Modification A* (Fig. 2.21)
 - After fixation of the upper platform into the sliding carriage and mounting of adhesive onto the lower platform, the z -traverse is moved towards the lower platform to adhere the sample onto the lower specimenholder. To prevent adhesive curing before the specimen sticks onto the lower platform and ensure suitable testing conditions, the velocity of z -traverse was changed to 3 mm/min (instead of 1.5 mm/min).
- *Modification B* (Fig. 2.21)
 - This block has been omitted because of the fact that even if no adhesive was applied, the upper blocks (set to ‘kraftgeregelt’) ensured measurement-startup at a tension free state.
- *Modification C* (Fig. 2.23)
 - According to the query whether a step test should be made and confirming with ‘Nein’, it is possible to accomplish a compression test. After confirmation, *preconditioning* within the adjusted number of cycles is made (strain is set to 30% compression).

2.2.4.3.3 Modifications in the data-input interface

In order to perform the compression protocol, the required parameters (strain, number of cycles) were added to the layout wizard (Fig. 2.24 (D)). Various parameters, which can be adjusted via the input mask, also shown in the figure are:

- specimen dimensions: thickness \times width \times length (in mm),
- specified sample-name,
- velocity for both, simple shear and step testing,
- number of cycles (*preconditioning* and *main* cycles),
- and strain for simple shear and compression testing

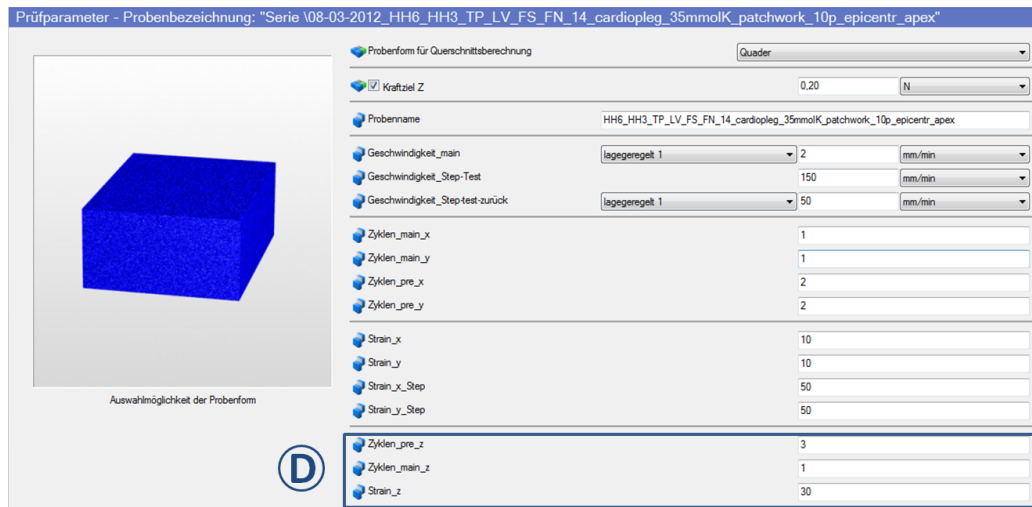


Figure 2.24: Layout-Assistant for various parameter adjustments

2.2.4.4 Testing protocol

After explanation of the preparation and fixation of specimens, and the experimental setup with all its software adjustments, this part of the thesis describes the detailed procedure protocol for shear properties of passive ventricular myocardium.

Triaxial shear testing protocol

For the triaxial shear testing, three adjoining (if possible) cubic specimens ($4 \times 4 \times 4$ mm) were prepared from the left ventricular free wall (Fig. 2.13) or alternatively front wall (depending on the available tissue). Their sides were aligned according to the *mean myofiber direction* (F), the direction *transverse to the fiber axis* (S) within the layer, and the direction *perpendicular* to the layers (N) (Fig. 2.15). Exact specimen dimensions were measured by using a geometrical triangle and transparent foil with mm-scale to avouch appropriate adhesion on specimenholders (thickness measurement using the videoextensometer, has proved to be unsuitable in terms of dehydration due to longer process).

Shear testing was performed under quasi-static loading conditions ($v=1$ mm/min) with different solutions (see chapter 2.2.2) for the respective tissue and heated within the laboratory heating immersion thermostat with heating basin (adjusted to $\sim 44^\circ\text{C}$ to achieve 37°C on specimen, controlled using a column thermometer) for suitable conditions during testing. Three cycles (two for preconditioning and one for further data analysis) of sinusoidal simple shear (0.1–0.5 in 0.1 steps of specimen thickness) were applied to the specimens in two orthogonal directions, first in the x - and then in the y -direction regarding to the experimental setup (Fig. 2.17). Consequently, for the six possible modes of simple shear three different specimens were needed. Resulting forces in three axes (x , y , z) were measured. On completion of shear testing, relaxation tests ('step test') at 0.5 shear strain were performed in the x - and y -direction in order to account for viscoelastic features of the tissue.

Therefore, a rapid displacement to 0.5 shear strain was imposed and the resultant forces were recorded for 300s. At least, due to more specified investigations on human tissue, three unconfined compression cycles (two for preconditioning and one for further data analysis) were applied (instead of relaxation tests, both would roughly harm the tissue) to the samples in z -direction at a maximum strain of 0.3 strain according to the determination of the tissue's compression behaviour.

2.2.4.4.1 Errors reported during testing

Although, the most common errors were already fixed in the program, sometimes they still occur without any evident reasons. An extremely annoying error sometimes occurred after passing the main cycle in x -direction at beginning with preconditioning in y -direction:

- (i) *testXpert.Fehler Nr. 23402*; Regelabweichung in Regler Traverse WN: 191977 ist zu groß

Sometimes this error resulted in an electrical bypass shutting down the whole laboratory equipment, after restarting the test without removing the specimen. This problem could be avoided by allocating the power supplies, for the three controller towers (especially y -controller), to different power outlets.

2.2.5 Data Analysis

The program relating to suitable data analysis of measurement series is realized as a MATLAB® GUI (graphic user interface) and is based on the bachelor thesis by Maier (2011). Therefore required export files are saved as type *.tra*, which specifies an ASCII format that can be read by *Matlab*® equal to an *.dat*-file (Maier, 2011). The additional parameter 'Prüfzeit' which is set to zero between preconditioning and main cycles, is indispensable to allow *Matlab*® identifying the data of interest. The program, which has due to different requirements been extensively modified, enables to handle various export files (one or more) well arranged, without any preprocessing and is presented in the following.

2.2.5.1 Modified MATLAB®-GUI

Figure 2.25 visualizes an overview of the modified GUI, all buttons appear in three variations: dataset in x -direction, dataset in y -direction and both of them, the corresponding program-code for the specified directions differ only hardly. After initializing the path for the obtained export files, it is possible to select one or more (press 'Strg') samples, whereby the MATLAB® -function *textread* picks out the information of interest relating to specimen dimensions, the number of cycles and strains, and adjusted velocities.

2.2.5.1.1 The GUI and its functions

Referring to different requirements relating to different studies on the cardiovascular system, (1) triaxial shear testing on human aortic wall tissue (Maier, 2011) and (2) shear properties of passive porcine and human ventricular myocardium, the following represent the main functions of the realized GUI which are of utmost importance for the current thesis:

- ‘*Steptest*’
 - If button ‘*Steptest*’ is pressed, the program plots the data according to the chosen dataset (x or y -direction).
- ‘*Originals*’
 - If ‘*Originals*’ is confirmed, the program reads the header of the selected files (number of zeros in parameter ‘*Prüfzeit*’) and automatically detects the main cycle, which is plotted with its specified specimen names (important for differentiating between various curves) and written into the legend.
 - Due to the export of the recorded data for the stress-strain relationship, an error which resulted in an incorrect scaling (a factor by times of ten) at the y -axis (shear stress in kPa), was solved.
- ‘*Stress Strain (Offset corr.)*’
 - In contrast to ‘*Originals*’, ‘*Stress Strain (Offset corr.)*’ was realized to compare suitable plots, by fitting them in that way that the resulting curves are shifted into their zero point on the scale (Fig. 2.26).
 - For the implementation of the offset shifting function, the dataset was splitted in two different sets of length ($1/3$ and the remaining $2/3$), because of the fact that due to the obtained curves (starting position is equal to end position), the zero point ($x = 0$) is intersected more than once. Subsequent the minima of the absolute values of the datasets were detected, their locations could be used to identify the ‘real’ points of zero crossing, and further it was possible to shift the curve into the origin position.

In addition to the offset-shifting, the ezyfit-toolbox was integrated to allow many further fitting-algorithms (e.g. noise-reduction).

For a detailed description of the several functions and block diagrams, the reader is referred to Maier (2011).

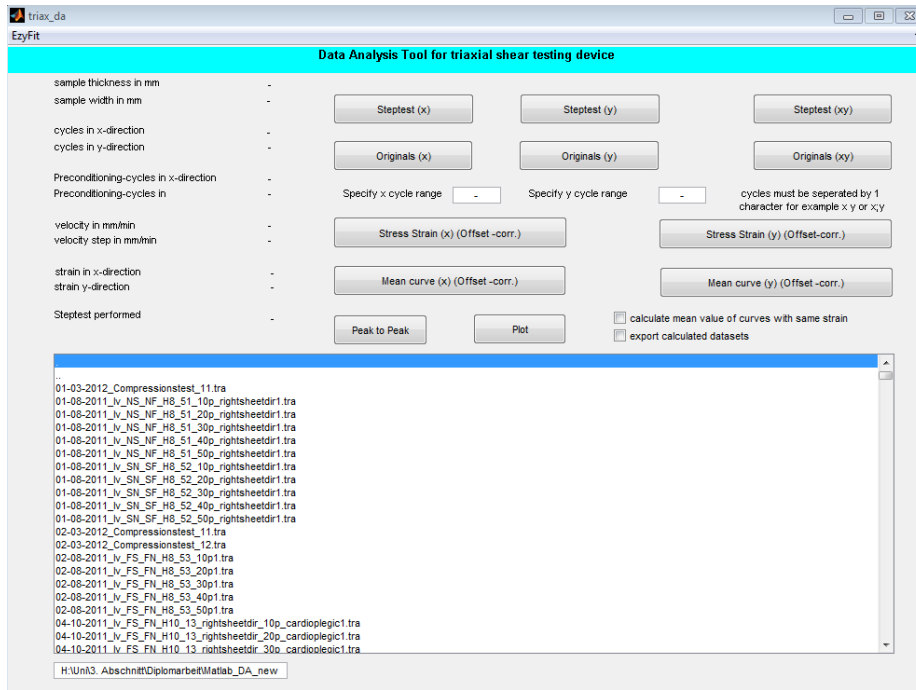


Figure 2.25: Overview of the realized MATLAB® GUI



Figure 2.26: Plot of the original dataset of a typical stress-strain curve of a human myocardium in *FN*-mode at 30% shear displacement (blue) and again with shifted offset (red)

3 Results

In consequence, this thesis emphasized the development of a standardized protocol for the triaxial examination of shear properties of passive porcine and human ventricular myocardium. In addition to the measurement of the stress-strain relationship for all six possible modes of simple shear (NF/NS , SF/SN , FS/FN), unconfined compression testing was applied to human myocardial samples in order to obtain further important mechanical compression data, which are not present in the literature.

A total of 14 porcine hearts and seven human hearts (only pieces of organs due to the high demand on human tissue) with collectively over 150 cubic specimens, were tested. The following sections constitute the valuation of the most relevant mechanical data referring to this thesis.

3.1 Measurement data acquisition of porcine myocardial tissue

As already afore mentioned, porcine tissue was tested with different chemical buffer solutions (PBS, PBS with additional EGTA, CCPS and modified Ringer solution with 15 mmolK⁺/l). In order to achieve representative measurement data for human tissue in a passive state at body milieu (37°C), the appliance of the appropriated solution played a major role.

Table 3.1 represents an overview of the relevant characteristics according to the tested porcine hearts, their corresponding specimens and conditions during measurement (used solution at temperature) for suitable mechanical data acquisition.

After interpretation of measurement data relying to the varied used solutions, the modified Ringer solution with additional potassium (maintains passive testing), was found to achieve the most suitable conditions for testing the mechanical properties of porcine myocardium. Hence, the determination of the shear stress-strain relationship and relaxation testing of the investigation of porcine myocardium, visualized in the following graphs, was conducted according to this ‘blood-like’, physiological-solution.

Table 3.1: Overview of relevant characteristics of suitable tested specimens according to measurement series on porcine tissue;

Notations for locations and positions: *PH...* porcine heart, *LVFW...* left ventricular free wall, *LV-FW...* left ventricular front wall, *end...* endocardial, *mid...* midwall, *epi...* epicardial, *equ...* equator;

Notations due to solutions: *CCPS...* ‘conventional cardioplegic solution’, *Ringer...* modified Ringer solution with 15 mmolK⁺/l

Heart no. (weight [g])	Sample no. (# slice/spec.)	Location (pos.)	Specimen ($t \times w \times l$ [mm])	Solution T [°C]	Autolysis (age [h])	Shear mode (x/y)
PH #10 (360g)	#2/1	LVFW end./equ.	$4.7 \times 4.5 \times 4.5$	CCPS 37°C	2h (6h)	FS/FN
	#2/2	LVFW end./equ.	$4.3 \times 4.5 \times 4.5$	CCPS 36.5°C	2.5h (9h)	SF/SN
PH #11 (370g)	#1/2	LVFW mid./base	$4.8 \times 4.9 \times 4.9$	CCPS 37°C	0.5h (2h)	SF/SN
	#2/2	LV-FW end./base	$3.9 \times 4 \times 3.5$	CCPS 37°C	1h (4.5h)	FS/FN
	#3/3	LV-FW mid./apex	$4 \times 3.5 \times 3.5$	CCPS 36.5°C	1.5h (26h)	NF/NS
	#3/4	LVFW mid./equ.	$3.5 \times 3.8 \times 3.8$	CCPS 37°C	2h (29h)	SF/SN
PH #12 (355g)	#3/1	LVFW mid./equ.	$4.5 \times 4.4 \times 4.9$	Celsior 17°C	0.5h (3h)	SF/SN
	#3/3	LVFW mid./apex	$3 \times 3.8 \times 3.4$	Ringer 36.5°C	1.5h (27h)	FS/FN
	#4/1	LVFW mid./apex	$4 \times 3.7 \times 4.1$	Ringer 37.5°C	2.5h (30h)	FS/FN
	#4/2	LVFW mid./apex	$4.1 \times 4 \times 4.1$	Ringer 37°C	3.5h (34h)	SF/SN
PH #13 (385g)	#1/2	LVFW mid./apex	$3.5 \times 3 \times 3.1$	Ringer 37°C	2h (12h)	NF/NS
	#2/4	LVFW mid./base	$3.8 \times 3.9 \times 3.8$	Ringer 36.8°C	4h (36h)	FS/FN
PH #14 (340g)	#1/2	LVFW epi./base	$2.8 \times 2.9 \times 3.5$	Ringer 37°C	0.5h (2h)	FS/FN
	#1/3	LVFW epi./equ.	$3.4 \times 2.8 \times 2.8$	Ringer 37.2°C	1.5h (5h)	NF/NS

3.1.1 Results for the shear stress-strain relationship of specimens in Ringer solution

Three cycles, two for preconditioning and one for further data analysis (main cycle) of sinusoidal simple shear were carried out (adjusted velocity, $v=1\text{mm/min}$) for the respective tissue in all six modes of simple shear. The following illustrations allegorize the relation between shear stress, assigned on the axis of ordinates (y -axis) in kPa, and shear strain (x -coordinate) in $\frac{\%}{100}$, which is known as shear strain (short: displacement of the top face of specimen relative to the bottom face).

Representative results for all six possible modes of simple shear

Figures 3.1, 3.2 and 3.3 visualize the quasi-static shear properties of the representative shear stress-strain relationship for cubic porcine myocardial samples (same conditions for all samples, which used for analysis) of PH #12 and #13 (dimensions: $\sim 4 \times 4 \times 4\text{mm}$) with axis aligned with the principal material axis (FSN- coordinate system, see chapter 2.2.3.2.1) at the left ventricular free wall. Cycles of preconditioning, not shown in representative figures, clearly indicated higher stress levels in both (positive and negative x and y) directions, than in the subsequent plotted cycle. Hence, cycles at startup of tests are always stiffer than the following (even if the applied shear stress is a minimum), independent of the imposed shear strain.

The representative graphs below, in which shear strain was increased from 0.1 (in steps of 0.1) to 0.5 in relation to specimen thickness, exhibit smallest shear stress magnitudes in *NF/NS*- mode (Fig. 3.1) and reach their maximum in *FS/FN*- mode (Fig. 3.3) for an equal amount of deformation.

Averaging (mean value) of measurement series of porcine myocardium

The results according to all six possible modes of simple shear at 30 % maximum strain from six different porcine hearts are demonstrated in Fig. 3.4 to 3.9. Furthermore, the set of those six varying stress-strain curves were averaged and represented in form of the mean value (black line). At comparison it can be shown that the mean value of each mode is very similar to its representative plot (Fig. 3.1 to 3.10).

3.1.2 Results for relaxation testing concerning to modified Ringer solution

Subsequent, after performing sinusoidal simple shear, a relaxation test ('step test'), also in the x - and y -direction, was executed in order to take account the viscoelastic features of the tissue. Concerning this matter, a rapid displacement to 0.5 shear strain was imposed and the resultant forces were recorded for 300s for all six modes. Figures 3.11, 3.12 and 3.13 representate the abrupt arise to a maximum ($v = 150\text{mm/min}$) and after reaching the 'holding' position, curves decrease ($v = 50\text{mm/min}$), until the specimen returns in its initial position (elapsed time-duration: 300s).

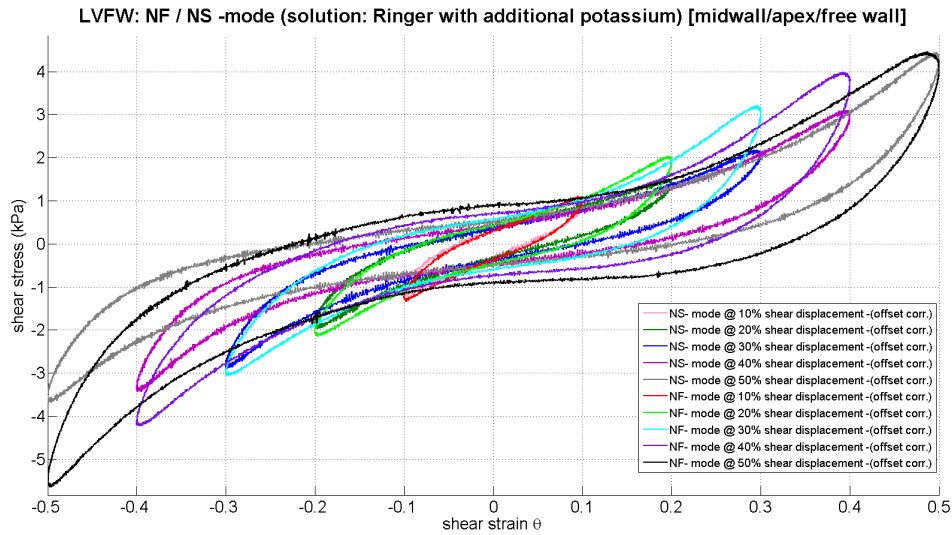


Figure 3.1: Ratio between shear stress and shear strain (main cycles, offset corrected) in *NF* and *NS* mode increasing from 10% to 50%.

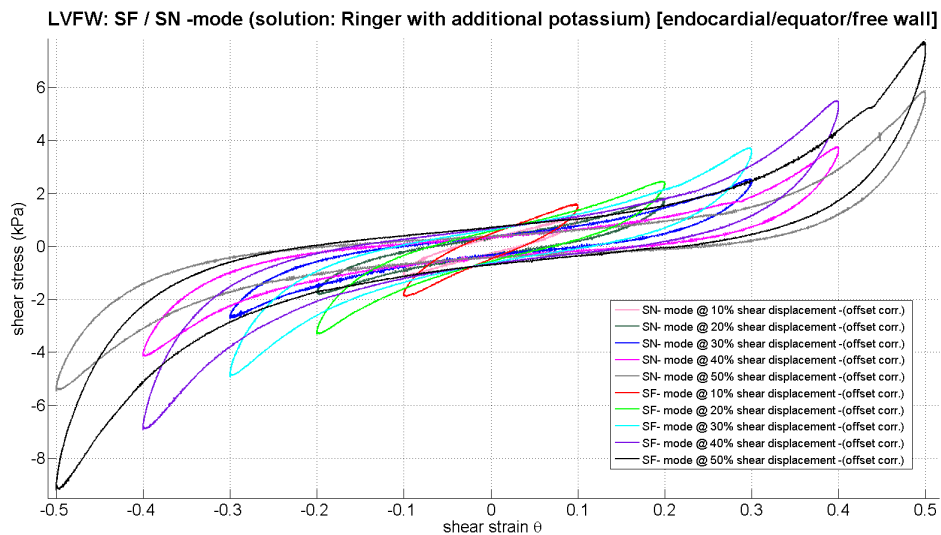


Figure 3.2: Shear stress-strain relationship (offset corrected) in *SF* and *SN* mode increasing from 10% to 50% shear strain.

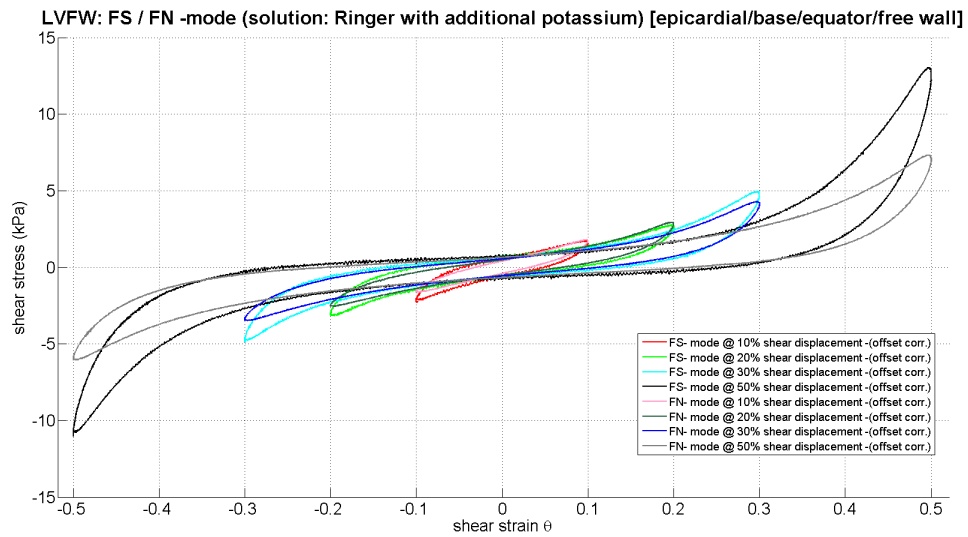


Figure 3.3: Main cycles (offset corrected) of the ratio of shear stress to shear strain in *FS* and *FN* mode increasing from 10% to 50%.

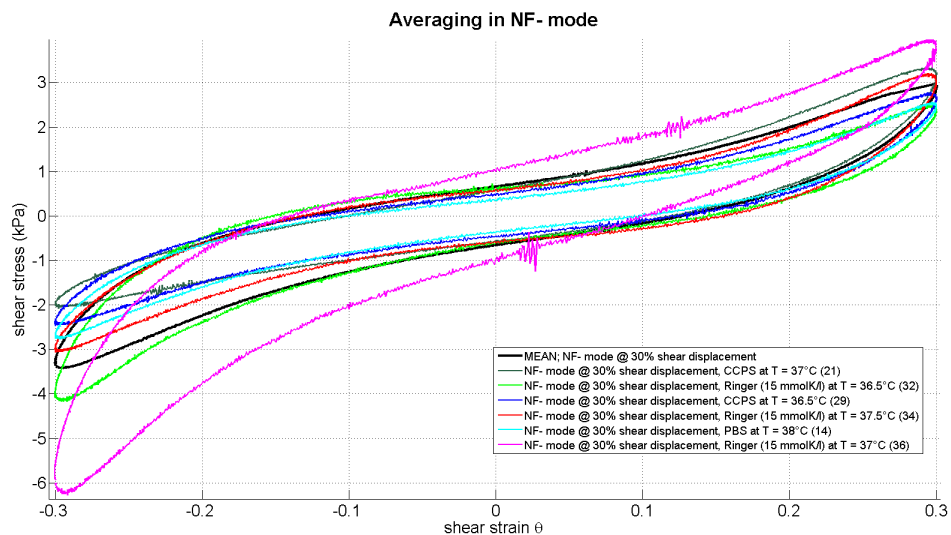


Figure 3.4: Averaging (mean value) of a set of six different porcine hearts at a maximum shear strain of 30 % in *NF*-mode (black bordered curve).

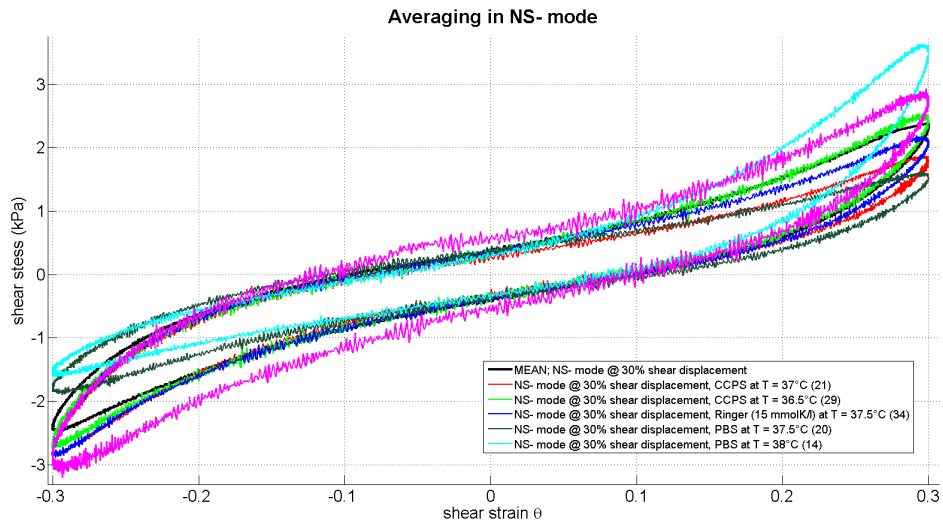


Figure 3.5: Averaging (mean value) of a set of six different porcine hearts at a maximum shear strain of 30 % in NS-mode (black bordered curve).

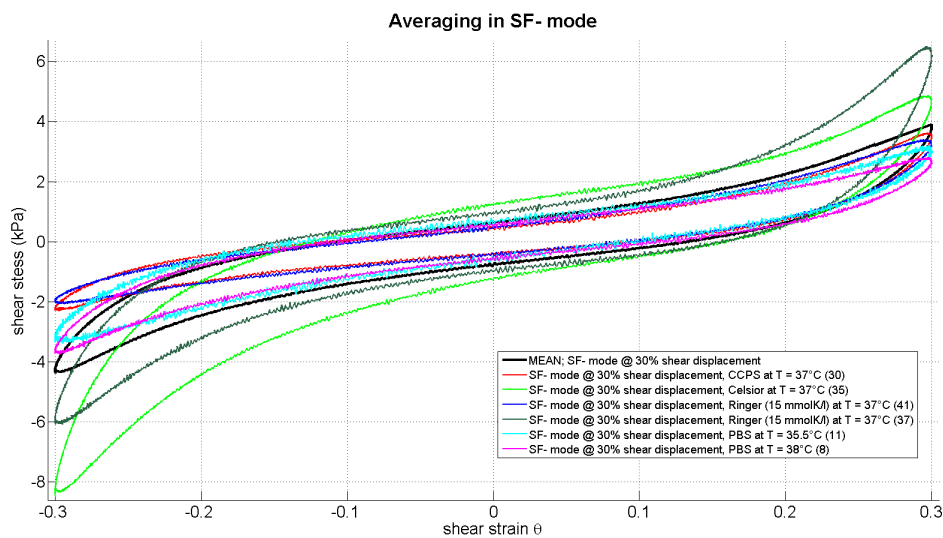


Figure 3.6: Averaging (mean value) of a set of six different porcine hearts at a maximum shear strain of 30 % in SF-mode (black bordered curve).

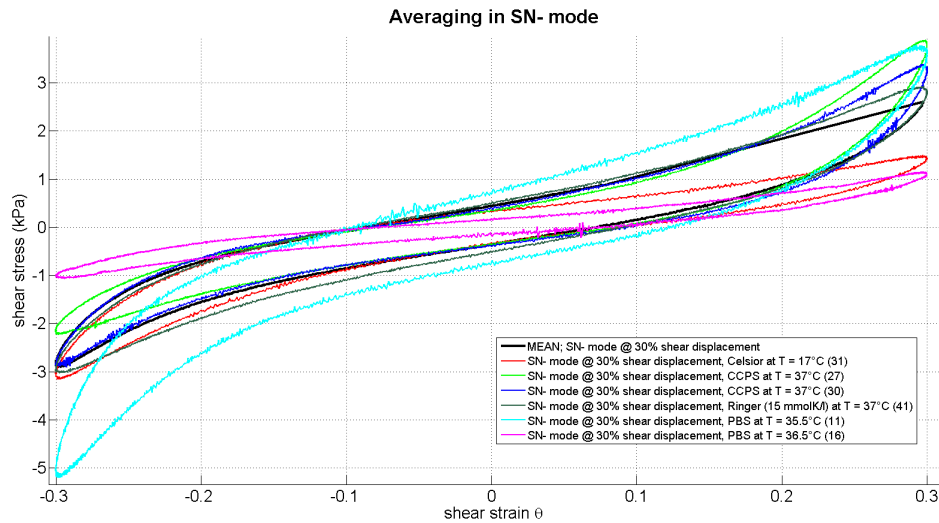


Figure 3.7: Averaging (mean value) of a set of six different porcine hearts at a maximum shear strain of 30 % in SN-mode (black bordered curve).

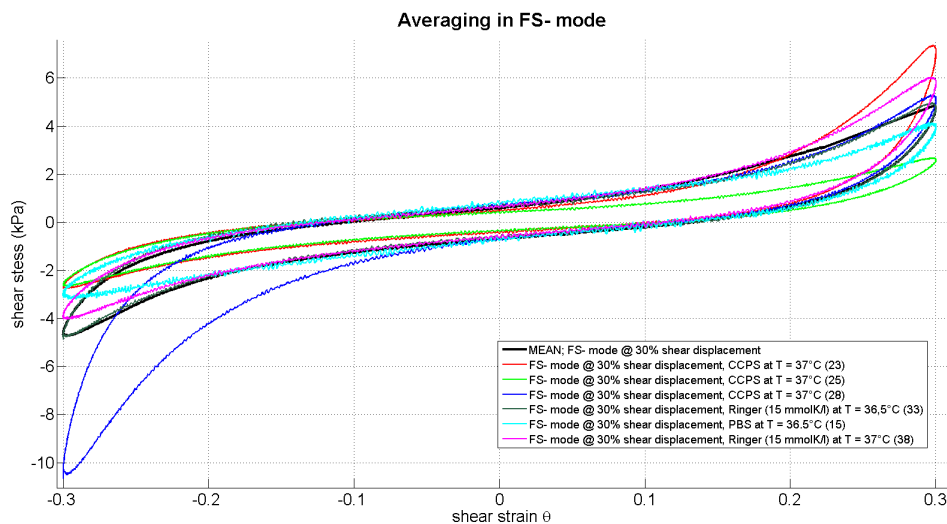


Figure 3.8: Averaging (mean value) of a set of six different porcine hearts at a maximum shear strain of 30 % in FS-mode (black bordered curve).

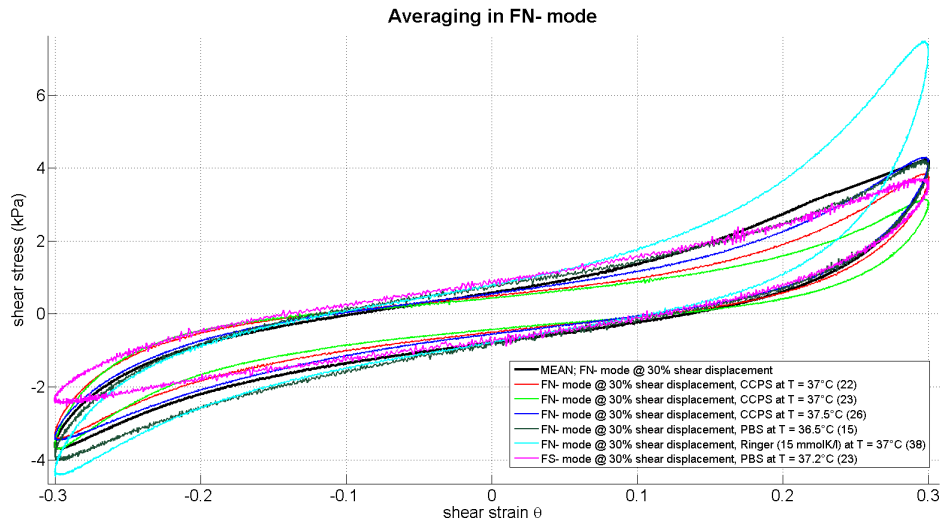


Figure 3.9: Averaging (mean value) of a set of six different porcine hearts at a maximum shear strain of 30 % in *FN*-mode (black bordered curve).

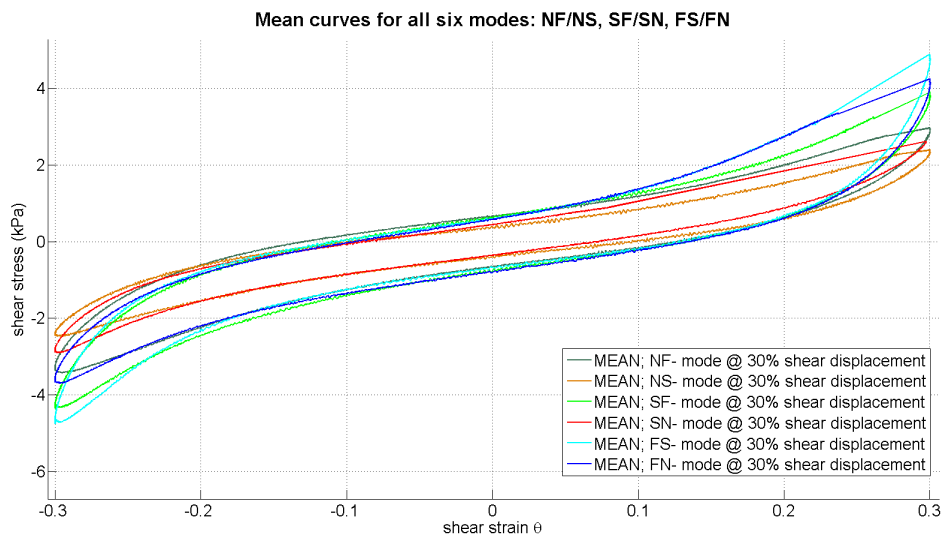


Figure 3.10: Mean curves for a set of six different porcine hearts at a maximum shear strain of 30 % in all modes of simple shear.

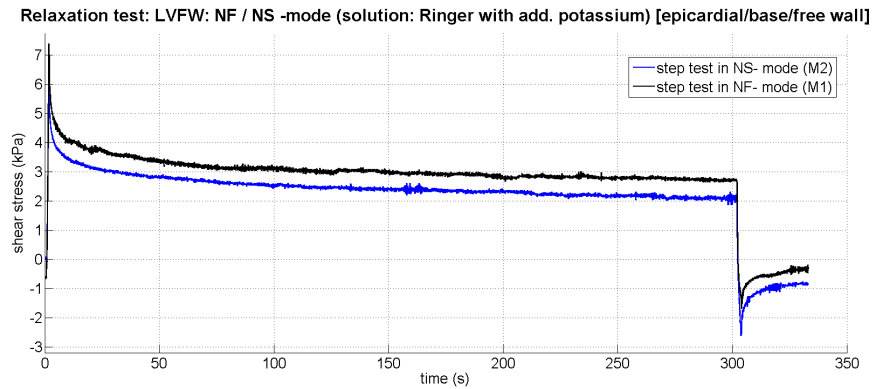


Figure 3.11: Relaxation test (porcine tissue) after a rapid displacement of 0.5 shear strain for 300 s in *NF*-direction (black curve) and *NS*-direction (blue curve).

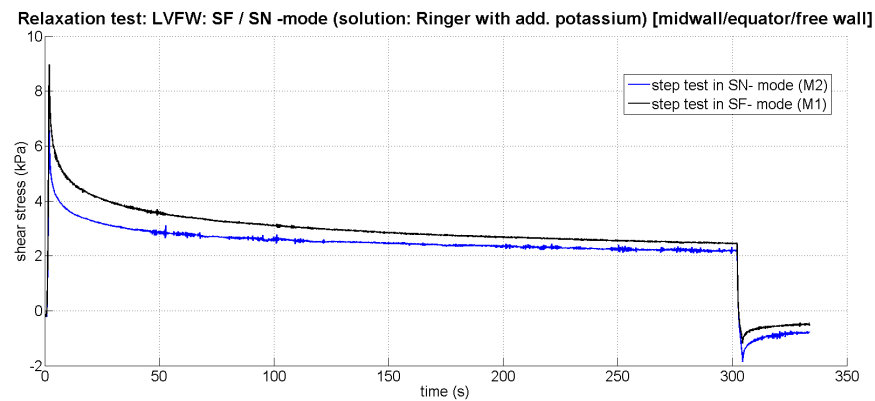


Figure 3.12: Relaxation test (porcine tissue) after a rapid displacement of 0.5 shear strain for 300 s in *SF*-direction (black curve) and *SN*-direction (blue curve).

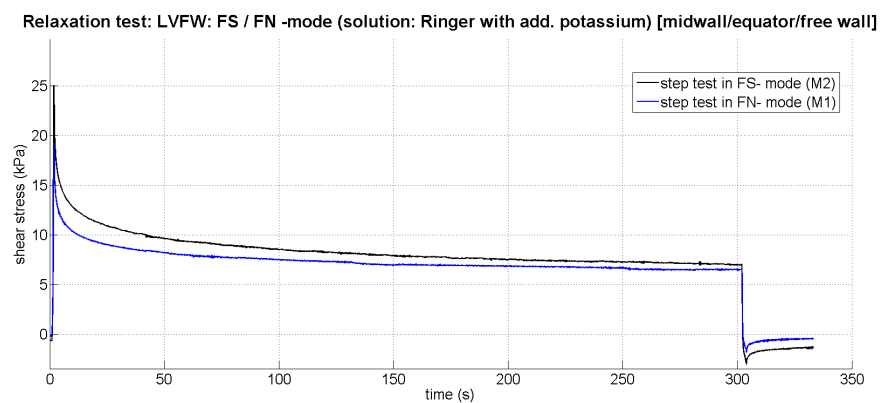


Figure 3.13: Relaxation test (porcine tissue) after a rapid displacement of 0.5 shear strain for 300 s in *FS*-direction (black curve) and *FN*-direction (blue curve).

3.2 Mechanical data acquisition of human myocardial tissue

Referring to the study of the stress-strain relationship of porcine tissue, human samples were tested within modified Ringer solution or CCPS with additional potassium (see Discussion 4). Because significant differences in relation to the respective tissue (different species) were already seen during preparation, very different results for human samples can be expected.

Table 3.2 represents an overview of relevant informations of the received myocardial samples of human heart tissue (*Notations TU MYO treats on specimens received from the Institute of Pathology, TP regards to samples originated from the Clinical Department of Transplant Surgery*).

All in all, seven human myocardial specimens (lv: free wall, front wall or rear wall) could have been received, four tissue samples originated from Transplant Surgery and three regard to the Institute of Pathology. Therefore, resulting cubic specimens with respect to their properties for preparation (position, solution) and measurement are compared in Tab. 3.3.

3.2.1 Tissue received from the Institute of Pathology

The main difference in received samples lies on fluctuations in the duration of autolysis: While samples received from the Department of Pathology already exhibit cell damage (due to autolysis duration >20h), specimens referring to Transplant Surgery were still in a passive state due to immediate inactivation of the tissue (inherently *in vivo* perfusion). This circumstance may assume very different results of the human tissue between those two departments. Other factors which may influence the results (age of patient, gender, primary disease, heart pathology, cause of death, body/heart-weight) are allocated in 4.2.3.

3.2.1.1 Results for the shear stress-strain relationship according to human samples from the Institute of Pathology

In contrast to porcine heart tissue, which are bred over a short period (approximately six months) before they get slaughtered, human tissue, must inherently show different mechanical properties (reflected especially in minimized magnitudes). The associated tissue softening of human myocardial tissue impeded exact cubic specimen preparation, thus preparation techniques had to be improved consistently. Furthermore, consistent specimen orientation, axis aligned corresponding to the FSN-coordinate system, was not guaranteed for all samples due to the much more inhomogeneities and fat deposits in human heart tissue.

Table 3.2: Overview of relevant informations due to all received myocardial samples of human heart tissue; Origins: Departments of Pathology and Transplant Surgery;
 Notations: *HH...human heart, Ref. No...reference number, LVFW...left ventricular free wall, IVW...interventricular wall (septum)*

Notations due to solutions: *CCPS... 'conventional cardioplegic solution'*

Heart no. (HH #)	Characteristics of received human heart samples										Patient information		
	Ref. No. (Dep. #)	Weight [g]	Wall-thick. (LVFW/IVW)	Heart pathology	Autolysis duration	Sum of tests	Storage for prep.	Age/ Gender	Weight/ Size	Cause of death			
HH #01	TU TP01	490	19mm/21mm	hypertrophy twice as big hypertens.	2h	4	Celsius at 4°C	74a male	115kg 1.6m	died during surgery			
HH #02	TU MYO 01/12	290	13mm/14mm	coronary sclerosis	28h	4	CCPS at 4°C	77a female	55kg 1.6m	inner layer infarct			
HH #03	TU MYO 02/12	400	16mm/18mm	hypertrophy dilated	19h	3	CCPS at 4°C	32a female	65kg 1.7m	un- known			
HH #04	TU MYO 03/12	220	18mm/19mm	coronary sclerosis hypertrophy	12.5h	4	CCPS at 4°C	93a female	55kg 1.6m	inner layer infarct			
HH #05	TU TP02	450	13mm/15mm	diast. dysfunct. I fibrin dep.	3h	3	Celsius at 4°C	41a male	unknown	fell due to alcohol			
HH #06	TU TP03	256	7mm/8mm	non failing (small)	frozen	4	Celsius at 4°C	30a female	unknown	fell from ladder			
HH #07	TU TP04	351	7mm/8mm	EF 60% non failing	4h	3	Celsius at 4°C	69a female	unknown	fell after alcohol			

A typical received myocardial piece at the LVFW from the Department of Pathology is illustrated in Fig. 3.14 (A), the red outlined area in (B) retributes flinty calcium deposits at the base, (C) visualizes a prepared slice for further cubic preparation (D).

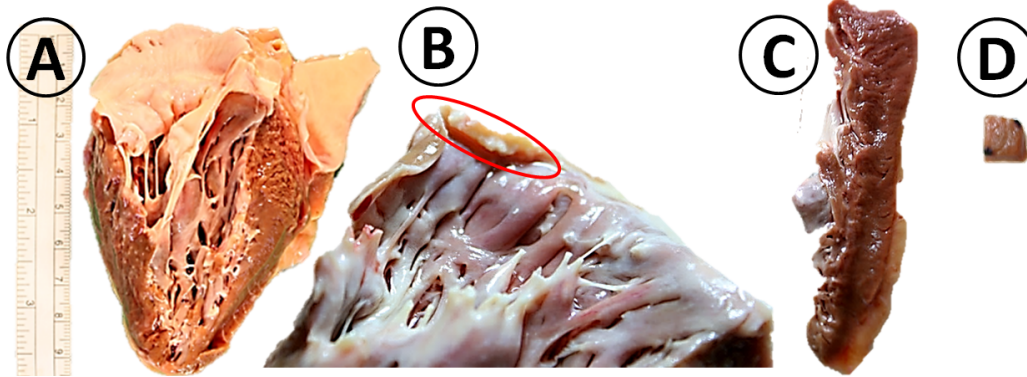


Figure 3.14: (A) Myocardial piece (Clinical Department of Pathology) at the LVFW. Red outlined area in (B) retributes flinty calcium deposits at the base, (C) visualizes a prepared slice and (D) indicates a labeled cubic specimen for shear testing.

The protocol for the investigation of the shear stress-strain relationship of human tissue remained unchanged ($v=1\text{mm/min}$), admittedly the velocity for the z -traverse at adhering the specimen to the lower platform was modified (increased) to 3mm/min to ensure proper specimen fixation. In addition, to ensure inactivation of cardiomyocytes, the content of potassium was increased in CCPS (one ampoule $20\text{mmolK}^+/\text{l}$) to get $36\text{mmolK}^+/\text{l}$ in total.

Representative results for all six possible modes of simple shear

Figures 3.15, 3.16 and 3.17 show the representative results (shear strain) of the triaxial shear test primarily of HH #03 (see Tab. 3.2), received from the Department of Pathology. Unfortunately, shear testing in SF/SN - mode was not applied up to 50% (10%-40% available) shear strain due to an internal error in the controller of the traverse in y -direction.

Averaging (mean value) of measurement series of human myocardium

The results for all six possible modes of simple shear at 30 % maximum strain are illustrated in the form of the mean value in Fig. 3.18, 3.19 and 3.20. Directions in SF/SN and FS/FN mode were only averaged for two of three samples due to the fact that the remaining did not show representative results.

3.2.1.2 Results for relaxation testing

Relaxation tests were only performed for two different specimens from HH #02 and #04, corresponding results are illustrated in Fig. 3.21 and 3.22

Table 3.3: Overview of relevant characteristics of tested specimens according to measurement series on human tissue (dissection location, specimen dimensions, solution for measurement at particular temperature) at $v=1$ mm/min. Autolysis-duration can be seen as the timespan, starting at excision of sample and ends until the sample was inlaid into CCPS. Age, in contrast, appreciates the period of time starting also at excision of sample and ends at specimen fixation (adhering onto the specimenholder).

Notations for locations and positions: *HH...human heart, LVFW...left ventricular free wall, LV-FW...left ventricular front wall, LV-RW...left ventricular rear wall, end...endocardial, mid...midwall, epi...epicardial, equ...equator*;
 Notations due to solutions: *CCPS... 'conventional cardioplegic solution' with 35mmolK⁺/l, Ringer... modified Ringer solution with 15 mmolK⁺/l*

Heart no.	Sample no. (# slice/spec.)	Location (pos.)	Specimen dim. ($w \times l \times t$ [mm])	Solution T [°C]	Autolysis (age [h])	Shear mode (x/y)
HH #01 (TP)	#01 (1/1)	LVFW end./equ.	$4.7 \times 4.7 \times 3$	Ringer 37.3°C	2h (11h)	FS/FN
	#02 (1/2)	LVFW epi./equ.	$5.2 \times 4 \times 4.2$	Ringer 37°C	2.5h (15h)	SN/SF
	#03 (2/1)	LVFW epi./base	$3.4 \times 3.3 \times 3$	Ringer 37.1°C	2.5h (18h)	NF/NS
	#04 (2/2)	LVFW epi./equ.	$4 \times 3.2 \times 3.2$	Ringer 37°C	3h (21h)	FS/FN
HH #02 (Patho)	#05 (1/1)	LV-FW epi./equ.	$6 \times 5.5 \times 4.1$	CCPS 37.4°C	28h (29h)	NS/NF
	#06 (1/2)	LV-FW epi./equ.	$5 \times 5 \times 4.5$	CCPS 37°C	28.5h (34.5h)	FS/FN
	#07 (2/1)	LV-FW mid./apex	$5.2 \times 5.2 \times 3.6$	CCPS 37°C	29h (39.5h)	SF/SN
	#08 (3/1)	LV-FW epi./equ.	$5.9 \times 5.9 \times 4.5$	CCPS 37.1°C	30h (43h)	FS/FN
HH #03 (Patho)	#09 (1/1)	LVFW epi./base	$4.5 \times 4.5 \times 4.15$	CCPS 37°C	20h (36.5h)	FS/FN
	#10 (2/1)	LVFW mid./base	$4.8 \times 4.8 \times 4.5$	CCPS 37.1°C	21h (41h)	NS/NF
	#11 (2/2)	LVFW mid./base	$4 \times 4 \times 4.1$	CCPS 37.1°C	22h (44.5h)	SF/SN

Table 3.3: Overview of relevant characteristics of tested specimens according to measurement series on human tissue.

Heart no.	Sample no. (# slice/spec.)	Location (pos.)	Specimen dim. ($w \times l \times t$ [mm])	Solution T [°C]	Autolysis (age [h])	Shear mode (x/y)
HH #04 (Patho)	#12 (1/2)	LFW epi./base	$4 \times 4 \times 4.85$	CCPS 37.5°C	14h (18h)	FS/FN
	#13 (1/3)	LFW epi./equ.	$4.9 \times 4.9 \times 4.95$	CCPS 37.4°C	15h (20h)	SF/SN
	#14 (1/4)	LFW epi./equ.	$4.95 \times 4.95 \times 4.95$	CCPS 37.3°C	16h (23h)	NF/NS
	#15 (1/1)	IVW epi./equ.	$4 \times 4 \times 3.4$	CCPS 36.5°C	13.5h (28h)	FS/FN
HH #05 (TP)	#16 (1/2)	LV-FW epi./equ.	$3 \times 3 \times 3$	CCPS 37°C	1h (10h)	FS/FN
	#17 (1/3)	LV-FW epi./equ.	$4 \times 4 \times 4.4$	CCPS 37°C	2h (14h)	NF/NS
	#18 (2/1)	LV-FW epi./apex	$3 \times 3 \times 3$	CCPS 37°C	2.5h (21h)	SF/SN
HH #06 (TP)	#19 (1/1)	LFW epi./base	$3.5 \times 3.5 \times 3$	CCPS 17°C	frozen (24h)	NF/NS
	#20 (1/2)	LFW epi./equ.	$4 \times 4 \times 4.4$	CCPS 19°C	frozen (27h)	FS/FN
	#21 (1/3)	LFW mid./equ.	$3.8 \times 3.8 \times 4$	CCPS 20°C	frozen (30h)	SF/SN
	#22 (1/4)	LFW mid./apex	$4 \times 4 \times 4$	CCPS 20°C	frozen (33h)	FN/FS
HH #07 (TP)	#23 (1/1)	LVRW mid./apex	$3.8 \times 3.8 \times 3.1$	CCPS 17°C	1h (4.5h)	NF/NS
	#24 (1/2)	LVRW mid./apex	$3.5 \times 3.5 \times 2.95$	CCPS 19°C	2h (7.5h)	SF/SN
	#25 (1/3)	LVRW epi./apex	$3.8 \times 3.8 \times 3.1$	CCPS 15°C	2.5h (10h)	FS/FN

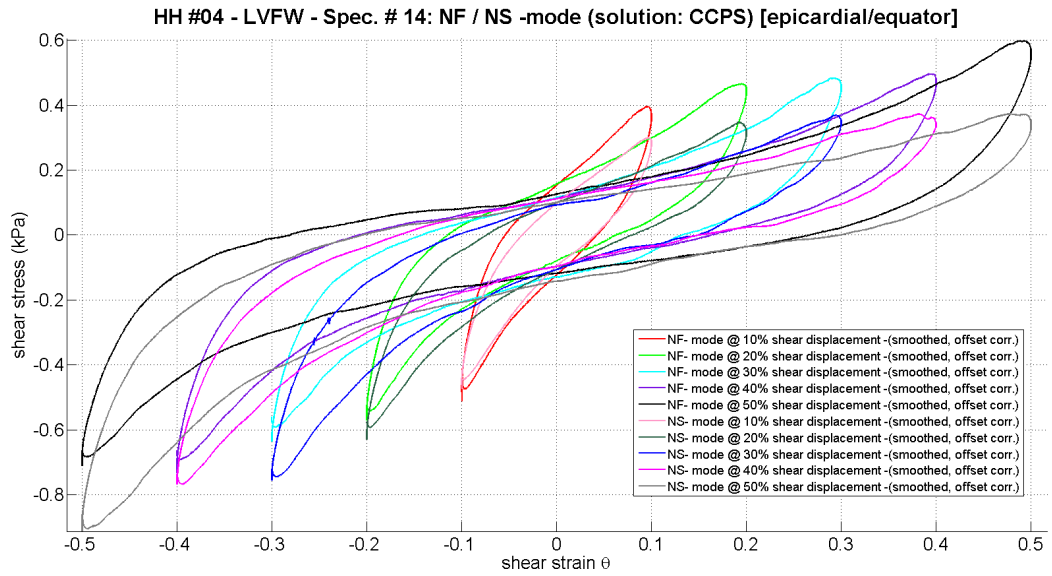


Figure 3.15: Shear stress-strain relationship (offset corrected and smoothed) in *NF* and *NS* mode increasing from 10% to 50% shear strain.

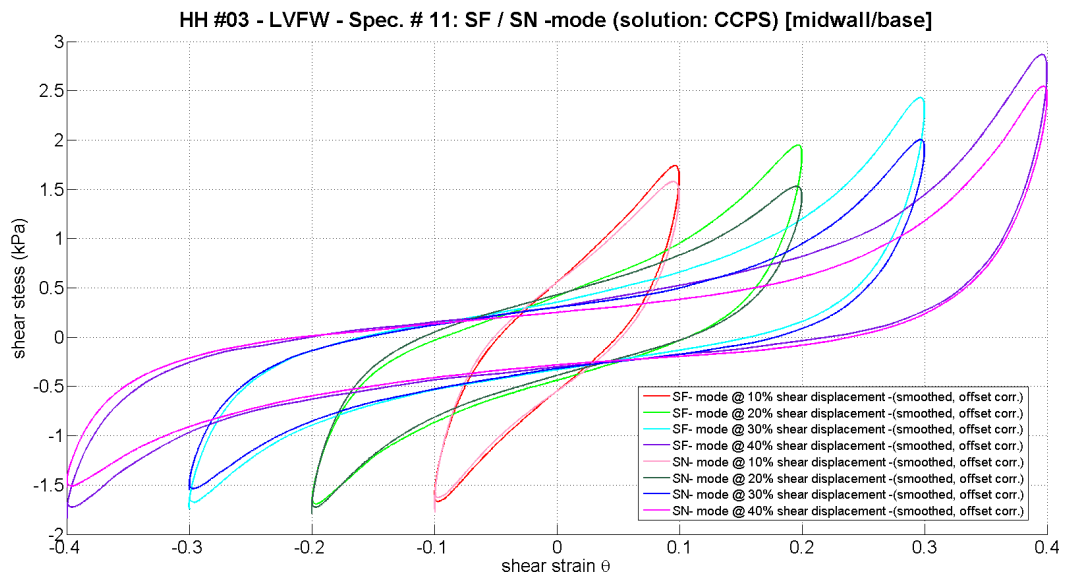


Figure 3.16: Shear stress-strain relationship (offset corrected and smoothed) in *SF* and *SN* mode increasing from 10% to 40% shear strain.

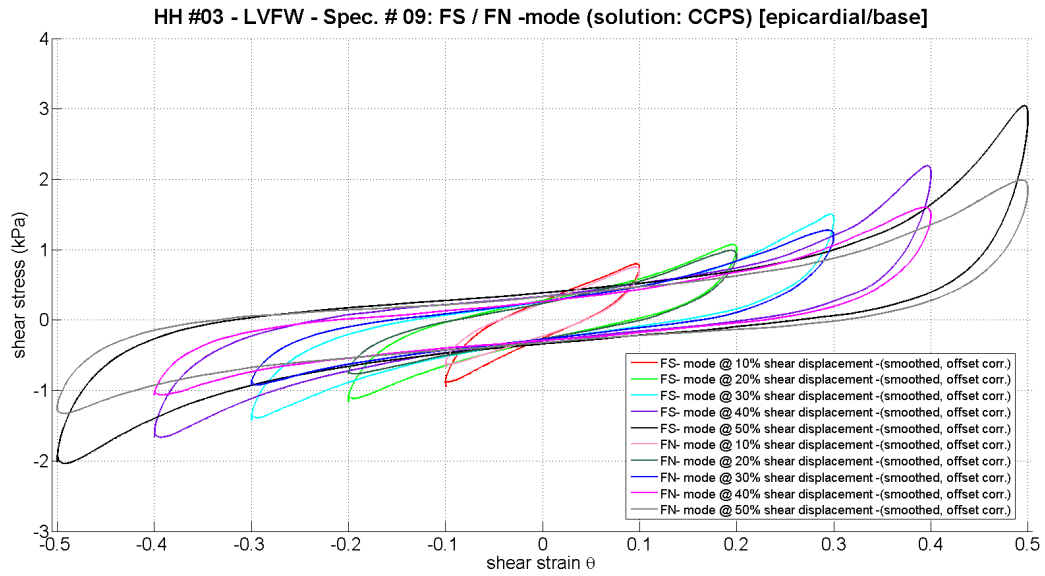


Figure 3.17: Shear stress-strain relationship (offset corrected and smoothed) in FS and FN mode increasing from 10% to 50% shear strain.

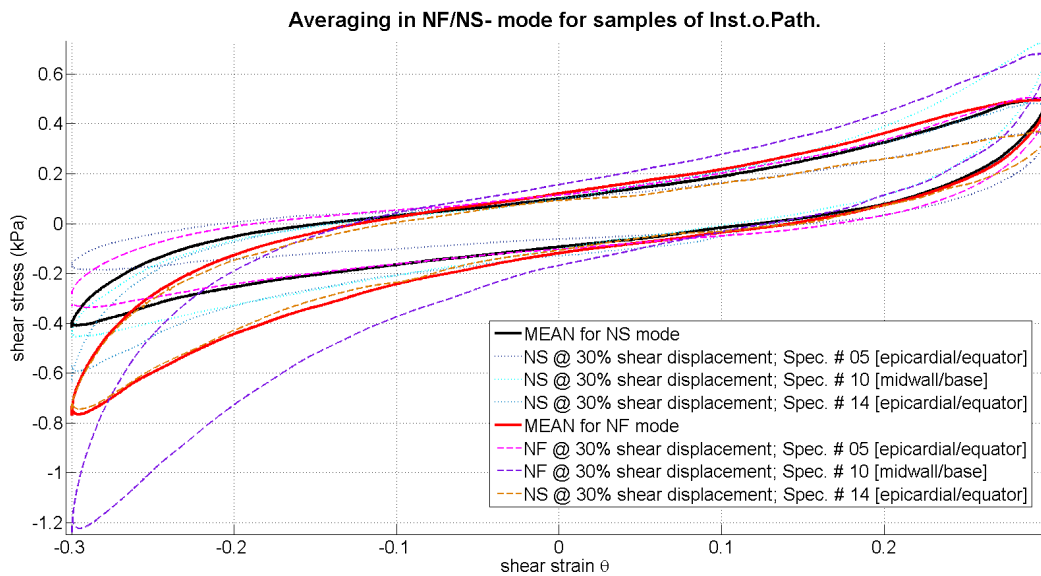


Figure 3.18: Averaging (mean value) of a set of three different human cubic specimens at a maximum shear strain of 30% in NF-mode (red bordered curve) and NS-mode (black bordered curve).

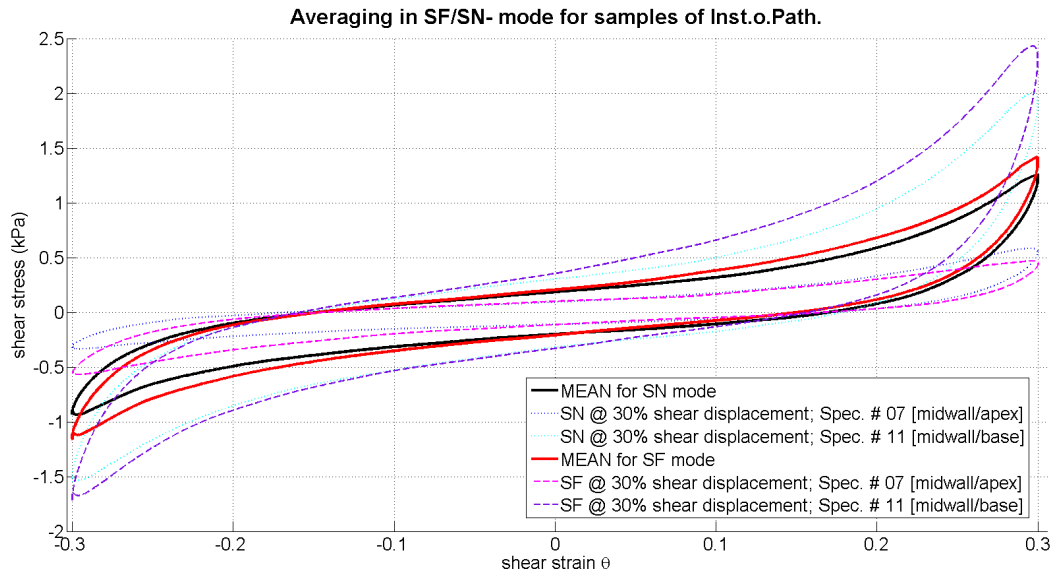


Figure 3.19: Averaging (mean value) of a set of two different human cubic specimens at a maximum shear strain of 30 % in *SF*-mode (red bordered curve) and *SN*-mode (black bordered curve).

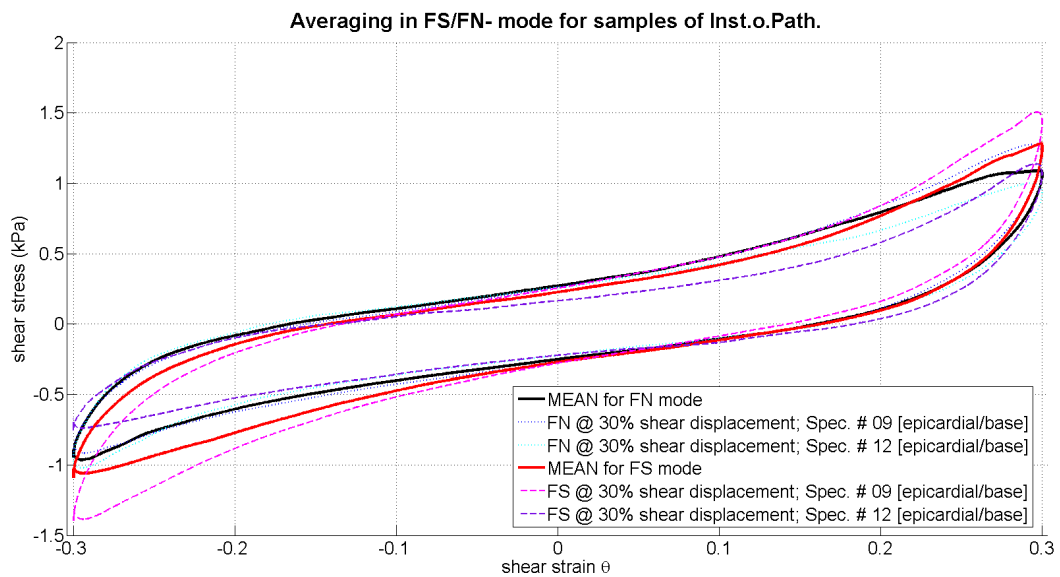


Figure 3.20: Averaging (mean value) of a set of two different human cubic specimens at a maximum shear strain of 30 % in *FS*-mode (red bordered curve) and *FN*-mode (black bordered curve).

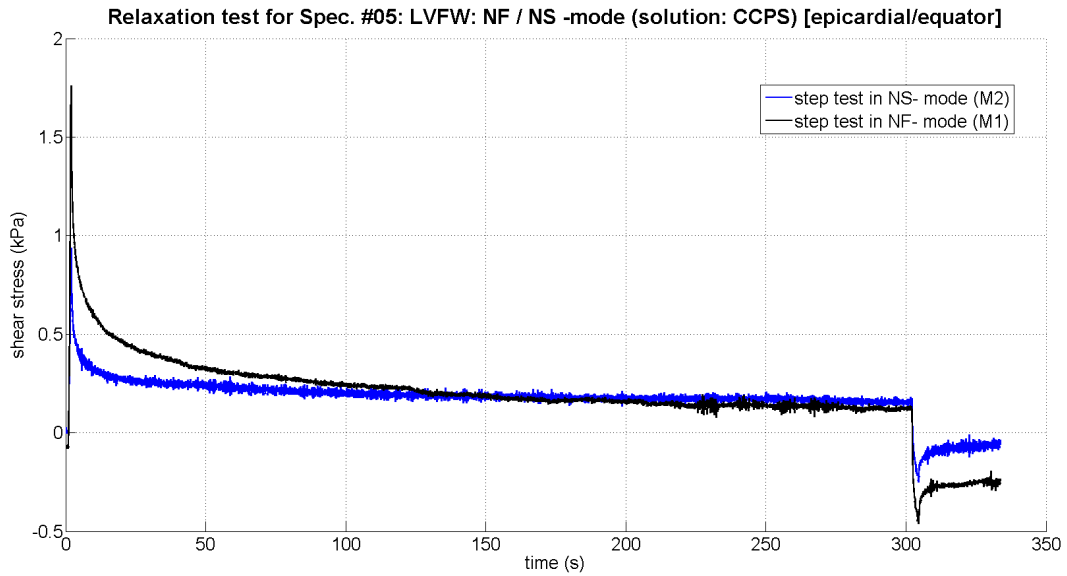


Figure 3.21: Relaxation test (human tissue) after a rapid displacement to 0.5 shear strain for 300 s in *NF*-direction (black curve) and *NS*-direction (blue curve).

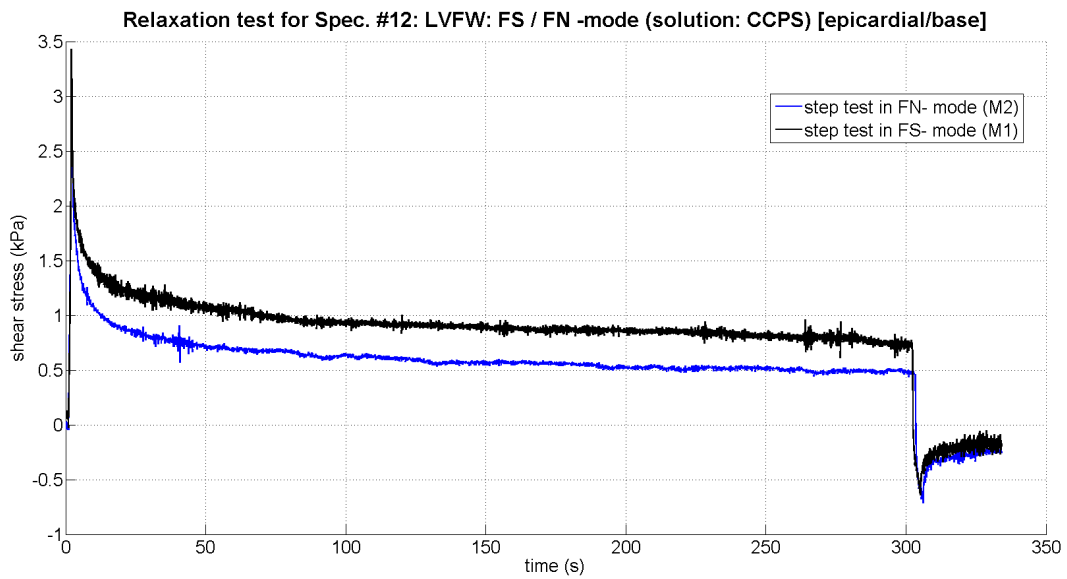


Figure 3.22: Relaxation test (human tissue) after a rapid displacement to 0.5 shear strain for 300 s in *FS*-direction (black curve) and *FN*-direction (blue curve).

3.2.2 Tissue received from the Department of Transplant Surgery

Immediate inactivation of cardiac myocytes (inhibit cell damage), respectively conveying the myocardium into a state of ‘standby’ (activation within a period of twelve hours possible), must inevitably lead to different results. The progress of a received left ventricular myocardial piece (HH #01 (A): strong hypertrophied, very adipose) from the Clinical Department of Transplant Surgery up to prepared sample (D) is shown in Fig. 3.23. A second received piece, which shows fibrin deposits (harmless) at the pericardial face (white outlined area), is visualized in Fig. 3.23 (E).

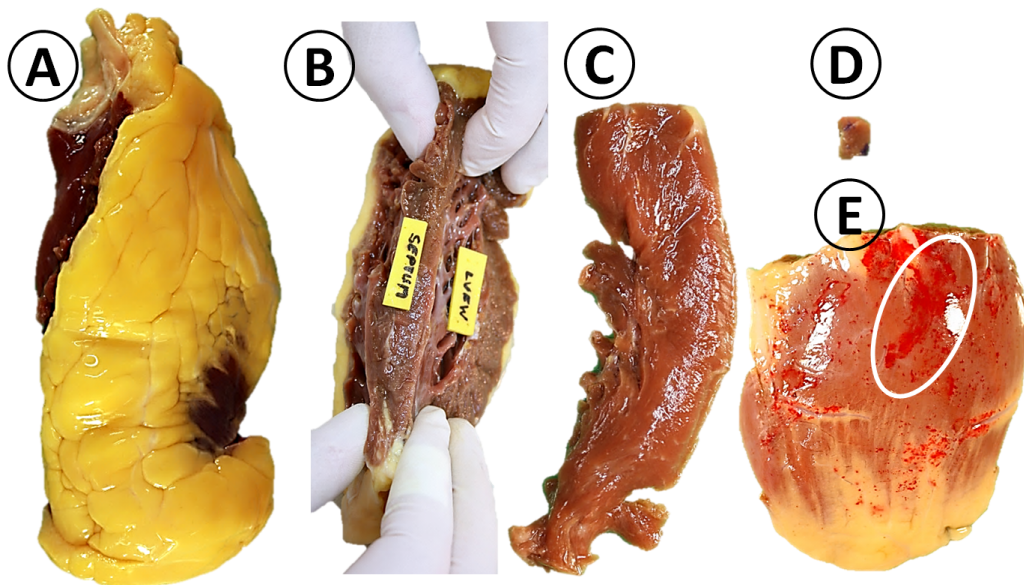


Figure 3.23: (A) Received myocardial piece (Clinical Department of Transplant Surgery) from the left ventricular front wall (very adipose) with its labeled walls (B), (C) visualizes a prepared slice, (D) indicates a labeled cubic specimen for shear testing (fat deposits at myocardial sheets) and (E) shows a different received specimen with fibrin deposits (white outlined area) on its surface.

3.2.2.1 Results for the stress-strain relationship according to human samples from the Clinical Dep. of Transplant Surgery

The measuring process remained unchanged, i.e. the same approach as described in chapter 3.2.1.1, was applied. Indeed, specimen preparation was even more difficult due to the small received myocardial tissue, referring to the high demand. As a consequence, only one slice of each myocardial piece could be prepared, at which the tissue often was very inhomogeneous (see Fig. 3.23 (C)).

Further, during triaxial shear testing of different specimens referring to the Dep. of Transplant Surgery, phenomena like ‘activation’ occurred (see Discussion 4.2.1), so there was a need for action, more specifically reconsidering the matter to ensure inactivation (e.g. choice of cardioplegic solution and temperature adjustment to a lower level). Hence, data for the relating specimens differ significantly from each other, which makes an allegation of the mean value not instructive.

Representative results for all six possible modes of simple shear due to CCPS at 37°C

But, however Fig. 3.24, 3.25 and 3.26 show the results of the stress-strain relationship for HH #05, tested within CCPS at 37°C (tissue seems to be activated, which will be discussed in 4.2.1.1).

Representative results for all six possible modes of simple shear due to CCPS at 15°-19°C

Counteracting the activation of the tissue, the second approach of cardioplegia, *hypothermia* (see chap. 2.2.2.2) had to be implemented. Due to the absence of suitable cooling utilities, testing could be performed at temperatures between 15° and 19°C (difference of 18°-22°C relating to body temperature). Figures 3.27, 3.28 and 3.29 illustrate the approach of cardioplegia at lower temperatures (‘strain softening’, see discussion 4.2.1) for HH #07 at the left ventricular rear wall.

All four human hearts were tested under different conditions, the remaining two, which are not listed here (would exceed the scope), were tested within Ringer solution (35mmolK⁺/l) at 37°C (HH #01), and CCPS at 17°-20°C (HH #06, frozen) and are part of discussion (see chapter 4.2.1.1).

3.2.2.2 Results for relaxation testing

‘Step tests’ (relaxation tests) were only performed for two different specimens (performing both, relaxation and compression tests would roughly harm the tissue) relating to HH #01 and #05, for the investigation of additional viscoelastic features of human myocardial samples, illustrated in Fig. 3.30 and 3.31.

3.2.2.3 Determination of (unconfined) compression properties

According to more specified investigations on human tissue, three unconfined compression cycles (two for preconditioning and one for further data analysis) were applied to samples in *z*-direction at a maximum strain of 0.3 strain according to the determination of the tissue’s compression behaviour (results will be discussed in chapter 4.2.2).

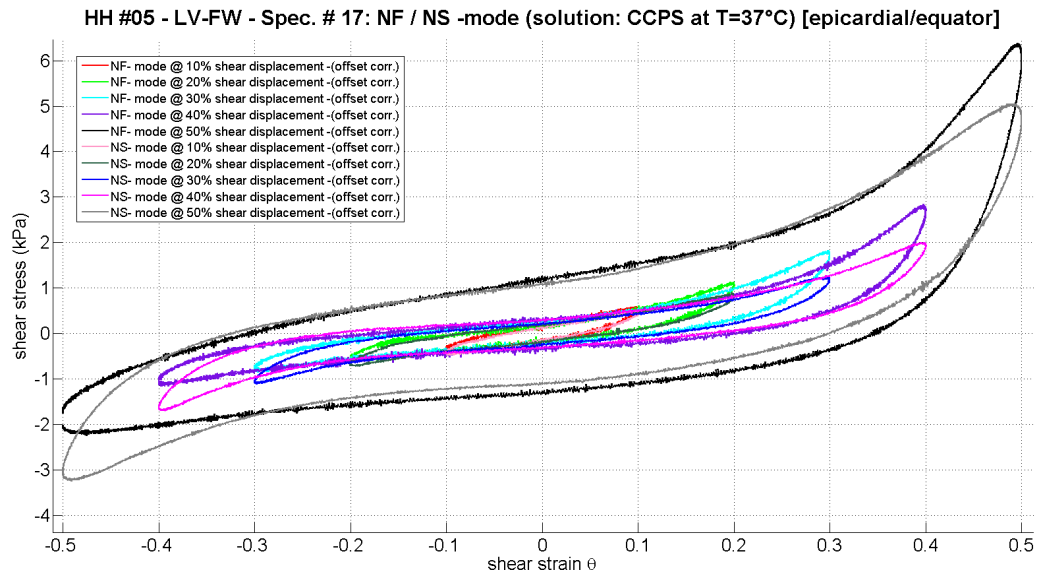


Figure 3.24: Shear stress-strain relationship (offset corrected) in *NF* and *NS* mode for Spec.#17 increasing from 10% to 50% shear strain.

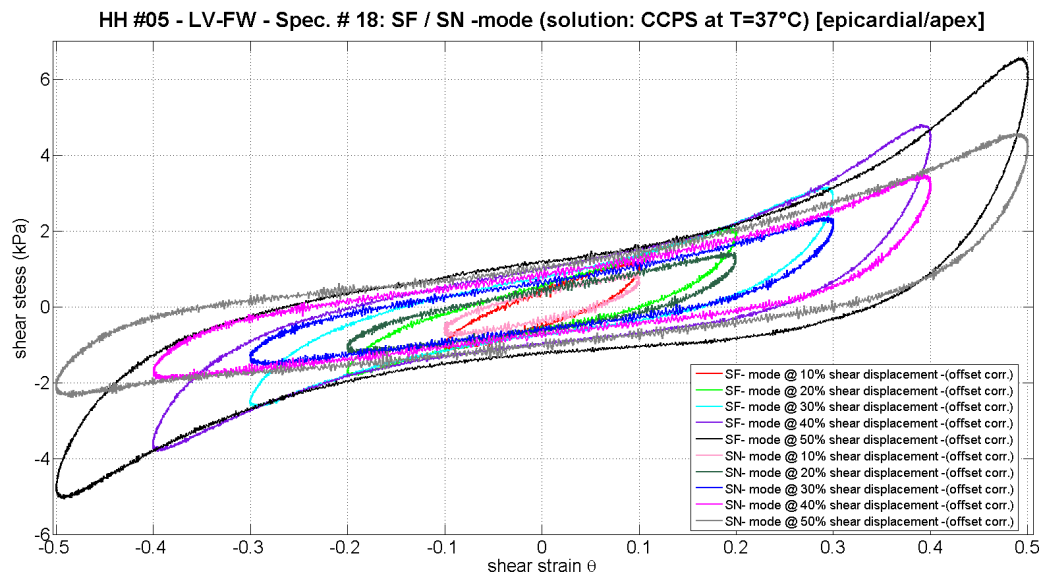


Figure 3.25: Shear stress-strain relationship (offset corrected) in *SF* and *SN* mode for Spec.#18 increasing from 10% to 50% shear strain.

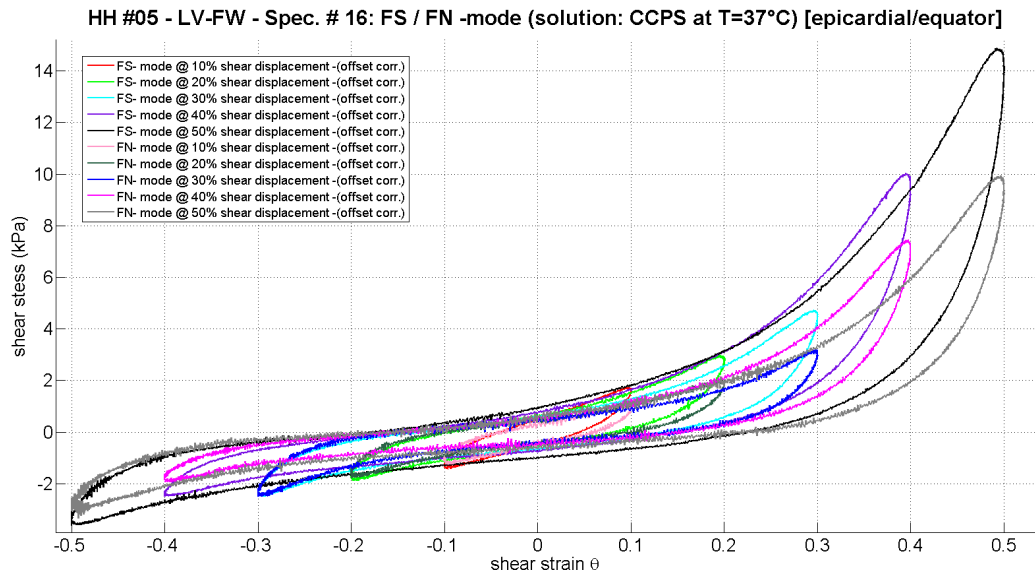


Figure 3.26: Shear stress-strain relationship (offset corrected) in *FS* and *FN* mode for Spec.#16 increasing from 10% to 50% shear strain ('strain softening').

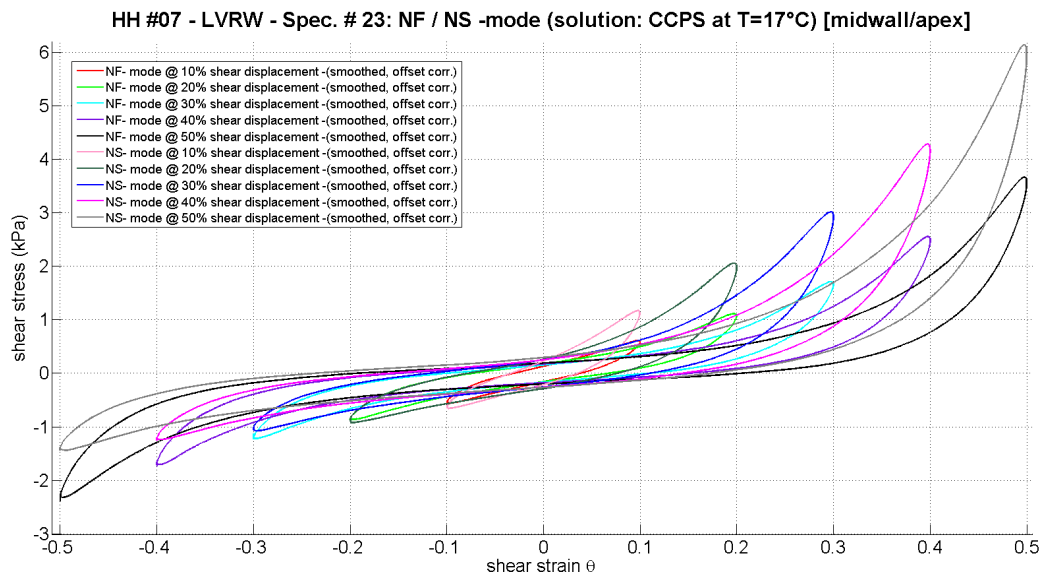


Figure 3.27: Shear stress-strain relationship (smoothed and offset corrected) in *NF* and *NS* mode for Spec.#23 increasing from 10% to 50% shear strain at 17°C.

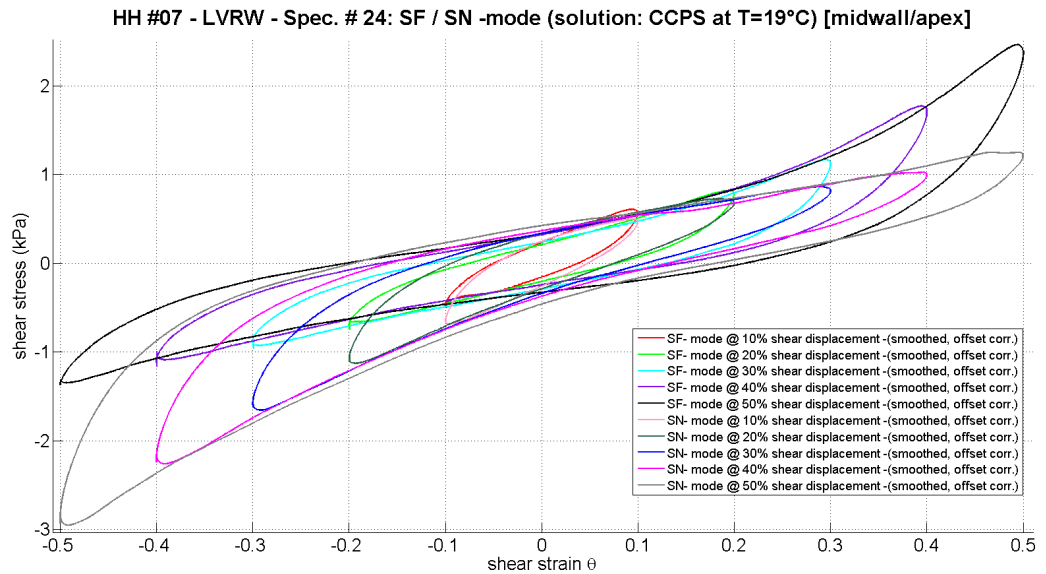


Figure 3.28: Shear stress-strain relationship (smoothed and offset corrected) in *SF* and *SN* mode for Spec.#24 increasing from 10% to 50% shear strain at 19°C.

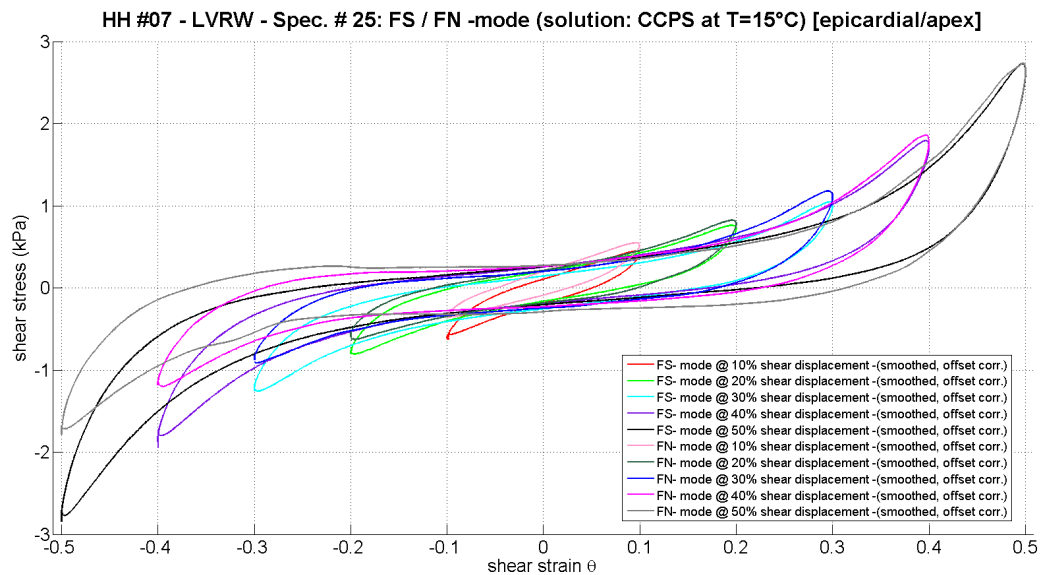


Figure 3.29: Shear stress-strain relationship (smoothed and offset corrected) in *FS* and *FN* mode for Spec.#25 increasing from 10% to 50% shear strain at 15°C.

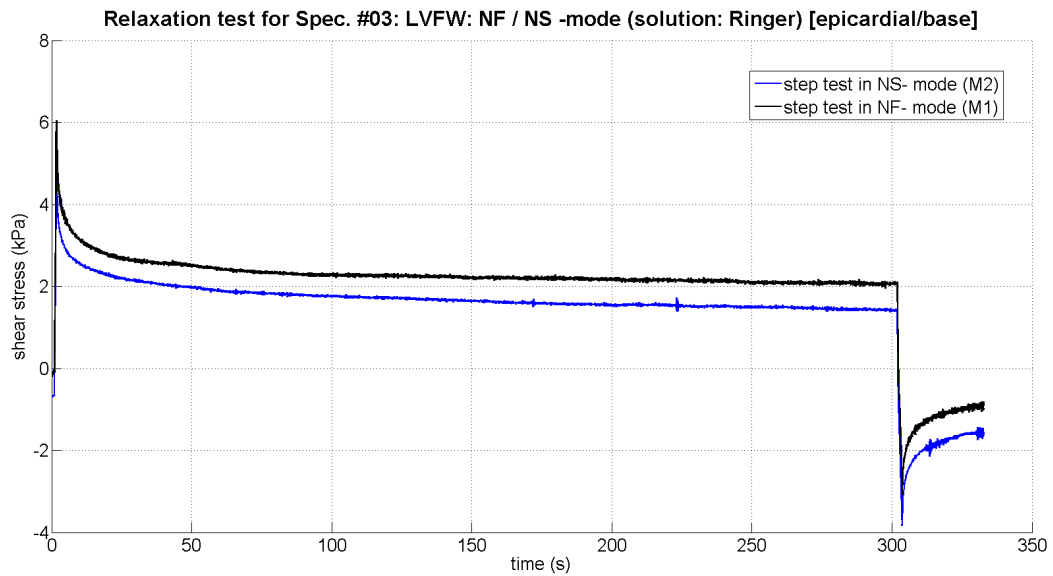


Figure 3.30: Relaxation test (human tissue) after a rapid displacement of 0.5 shear strain for 300 s in *NF*-direction (black curve) and *NS*-direction (blue curve) for Spec.#03.

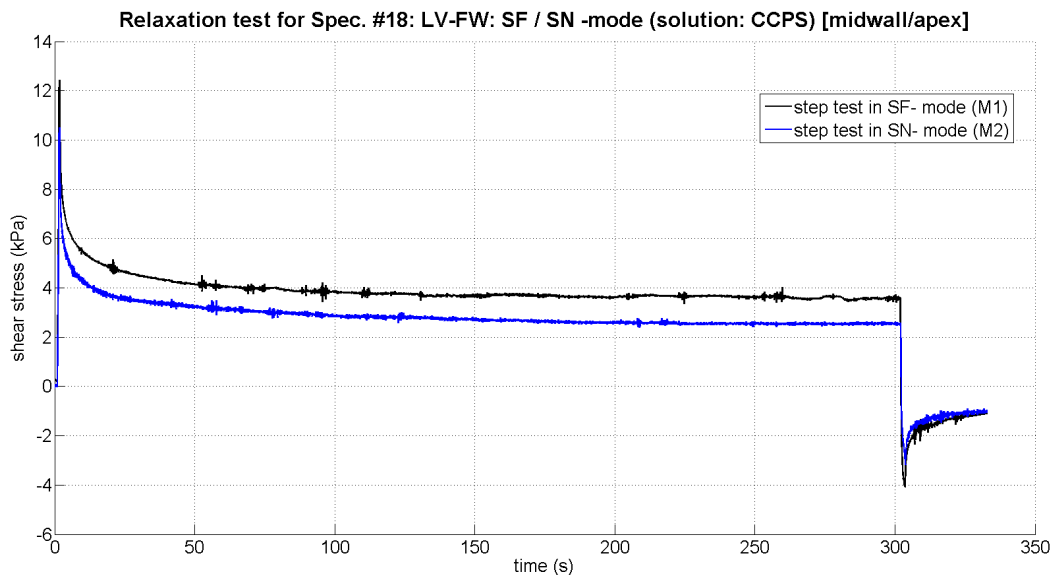


Figure 3.31: Relaxation test (human tissue) after a rapid displacement of 0.5 shear strain for 300 s in *SF*-direction (black curve) and *SN*-direction (blue curve) for Spec.#18.

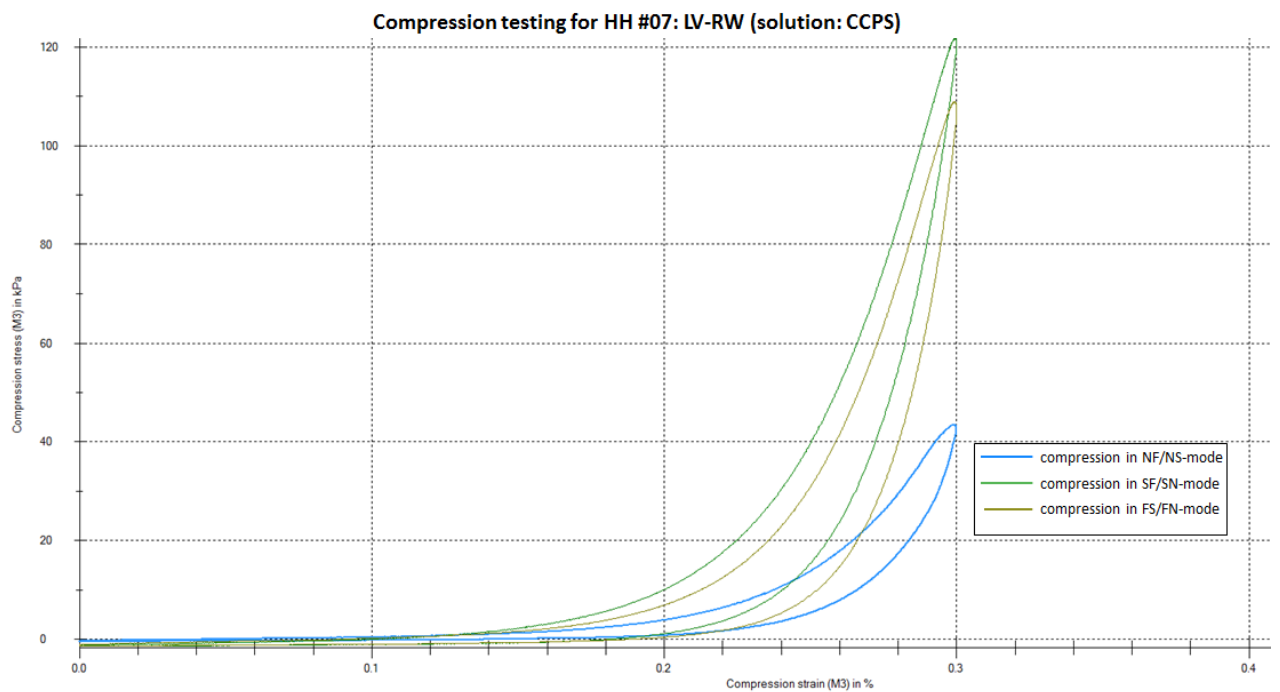


Figure 3.32: Compression test (human tissue) at 30% compression strain of HH #07 within CCPS at room temperature.

4 Discussion

The following section deals with the analysis and discussion of the investigated experimental data (chapter 3), a comparison of the observed mechanical behaviour of porcine tissue due to Dokos et al. (2002) and differences relating to human tissue. Further, states that influenced the measuring process, limitations and problems are well discussed.

4.1 Data analysis of porcine tissue

In order to make an appropriate evidence on the mechanical behaviour of porcine tissue, the results of specimens according to its locations in the myocardium (RVF, IVW, LVFW) and conditions during measurement (used chemical solution) have to be compared. Therefore, an instructive method for a qualitative comparison of mechanical properties is done via the determination of deviations according to the minima and maxima as well as for the hysteresis referring to the shear stress-strain relationship. Figure 4.1 illustrates the mean values of a cubic sample in *NS*-shear mode at an imposed shear strain of 0.3 at the RVFW (blue curve), IVW (green curve) and the LVFW (red curve).

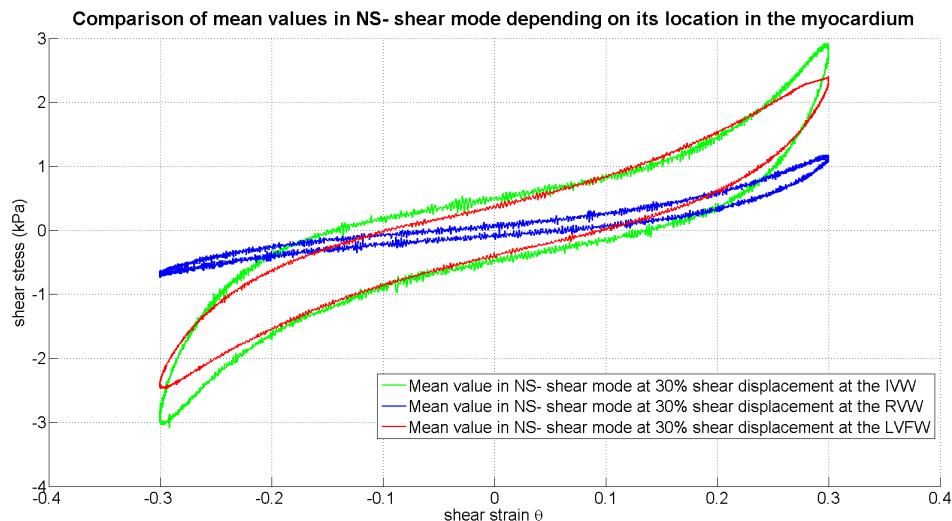


Figure 4.1: Mean curve of the shear stress-strain relationship in *NS*-shear mode (offset corrected) at 30 % shear strain of the RVFW (blue), IVW (green) and LVFW (red).

Table 4.1 compares the empirical derived data, concerning to the absolute value (peak to peak) due to the ascertained minima and maxima and the amount for the hysteresis of the respective ventricular wall. Hence, it can be obtained, that the interventricular wall is approximately 20% stiffer than the left ventricular free wall, quite in contrary to the RVFW, which is significantly softer.

Table 4.1: Comparison of minimas and maximas of the shear stress-strain relationship of cubic specimens at the RVFW, IVFW and LVFW in NS-shear mode at 0.3 shear strain.

Notations: RVFW...right ventricular free wall, IVFW...interventricular wall (septum), LVFW...left ventricular free wall

Ventricular wall	MIN. [kPa]	MAX. [kPa]	Peak to peak [kPa]	Hysteresis [kPa]
RVFW	-0.65	1.2	1.85	0.17
IVW	-2.85	2.83	5.68	0.936
LVFW	-2.4	2.29	4.69	0.71

Referring to the ratios of shear stress and shear strain, Fig. 3.1, 3.2 and 3.3 (chapter 3.1.1), accurately visualized the orthotropic mechanical behaviour of passive porcine myocardium. The tissue exhibited largest shear stress magnitudes in *FS/FN*-mode, and in contrast lowest in *NF/NS*-mode, the shear mode in *SF/SN*-mode lies between them. Resultant, largest mechanical stiffness is observed in the direction of cardiac myofibers, followed by the orientation of myocardial sheets. Greater stiffness in the direction of myofibers, may especially be declared due to the extension of cardiac myofibers and additionally by the contribution of *endomysial* collagen cords, surrounding myofibers. Passive triaxial shear testing of porcine myocardium clarifies strain softening in all six possible modes of simple shear, which is most affected in terms of cardioplegia. Contrary, the amount of hysteresis decreases in the cardioplegic environment compared to PBS (up to two times lower), coexistent with the increase of minima/maxima in the shear stress-strain diagrams.

Further, it was observed that the proportion of hysteresis transverse to myofibers was always less than in the direction of myofibers, which can also be characterized due to the influence of collagen, respectively liquid rearrangements inside and outside the cell. Biggest fluctuations in magnitudes in the direction of myofibers (*FS/FN*-mode), at which the shear stress-strain curve abrupt and rapidly increases, is observed at an imposed shear strain of 0.4, whereas the maximum is reached in *FS*-direction at ~ 15 kPa. In order, for the determination of viscoelastic properties of the tissue illustrated by the hysteresis on the one hand, additional relaxation tests at 0.5 shear strain were performed on the other hand (Fig. 3.11, 3.12 and 3.13).

The corresponding results, as well as the magnitudes of the illustrated plateaus (\sim times by three less compared to the maximum), are highly dependent relating to the principal material axes (same behavior, maximum in *FS*-direction, minimum in *NS*-direction).

Comparison with existing data - Dokos et al. 2002

Concluded, according to porcine myocardium, the shear properties of porcine myocardium, independent on the applied buffered solution, are viscoelastic and nonlinear and highly dependent on the orientation of cardiac myofibers and sheets (orthotropic). Quantitative, Dokos et al. (2002) could report higher magnitudes (shear stress), which can be explained due to the different set of CPS (also included BDM) in terms of the proper inactivation. Additionally, owing to stress caused due slaughtering, porcine tissue may develop a stress-induced cardiomyopathy, which can also result in lower magnitudes of shear stress.

4.2 Data analysis of human tissue

All subjects of human cadavers were approved by the Ethics Committee, Medical University Graz.

This thesis reports the outcome of experimental data referring to the mechanical behaviour of a total of seven human hearts, with excised cubic specimens at different locations (depending on the received myocardial piece). As already afore mentioned, the setup for transport, preparation and triaxial shear testing had to be consistently improved due to the higher sensibility on human tissue. Owing to the very small amount of the tissue (only one slice was extracted) and substantially much lower wall thicknesses (see Tab. 1.1) of human ventricles, the extraction of adjacent cubic specimens was not always possible, leading sometimes to improper possibilities of comparison referring to the differences in the laminar structure depending on its orientation (epicardial, endocardial, base, apex), as mentioned in chapter 1.3.2.2.2 (cleavage planes are at about 45° to the base, rotating towards the apex). Furthermore, during preparation, it could be shown that adipose tissue (augmented in increased age compared to porcine tissue) seems to have the ambition to deposit adjacent on laminar sheets. Thereby, much higher inhomogeneities and sparsely fat populated cleavage planes, sometimes resulted in damage of cubic samples during preparation. Those specimens were unfeasible for the investigation of shear properties, resultant in loss of tissue and in addition constricted specimen number.

Myocardial pieces of human cadavers were either received from the Clinical Department of Transplant Surgery, or from the Institute of Pathology, referring to Tab. 3.2. Concerning to the immediate death of patients and the elapsed time until the beginning of autopsy, the progress of autolysis is already well advanced. In contrast, human tissue from the Dep. of Transplant was immediately inactivated (see chap. 2.1.1.1.1) before and immediately after excision from the donor and supplied with several components such as nutrients, counteracting myocyte damage to prevent cell death.

Depending on origin, very different datasets on the investigations of the shear stress-strain behavior were expected, which are discussed in the following. It is assumed that the mechanical stiffness of the tissue originated from the Dep. of Transplant (inactivated) is stiffer in relation to those of the Inst. of Path. (autolysis-duration: 12.5 h - 28 h), which already included extincted cells.

Other factors, which influenced the test results such as, geometrical aspects of cubic samples, adhesion (glue) of specimen (during testing), temperature of cardioplegia and primary diseases as well as e.g. cardiac pathology of the donor are as well discussed in the following.

4.2.1 Comparison of mechanical properties: strain softening vs. myocyte activation

The results according to the tested specimens (Tab. 3.3), originated from the Inst. of Pathology, clearly visualized strain softening for all six possible modes of simple shear, whereas the proportion was lowest in the direction of myofibers (Fig. 3.17). This behaviour (also called the ‘Mullins effect’) is explained due to the reduced shear stress (y -axis) at continuous development of shear strain (x -axis: 0.1-0.5) and is further defined by the behaviour of preconditioning, respectively viscoelasticity and may be due to damage on elastic components (Emery et al., 1997). It was observed, that specimens of HH #02,#03,#04 (Inst. of Path.), partially differ greatly in their magnitudes of simple shear modes. The shear stress-strain relationship in *NF/NS*-mode of HH #04 for instance, demonstrated a minimum at -0.7 kPa and attained its maximum at 0.6 kPa (Fig. 3.15), these curves were therefore strongly afflicted with noise. Hence, the plots had to be fitted using a smoothing algorithm in MATLAB. But, however the averaged mean values were highlighted in Fig. 3.18, 3.19 and 3.20.

Shear properties, more accurately dependencies on different shear modes (e.g. *NF/NS* to *FS/FN*), could not be distinguished clearly for each of the afore mentioned datasets. This phenomena is explained due to the long period of autolysis and their resulting effects (see chap. 4.2.1.1). Despite this, small differences were detected, which allude to the orthotropic character of the tissue.

Quite in contrary, specimens of HH #01,#05, referring to the Dep. of Transplant Surgery, visualize similar results. Magnitudes of all samples were increased as well as their areas of hysteresis. HH #01 were tested within the use of the modified Ringer solution (15 mmolK⁺/l), not known that the missing ingredients compared to Celsior® or CCPS can also lead in cell damage. Additional, due to the high fat content in the tissue and testing at body temperature ($T = 37^{\circ}\text{C}$) for HH #01, the protein components were liquefied and extruded during the measuring process, hence, cubic specimen were detached from specimenholders. Resultant, HH #01 were therefore not reproducible.

The tests for the remaining specimens of investigations on tissue referring to the Dep. of Transplant were improved, the use of a different solution (CCPS) with increased potassium content ($\sim 35 \text{ mmolK}^+/\text{l}$) and healthier tissue (less adiposed), led to much more appropriate experimental data.

4.2.1.1 Effects caused by improper autolysis duration and activation

Autolysis is known as the self-decomposition of already dead cardiac myocytes. If a certain period of autolysis ($> 20 \text{ h}$) is exceeded, seen at specimens of the Inst. of Path., cells are already destroyed, only extracellular matrix and cell deposits remain. Hence, data of shear stress at an imposed shear strain is therefore mostly depending on the extracellular collagen cords (mainly endomysial collagen, Fig. 1.8). Therefore resulting small differences, seen in the mean values of HH #02,#04 (Inst. o. Pathology) according to its material axis, are explained due to destroyed myofibers and the associated decrease in stiffness in the direction of them. It can be assumed, that the anisotropic mechanical behaviour of the tissue due to the progression of autolysis is getting more isotropic. HH #03 (MYO 2/12 is not directly comparable to the remaining two samples (TU MYO 1/12 and 3/12), because autolysis seems to be slowed due to the more youthful age of the tissue (32 a), which is coexistent with the less advanced natural decay (during lifetime of the donor) of cardiac myocytes. It can be hypothesized, that this circumstance led to the basically stiffer mechanical behaviour (Fig. 3.16 and 3.17).

Specimens according to the measurement series on the immediate inactivated tissue after separation from the donor (Dep. of Transplant Surgery), suddenly resulted in activation during measurement, seen in HH #01 and HH #05 (Fig. 3.24,3.25) and partially in HH #07 (Fig. 3.28). Generally the activation of the myocardial tissue is inhibited due the use of a cardioplegic solution. The higher potassium concentration of such a CPS increases the permeability of the cell membrane for potassium. Further, the resting potential is decreased due to the minimized K^+ -concentration-gradient. Hence, the cell gets depolarized, which immobilizes the cell membrane and inhibits ion exchange.

Mechanical stress, imposed to the myocyte, may abolish depolarization and cause an activation (mechano-transductive-activation). Investigations on human shear properties have shown, that the inactivation of the tissue is additionally explained by the contribution of temperature incorporated to cardioplegia. Hypothermia is the second major component for cardioplegia, because of the fact that a cardioplegic solution has its domain temperature between 2 and 4°C.

Therefore, HH #06 and HH #07 were tested at lower temperatures (15°-19°C). Figures 3.27 and 3.29 illustrate the shear stress-strain relationship in *NF/NS*- mode at 17°C and *FS/FN*-mode at 15°C. This specimens indicated strain softening in contrast to Fig. 3.28 in *SF/SN*-mode at 19°C where tissue got activated again. Hence, it can be assumed, that the tissue at measurement temperatures higher than 20°C, prefers to activate.

HH #06 is not comparable to HH #07, although it was measured at lower temperatures, because cell death occurs due to freezing of the tissue, which inevitably lead to different results.

Table 4.2: Comparison of minimas and maximas of the shear stress-strain relationship of cubic specimens at the LVFW in all modes of simple shear at 0.3 shear strain for a representative shear stress-strain plot received from the Inst. of Pathology (left) and from the Dep. of Transplant (right).

Notations: Ratio... $[\frac{\%}{100}]$...inactivated tissue in relation to activated tissue

Shear mode	Inactivated tissue			Activated tissue			Ratio [%/100]
	MIN. [kPa]	MAX. [kPa]	Peak to peak [kPa]	MIN. [kPa]	MAX. [kPa]	Peak to peak [kPa]	
<i>NF</i>	-0.59	0.50	1.09	-0.8	1.8	2.6	1 : 2.38
<i>NS</i>	-0.73	0.37	1.1	-1.1	1.15	2.25	1 : 2.04
<i>SF</i>	-1.71	2.45	4.16	-2.5	3.0	5.5	1 : 1.32
<i>SN</i>	-1.51	2.01	3.52	-1.5	2.2	3.7	1 : 1.05
<i>FS</i>	-2.1	3.05	5.15	-3.5	15	18.5	1 : 3.59
<i>FN</i>	-1.3	2.3	3.6	-3.0	10	13	1 : 3.61

Tab. 4.2 illustrates the increased ratio of activated tissue compared to inactivated tissue.

4.2.2 Unconfined compression behaviour of the human myocardium

Investigations on unconfined compression testing determined highest magnitudes of compression stress in *SF*-direction, contrary to triaxial shear investigations, which had their maximum in *FS*-direction. *NF*-direction representate similar results with lowest magnitudes of compression stress. It can be assumed, that compressing the cubic specimen in *z*-direction (*SF*-cube) has increased stress magnitudes due to tensile stresses of cleavage planes (sheets) at the sample borders containing perimysial collagen and additional tensile stress acting on the transverse myofibers containing endomysial collagen (see also Fig. 2.15). Compression of a specimen fixed in *NF*-mode indicated lowest compression stress magnitudes, which may explained due to tensile stress of cardiac myofibers and sheets, imposed only transverse to the compression axis (their contribution of stress in *z*-axis is only indirectly effective).

4.2.3 Pathological aspects: gender, age, cardiac myopathy

Heart related diseases like cardiac myopathy (hypertrophy), coronary sclerosis and diastolic dysfunction of the tested human specimens did not show influences according to the mechanical behavior of triaxial shear properties, only changes in wall thickness were recognized. During this thesis it was not possible to determine the impact of these diseases according to the small amount of available samples.

Differences according to the age and gender of the donor were probably detected during triaxial shear testing. Whereas tissue of older donors (HH #04: female, 93 a) clearly indicated tissue softening, specimen from younger donors demonstrated much stiffer results. Hence, it can also be assumed that the progress of autolysis is decelerated in younger tissue samples.

Bibliography

- Ackemann, J., Gross, W., Mory, M., Schaefer, M., and Gebhard, M. M. (2002). Celsior versus custodiol: early postischemic recovery after cardioplegia and ischemia at 5 degrees c. *Ann. Thorac. Surg.*, 74:522–529.
- Adams, W., Trafford, A. W., and Eisner, D. A. (1998). 2,3-butanedione monoxime (bdm) decreases sarcoplasmic reticulum ca content by stimulating ca release in isolated rat ventricular myocytes. *Pflugers Arch.*, 436:776–781.
- Bankl, H. (1998). *Arbeitsbuch Pathologie - Einfhruung in die Pathologie - Pathologisch-anatomisches Praktikum*. FACULTAS Studienbcher Medizin Band 10.
- Barallobre-Barreiro J., Fernandez-Caggiano M., D. A. A. A. (2012). The cardio research web project.
- Bett, G. C. and Rasmusson, R. L. (2002). *Quantitative Cardiac Electrophysiology*. Taylor & Francis.
- Cheng, A., Langer, F., Rodriguez, F., Criscione, J. C., Daughters, G. T., Miller, D. C., and Ingels, N. B. (2005). Transmural sheet strains in the lateral wall of the ovine left ventricle. *Am. J. Physiol. Heart Circ. Physiol.*, 289:H1234–1241.
- Cohen, N. M. and Lederer, W. J. (1988). Changes in the calcium current of rat heart ventricular myocytes during development. *J. Physiol. (Lond.)*, 406:115–146.
- Cooper, G. M. (2000). *The Cell: A Molecular approach, 2nd edition*. Sinauer Associates.
- Costa, K. D., Holmes, J. W., and McCulloch, A. D. (2001). Modelling cardiac mechanical properties in three dimensions. *Philosophical Transactions of the Royal Society of London. Series A:Mathematical, Physical and Engineering Sciences*, 359(3):1233–1250.
- Crick, S. J., Sheppard, M. N., Ho, S. Y., Gebstein, L., and Anderson, R. H. (1998). Anatomy of the pig heart: comparisons with normal human cardiac structure. *J. Anat.*, 193 (Pt 1):105–119.
- Demer, L. L. and Yin, F. C. (1983). Passive biaxial mechanical properties of isolated canine myocardium. *J. Physiol. (Lond.)*, 339:615–630.
- Dokos, S., Smaill, B. H., Young, A. A., and LeGrice, I. J. (2002). Shear properties of passive ventricular myocardium. *American Journal of Physiology - Heart and Circulatory Physiology*, 283(1):H2650–H2659.

- Dorri, F. (2004). *A finite element model of the human left ventricular systole, taking into account the fibre orientation pattern*. PhD thesis, ETH Zurich.
- Dou, J. (2003). *Mapping Myocardial Structure- Function Relations with Cardiac Diffusion and Strain MRI*. PhD thesis, Massachusetts Institute of Technology (MIT).
- Emery, J. L., Omens, J. H., and McCulloch, A. D. (1997). Strain softening in rat left ventricular myocardium. *J Biomech Eng*, 119(1):6–12.
- Garikipati, K. and M. Arruda, E. (2008). *Symposium on Cellular, Molecular and Tissue Mechanics*. Springer.
- Gehrmann, F. (2010). A triaxial shear measurement device. Master's thesis, Insitute of Biomechanics, Graz University of Technology.
- Gilbert, S. H., Benson, A. P., Li, P., and Holden, A. V. (2007). Regional localisation of left ventricular sheet structure: integration with current models of cardiac fibre, sheet and band structure. *Eur J Cardiothorac Surg*, 32:231–249.
- Gray, H. (2008). *Gray's Anatomy - The Anatomical Basis of Clinical Practice*, volume 40. Edinburgh: Churchill Livingstone.
- Guo, W., Chen, N., Chen, Y., Xia, Q., and Shen, Y. (2005). Activation of mitochondrial atp-sensitive potassium channel contributes to protective effect in prolonged myocardial preservation. In *Engineering in Medicine and Biology Society, 2005. IEEE-EMBS 2005. 27th Annual International Conference of the*, pages 4027 –4030.
- Ho, S. Y. (2009). Anatomy and myoarchitecture of the left ventricular wall in normal and in disease. *Eur J Echocardiogr*, 10:3–7.
- Holzapfel, G. (2000). *Biomechanics of soft tissue*, volume Handbook of material behavior, Nonlinear Models and Properties. Academic Press, handbook of material behavior, nonlinear models and properties edition.
- Holzapfel, G. A. (2009). *Biomechanics - Lecture Notes*. Holzapfel, Gerhard A, Graz University of Technology.
- Holzapfel, G. A. and Ogden, R. W. (2009). Constitutive modelling of passive myocardium: a structurally based framework for material characterization. *Philosophical Transactions of the Royal Society A: Mathematical, Physical and Engineering Sciences*, 367(2):3445–3475.
- Horgan, C. O. and Murphy, J. G. (2011). Simple shearing of soft biological tissues. *Proceedings of the Royal Society A: Mathematical, Physical and Engineering Science*, 467(2127):760–777.

- Hsueh, W. A., Law, R. E., and Do, Y. S. (1998). Integrins, adhesion, and cardiac remodeling. *Hypertension*, 31:176–180.
- Humphrey, J. (2002a). *Cardiovascular Solid Mechanics: Cells, Tissues, and Organs*. Springer.
- Humphrey, J. D. (2002b). *Continuum biomechanics of soft biological tissues*. Department of Biomedical Engineering and The M. E. DeBakey Institute, 233 Zachry Engineering Center, Texas A&M University, College Station, TX 77843-3120, USA.
- Klabunde, R. E. (2011). *Cardiovascular Physiology Concepts*. Wolters Kluwer.
- LeGrice, I. J., Smaill, B. H., Chai, L. Z., Edgar, S. G., Gavin, J. B., and Hunter, P. J. (1995). Laminar structure of the heart: ventricular myocyte arrangement and connective tissue architecture in the dog. *Am. J. Physiol.*, 269:H571–582.
- Maier, F. (2011). Triaxial shear testing of human aortic wall tissue. Master's thesis, Institute of Biomechanics, Graz University of Technology.
- McCulloch, A. D. and Omens, J. H. (2006). Myocyte shearing, myocardial sheets, and microtubules. *Circ. Res.*, 98:1–3.
- Paulsen, Friedrich; Waschke, J. (2006). *Atlas der Anatomie des Menschen*. Sobotta.
- Pope, A. J., Sands, G. B., Smaill, B. H., and LeGrice, I. J. (2008). Three-dimensional transmural organization of perimysial collagen in the heart. *Am. J. Physiol. Heart Circ. Physiol.*, 295:H1243–H1252.
- Rohmer, D., Sitek, A., and Gullberg, G. T. . (2007). Reconstruction and visualization of fiber and laminar structure in the normal human heart from ex vivo diffusion tensor magnetic resonance imaging (dtmri). *Invest Radiol*, 42(4):777–789. [DOI:10.1097/RLI.0b013e3181238330] [PubMed:18030201].
- Spinale, F. G. (2007). Myocardial matrix remodeling and the matrix metalloproteinases: influence on cardiac form and function. *Physiol. Rev.*, 87:1285–1342.
- Walker, C. A. and Spinale, F. G. (1999). The structure and function of the cardiac myocyte: a review of fundamental concepts. *J. Thorac. Cardiovasc. Surg.*, 118:375–382.
- Watanabe, Y., Iwamoto, T., Matsuoka, I., Ohkubo, S., Ono, T., Watano, T., Shigekawa, M., and Kimura, J. (2001). Inhibitory effect of 2,3-butanedione monoxime bdm on na^+/ca^{2+} exchange current in guinea-pig cardiac ventricular myocytes. *Br. J. Pharmacol.*, 132:1317–1325.
- Weber, K. T. (1989). Cardiac interstitium in health and disease: the fibrillar collagen network. *J. Am. Coll. Cardiol.*, 13:1637–1652.

Wikipedia.org (2012). en.wikipedia.org.

Yin, F. C., Strumpf, R. K., Chew, P. H., and Zeger, S. L. (1987). Quantification of the mechanical properties of noncontracting canine myocardium under simultaneous biaxial loading. *J Biomech*, 20:577–589.

5 Appendix

5 Appendix

Shear properties of passive ventricular myocardium

Print Reset



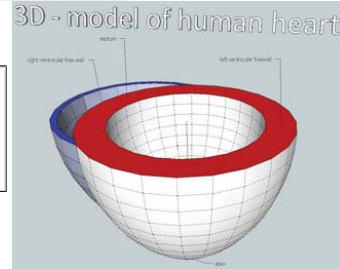
Measurement Protocol - TRIAX - Myocardium



Fig 1a,b (left): explanted human heart

Fig 2 (right): 3D - model of human heart

No. #HH3_Patho_2



Heart # human pathology #02
 weight (g) 400
 wall-thickn. -LVFW (mm) 16mm
 wall-thickn. -RVFW (mm) 5mm

Measurement Date: 14.02.2012 , 14.02.2012
 Export -filename: HH2_LV_cardiopleg_35mmolK_patchwork_p
 data-analysis-file: #HH3_Patho_2_data_analysis.xls

details-Heart:
 PathoNr.: TU MYO 2/12
 Patient: w, 32a, 170cm, 65kg
 Time of death: 12.02.2012, 14.30h
 Pathology: heart hypertrophy
 sample: LVFW, front wall (lamella -cut due to autopsy), SEPT
 storage until preparation: CPS (16mmolK/l), 3°C

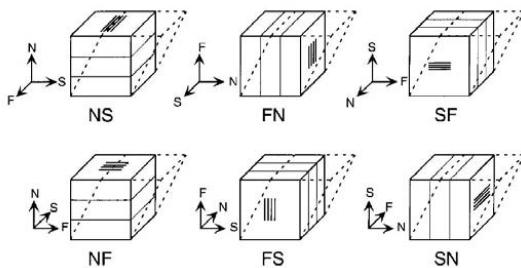
1a. Specimen details: Specimen #1

sliceNo./specNo: 11 specimen-size: length (M2) in mm: 4,5 width (M1) in mm: 4,5 depth (M3) in mm: 4,15
 place of dissection: LVFW specimen-position: epicardial , equator, base

specimen-orientation:
 X-direction: NF NS SF SN FS FN
 Y-direction: NF NS SF SN FS FN

autolyse - time (h): 19/17so el. time at room temp. (prep.) 0,5

storage: laboratory refridgertal details: cps, 2°C



Notes: stiffest human tissue tested! (age only 32a)
 low fat storage in tissue

Fig 2: Illustration of six possible modes of shear deformation adapted from Dokos et. Al

5.1 Measurement protocol on the basis of human myocardium

Shear properties of passive ventricular myocardium



2a. measurement details: Specimen #1

preconditioning cycles: measured strain: 10% 20% 30% 40% 50%

main cycles: steptest: yes no solution temperature: (°C)

spec. fixation: compression-test: yes no

solution: PH: adj. measurement velocity (mm/min):

Notes:

cardioplegic solution 35mmolK/I (1,

pictures taken: yes no



Specimen



Specimen

5 Appendix

Shear properties of passive ventricular myocardium

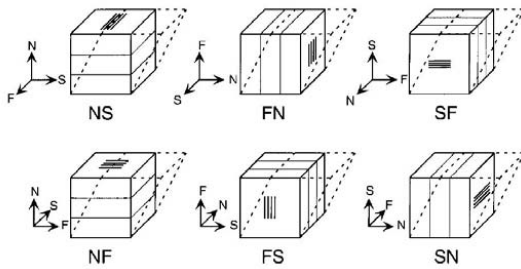


1b. Specimen details: Specimen #2

sliceNo./specNo: specimen-size: length (M2) in mm: width (M1) in mm: depth (M3) in mm:

place of dissection: specimen-position: ,

specimen-orientation: X-direction: NF NS SF SN FS FN
 Y-direction: NF NS SF SN FS FN



elapsed time since dissection (h): el. time at room temp. (prep.)

storage: details:

Notes: isotropy?: hard to recognize differences in orientations!

solution has become turbid over time, therefore addition of 'fresh' solution!

2b. measurement details: Specimen #2

preconditioning cycles: measured strain: 10% 20% 30% 40% 50%

main cycles: steptest: yes no solution temperature: (°C)

spec. fixation: compression-test: yes no

adj. measurement velocity (mm/min):

Notes:

new solution

pictures taken: yes no

5.1 Measurement protocol on the basis of human myocardium

Shear properties of passive ventricular myocardium



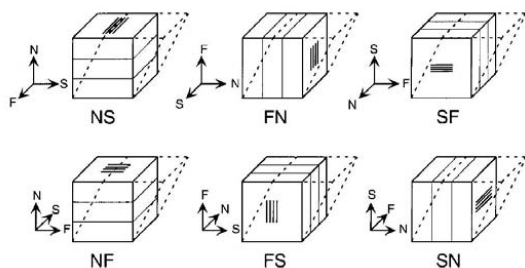
1c. Specimen details: Specimen #3

sliceNo./specNo: specimen-size: length (M2) in mm: width (M1) in mm: depth (M3) in mm:

place of dissection: specimen-position: ,

specimen-orientation: X-direction: NF NS SF SN FS FN

Y-direction: NF NS SF SN FS FN



elapsed time since dissection (h): el. time at room temp. (prep.)

storage: details:

Notes:

2c. measurement details: Specimen #3

preconditioning cycles: measured strain: 10% 20% 30% 40% 50%

main cycles: steptest: yes no solution temperature: (°C)

spec. fixation: compression-test: yes no

adj. measurement velocity (mm/min):

Notes: isotropy!
50%- stretch occurred an error: offset on y -traverse reported too high

pictures taken: yes no

5 Appendix

Excision protocol for myocardial samples

„Biomechanik humaner ventrikulärer Myokarde“

Sowohl für den biaxialen Zugversuch, als auch für den triaxialen Scherversuch werden Gewebeprobe(n) (bevorzugt aus dem linken Ventrikel und Septum) benötigt.

Die Entnahme soll bei Verstorbenen während einer routinemäßigen klinischen Obduktion erfolgen, um anschließende biomechanische, histologische und polarisations-mikroskopische Untersuchungen an den Myokardgewebeprobe(n) durchzuführen.

Die Myokardproben werden unterschiedlich für die jeweiligen Versuche präpariert, gemessen und analysiert. Abbildung 1 beschreibt schematisch die für die biomechanischen Versuche relevanten Regionen.

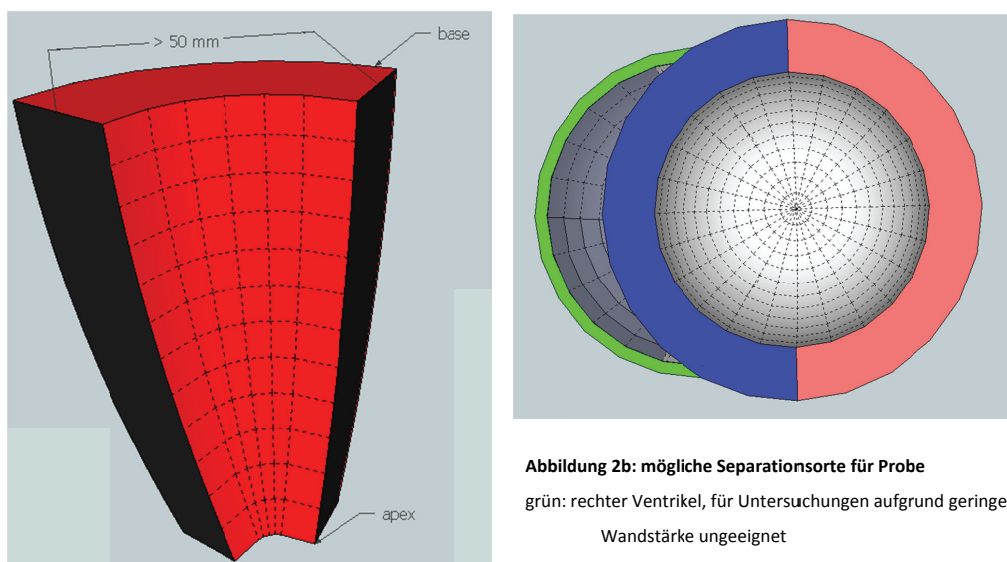
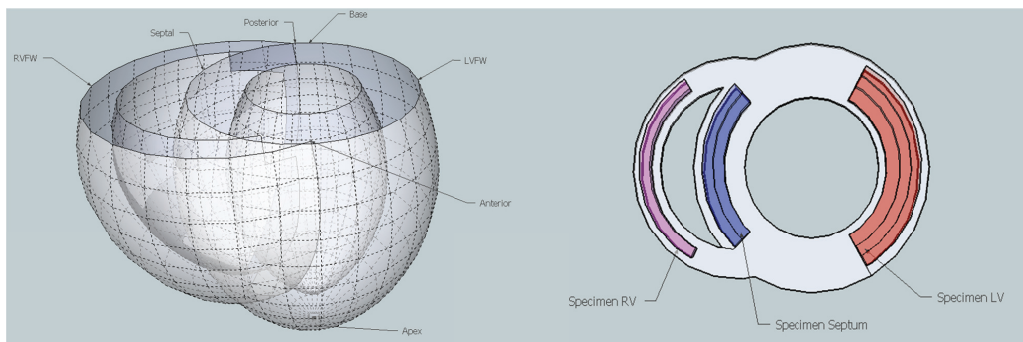


Abbildung 2a: separierter Keil für biomech. Untersuchungen

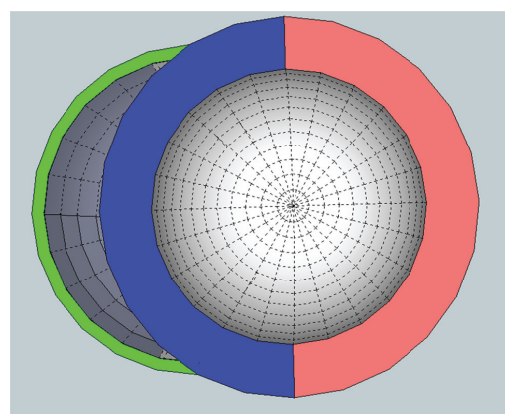


Abbildung 2b: mögliche Separationsorte für Probe

grün: rechter Ventrikel, für Untersuchungen aufgrund geringer Wandstärke ungeeignet

blau: Septum

rot: linker Ventrikel (free wall)

Die Abbildungen zeigen nur den Ventrikel, Atrien werden für biomech. Untersuchungen nicht herangezogen!

5.2 Dissection protocol for the Clinical Departments of Pathology and Transplant Surgery

Anforderungen für die Versuchsreihe:

- **Autolyse**, wenn möglich nicht länger als **24h** vorangeschritten!

Es werden sowohl „gesunde“ – als auch Herzen mit diversen Erkrankungen für die Untersuchungen herangezogen
- Separation eines **Keils** (Abb. 2a) aus den in Abbildung 2b färbig markierten Bereichen des Myokards (**base – apex**) mit einer Mindestgröße von 50 mm (ideal: >60mm) an der Basis.
- Wenn möglich soll an den schwarz markierten Flächen in Abbildung 2a ein **histologischer Schnitt** durchgeführt werden, um die Ausrichtung der „sheets“ bestimmen zu können, die für die biomechanischen Eigenschaften des Myokards eine wesentliche Rolle spielen.

Die weitere Aliquotierung der Proben erfolgt im Labor des Instituts für Biomechanik.

- Separation aus dem **rechten Ventrikel optional**, da Wandstärke grenzwertig für Versuch
- Entnommene Proben sollen direkt nach Entnahme in dem von uns bereitgestellten **Gefäß** (mit kardioplegische Lösung) mit Datum und Uhrzeit beschriftet und bis zur Abholung gekühlt (1°C – 4°C) gelagert werden.
- Für die Messung benötigte Daten des Verstorbenen:
 - Geschlecht
 - Alter
 - Gewicht
 - Herzgewicht
 - Wandstärke des linken- und rechten Ventrikels
 - Autolysezeit der Probe
 - etwaige Herzerkrankungen
- Organisatorisches:
Information über eine grundsätzlich geeignete Obduktion an Dr. Christian Viertler/Prof. Regitnig (Autolysezeit, keine spezielle Fragestellung seitens der Klinik bezüglich Herzerkrankungen...) durch Hrn. Donnerer. Danach Absprache mit dem jeweiligen Obduzenten bezüglich der Probenentnahme. Falls eine Probenentnahme möglich ist (keine spezielle klinische Fragestellung/Hinweis bezüglich Herzerkrankungen/-infarkt etc.), Probenentnahme durch den Obduzenten und Verständigung der TU durch Dr. Viertler od. Hr. Donnerer. Lagerung der Proben in kardioplegischer Lösung im Kühlschrank im Seziersaal bis zur Abholung.
- Kontaktdaten
 - Dr. Christian Viertler 0316/385 80961
 - Prof. Peter Regitnig 0316/385 81629
 - Augustin Donnerer 0316/385 81632

 - Michael Kutschera 0650/85 00 139 (Diplomand TU Graz)
 - Roland Kresnik 0650/22 31 166 (Diplomand TU Graz)

Vielen Dank für Ihre Kooperation!

5.3 Ethics applicant - Clinical Department of Transplant Surgery

2. Eckdaten der Studie

- 2.1 Art des Projektes: 2.1.1 Klinische Prüfung eines nicht registrierten **Arzneimittels**
 2.1.2 Klinische Prüfung eines registrierten **Arzneimittels**
 2.1.2.1 gemäß der Indikation 2.1.2.2 nicht gemäß der Indikation
 2.1.3 Klinische Prüfung einer neuen **medizinischen Methode**
 2.1.4 Klinische Prüfung eines **Medizinproduktes**
 2.1.4.1 mit CE-Kennzeichnung 2.1.4.2 ohne CE-Kennzeichnung
 2.1.4.3 Leistungsbewertungsprüfung (In-vitro-Diagnostika)
 2.1.5 **Nicht-therapeutische biomedizinische Forschung** am Menschen
(Grundlagenforschung)
 2.1.6 **Genetische Untersuchung**
 2.1.10 **Register**
 2.1.11 **Biobank**
 2.1.12 **Retrospektive Datenauswertung**
 2.1.13 **Fragebogen Untersuchung**
 2.1.14 **Psychologische Studie**
 2.1.15 **Pflegewissenschaftliche Studie**
 2.1.16 **Nicht-interventionelle Studie (NIS)**
 2.1.7 **Sonstiges** (z.B. Diätetik, Epidemiologie, etc.), bitte spezifizieren:

Zusatzinformation: 2.1.8 **Dissertation** 2.1.9 **Diplomarbeit**

2.2 Fachgebiet: **Transplantchirurgie, Biomechanik**

2.3 Arzneimittelstudie (wenn zutreffend)

2.4 Medizinproduktstudie (wenn zutreffend)

2.3.1 Prüfsubstanz(en):

2.4.1 Prüfprodukt(e):

2.3.2 Referenzsubstanz:

2.4.2 Referenzprodukt:

2.5 Klinische Phase: _____ (unbedingt angeben, bei Medizinprodukten die am ehesten zutreffende Phase)

2.6 Nehmen andere Zentren an der Studie teil: ja nein. Wenn **ja**:

2.6.1 im Inland

2.6.2 im Ausland

2.7 Liste der Zentren: **Klinische Abteilung für Transplantationschirurgie, Medizinische Universität
Graz
Institut für Biomechanik, Technische Universität Graz**

2.8 Liegen bereits Voten anderer Ethikkommissionen vor?

ja nein. Wenn **ja**, **Voten beilegen!**

2.9 Geplante **Gesamtzahl** der **Prüfungsteilnehmer/innen** (in allen teilnehmenden Zentren):

30

5.3 Ethics applicant - Clinical Department of Transplant Surgery

5. Angaben zur Versicherung (gemäß §32 Abs.1 Z.11 und Z.12 und Abs.2 AMG; §§47 und 48 MPG)

5.1 Eine Versicherung ist erforderlich: ja nein. Wenn ja:

5.1.1 Versicherungsgesellschaft

5.1.2 Adresse:

5.1.3 Telefon:

5.1.4 Polizzenummer:

5.1.5 Gültigkeitsdauer:

Diese Angaben müssen in der Patienten- / Probandeninformation enthalten sein!

7. Strukturierte Kurzfassung des Projektes (*in deutscher Sprache, kein Verweis auf das Protokoll*)

<p>7.1 Wenn Original-Projekttitle nicht in Deutsch: Deutsche Übersetzung des Titels: Biomechanik des humanem ventrikulärem Myokardiums (Biaxiale und triaxiale mechanische Untersuchung)</p>
<p>7.2 Zusammenfassung des Projektes (Rechtfertigung, Relevanz, Design, Maßnahmen und Vorgehensweise): Das mechanische Verhalten der Ventrikel des menschlichen Myokards (linker Ventrikel, rechter Ventrikel und Septum), im Speziellen der Muskelzellen und der umliegenden kollagenen Faserkomponenten, ist bis dato noch sehr dürftig erforscht. Eine systematische, biomechanische, mikrostrukturelle und histologische Untersuchung des humanen Herzmuskels soll daher durchgeführt werden. Daten aus biaxialen Zugversuchen am menschlichen Myokardgewebe existieren bis heute nur in sehr geringem Ausmaß, Daten aus triaxialen Scherversuchen existieren de facto gar nicht. Insbesondere sind die Einflüsse der zu Verbänden von mehrlagig angeordneten Muskelfasern zusammengesetzten sogenannten Sheet-Strukturen zu erfassen. Dazu werden Gewebescheiben in Hauptmuskelfaserrichtung mittels biaxialen Zugversuchen unter verschiedenen Lastprotokollen biomechanisch getestet. Neben den biaxialen Zugversuchen sollen die Schereigenschaften des Myokards auch mit Hilfe eines triaxialen Kraftaufnehmers, entsprechend der Koordinatenachsen die sich aus der Muskelfaserrichtung und Sheets ergeben, gemessen werden. Die daraus resultierenden Ergebnisse, sollen vor allem auch einer späteren mathematischen Modellierung dienen, welche die Einhaltung der drei Dimensionen unbedingt voraussetzt. Anschließend werden die laminare Struktur und Komponenten der geprüften Bereiche histologisch untersucht. Die folglich erhaltene räumliche Mikrostruktur der mechanisch relevanten Komponenten soll Aufschluss über noch nicht verstandene Einflüsse der Sheet-Strukturen auf die Stabilität des Herzwandgewebes geben. Derartig kombinierte biomechanische Daten von humanen Herzmuskelgeweben existieren bis heute nur in sehr geringem Ausmaß. Das Projekt erstreckt sich weniger über eine geplante Dauer, als über ein Versuchskontingent von mindestens 30 menschlichen Herzen. Dabei sollen jeweils beide Ventrikel eines menschlichen Herzens post-mortem getestet werden. Für die biaxialen mechanischen Untersuchungen sind die Herzen so zu beschneiden, dass sich je 3 Proben aus der lateralen Wand des linken Ventrikels, sowie je 2 Proben aus dem Septum und der medialen Wand des rechten Ventrikels extrahieren lassen. Für Untersuchungen der triaxialen Schereigenschaften werden, jeweils 3 Würfel vom linken und rechten Ventrikel in einem Winkel von 45° zur Base entnommen. Es sind keine Atria, Herzohren, Klappen oder versorgende Gefäße zur Untersuchung nötig. Die Proben werden im Rahmen der Organexplantation entnommen und in einer kardioplegischen Lösung bis zu den Präparationen und den Tests bei 2-4°C gelagert. Selbige dient dazu, fortschreitende Autolyse zu minimieren. Die Tests an den Proben aus dem Herzgewebe finden aufgrund der Autolyse auch innerhalb 24h statt. Nach Abschluss werden die Gewebeproben in Formalin fixiert, um die mikroskopischen Struktur-Untersuchungen durchführen zu können. Folgende Maßnahmen bzw. Voraussetzungen werden bei der Präparateentnahme berücksichtigt (die klinische Transplantation wird durch die Probenentnahme nicht beeinträchtigt - siehe auch 7.6.): 1) Die Ventrikelproben werden sofort nach der Gewinnung aus dem Herzen in kardioplegischer Lösung bei 4°C eingelegt. 2) Extraktion der quadratischen Proben für den biaxialen Zugversuch aus dem spezifizierten Herzgewebe der Ventrikel und zusätzliche Extraktion von würfelförmigen Proben aus den Ventrikel für den triaxialen Scherversuch. 3) Erfassung der Hauptfaserrichtungen der Gewebeer- und Gewebegrundflächen durch mikroskopische Untersuchung für die biaxialen Zugversuche. (biaxial) Erfassung der Sheet-Strukturen und Muskelfaserrichtung durch eine mikroskopische Untersuchung bzw. mit Hilfe eines Vergrößerungsglases für die triaxialen Scherversuche. (triaxial) 4) Zuschneiden der Proben in definierter Größe (25x25x2,5mm) (LxBxT) in der mittleren Hauptfaserrichtung. (biaxial) Zuschneiden der Proben in definierter Größe (4x4x4mm) (LxBxH) entsprechend eines definierten Koordinatensystems. (triaxial) 5) Biaxial: Proben mit quadratischem Grundriss für die biaxialen mechanischen Untersuchungen</p>

5.3 Ethics applicant - Clinical Department of Transplant Surgery

<p>werden aus dem Herzgewebe präpariert. Biaxiale Zugversuche mit verschiedenen Lastprotokollen bezüglich der Axial- und Umfangsrichtung werden an den Proben durchgeführt, wobei die Deformation der Probe berührungsfrei mit einem Videoextensometer bestimmt wird.</p> <p>Triaxial: Die extrahierten würfelförmigen Proben werden mit Hilfe eines Videoextensometers nachgemessen und deren Spannungs-Dehnungs-Kurven durch die Scherversuchsanlage aufgezeichnet.</p> <p>6) Histologische Untersuchungen der getesteten Proben hinsichtlich der Verteilung und des Vorkommens besagter Herzfaserverbände (den sog. Sheets) mit Spezialfärbung der elastischen und kollagenen Fasern.</p>
<p>7.3 Ergebnisse der prä-klinischen Tests oder Begründung für den Verzicht auf prä-klinischen Tests: In einer Pilot-Studie konnte gezeigt werden, dass biaxiale und triaxiale Tests an 15 frischen Schweineherzen eine deutliche Relevanz der Sheet-Struktur auf die biomechanischen Eigenschaften des ventrikulären Myokards erkennen lassen. Da diese Eigenschaften bei verschiedenen Spezies deutliche Unterschiede aufweisen, soll diese Abhängigkeit nun auch am humanen Myokard überprüft bzw. nachgewiesen werden.</p>
<p>7.4 Primäre Hypothese der Studie (wenn relevant auch sekundäre Hypothesen): Die biaxiale und triaxiale Untersuchung der biomechanischen Eigenschaften und deren Variation in Zusammenhang mit den erhaltenen Sheet-Strukturen der Gewebeprobe, soll den wesentlichen Einfluss der Herzmuskelfaserverbände (Sheets) auf die Systemeigenschaften des Myokardiums nachweisen und beschreiben. Dadurch werden grundlegende, mechanische und bis dato nicht existente Daten der Mechanik des ventrikulären Herzmuskelgewebes gewonnen und diese für computerunterstützte Simulationen nutzbar gemacht.</p>
<p>7.5 Relevante Ein- und Ausschlusskriterien:</p>
<p>7.6 Ethische Überlegungen (Identifizieren und beschreiben Sie alle möglicherweise auftretenden Probleme. Beschreiben Sie den möglichen Wissenszuwachs, der durch die Studie erzielt werden soll und seine Bedeutung, sowie mögliche Risiken für Schädigungen oder Belastungen der Prüfungsteilnehmer/innen. Legen Sie Ihre eigene Bewertung des Nutzen/Risiko-Verhältnisses dar):</p> <ol style="list-style-type: none"> 1. Die Probengewinnung wird nur an Herzen durchgeführt, die für Transplantationen ungeeignet sind. 2. Die Probengewinnung wird sorgfältig von einem Transplantationschirurgen im Rahmen Explantation durchgeführt. 3. Während der Probengewinnung wird ein Protokoll geführt, das die Daten des Patienten sowie die Art und Zweck der Herzmanipulation beinhaltet. 4. Die Probengewinnung erfolgt in pietätvoller Weise. 5. Die Probengewinnung dient keinem finanziellen Zweck. 6. Die Probengewinnung dient einer klaren Zielsetzung, die zukünftig der ärztlichen Betreuung von Patienten dient.
<p>7.7 Begründung für den Einschluss von Personen aus geschützten Gruppen (z.B. Minderjährige, temporär oder permanent nicht-einwilligungsfähige Personen; wenn zutreffend):</p>
<p>7.8 Beschreibung des Rekrutierungsverfahrens (alle zur Verwendung bestimmte Materialien, z.B. Inserate inkl. Layout müssen beigelegt werden): Entnahme von Gewebeprobe nach einer erforderlichen Herztransplantation an der klinischen Abteilung für Transplantationschirurgie der Medizinischen Universität Graz.</p>
<p>7.9 Vorgehensweise an der/den Prüfstelle(n) zur Information und Erlangung der informierten Einwilligung von Prüfungsteilnehmer/innen/n, bzw. Eltern oder gesetzlichen Vertreter/innen/n, wenn zutreffend (wer wird informieren und wann, Erfordernis für gesetzliche Vertretung, Zeugen, etc.):</p>
<p>7.10 Risikoabschätzung, vorhersehbare Risiken der Behandlung und sonstiger Verfahren, die verwendet werden sollen (inkl. Schmerzen, Unannehmlichkeiten, Verletzung der persönlichen Integrität und Maßnahmen zur Vermeidung und/oder Versorgung von unvorhergesehenen / unerwünschten Ereignissen):</p>

5 Appendix

7.11 Voraussichtliche Vorteile für die eingeschlossenen Prüfungsteilnehmer/innen:
7.12 Relation zwischen Prüfungsteilnehmer/in und Prüfer/in (z.B. Patient/in - Ärztin/Arzt, Student/in - Lehrer/in, Dienstnehmer/in - Dienstgeber/in, etc.):
7.13 Verfahren an der/den Prüfstelle(n) zur Feststellung, ob eine einzuschließende Person gleichzeitig an einer anderen Studie teilnimmt oder ob eine erforderliche Zeitspanne seit einer Teilnahme an einer anderen Studie verstrichen ist (von besonderer Bedeutung, wenn gesunde Proband/inn/en in pharmakologische Studien eingeschlossen werden):
7.14 Methoden, um unerwünschte Effekte ausfindig zu machen, sie aufzuzeichnen und zu berichten (Beschreiben Sie wann, von wem und wie, z.B. freies Befragen und/oder an Hand von Listen):
7.15 Optional: Statistische Überlegungen und Gründe für die Anzahl der Personen, die in die Studie eingeschlossen werden sollen (ergänzende Informationen zu Punkt 8, wenn erforderlich): In bekannter Literatur weisen Studien dieses Umfanges an tierischem Gewebe bereits gute Aussagekraft über die biomechanischen Zusammenhänge auf.
7.16 Optional: Verwendete Verfahren zum Schutz der Vertraulichkeit der erhobenen Daten, der Quelldokumente und von Proben (ergänzende Informationen zu Punkt 8, wenn erforderlich): Patientenbezogene Daten (Alter, Geschlecht, Krankheiten) werden nur in anonymisierter Form mit den Analyseergebnissen verglichen, so dass keine Beziehung zwischen den Daten einerseits und der Identität der Patienten andererseits hergestellt werden kann.
7.17 Plan zur Behandlung oder Versorgung nachdem die Personen ihre Teilnahme an der Studie beendet haben (wer wird verantwortlich sein und wo): -
7.18 Betrag und Verfahren der Entschädigung oder Vergütung an die Prüfungsteilnehmer/innen (Beschreibung des Betrages, der während der Prüfungsteilnahme bezahlt wird und wofür, z.B. Fahrtspesen, Einkommensverlust, Schmerzen und Unannehmlichkeiten, etc.): -
7.19 Regeln für das Aussetzen oder vorzeitige Beenden der Studie an der/den Prüfstelle(n) in diesem Mitgliedstaat oder der gesamten Studie: -
7.20 Vereinbarung über den Zugriff der Prüferin/des Prüfers/der Prüfer auf Daten, Publikationsrichtlinien, etc. (wenn nicht im Protokoll dargestellt): Daten die in Publikationen veröffentlicht werden unterliegen den strengen Kriterien der Journals und sind anonymisiert.
7.21 Finanzierung der Studie (wenn nicht im Protokoll dargestellt) und Informationen über finanzielle oder andere Interessen der Prüferin/des Prüfers/der Prüfer: Institutseigene Mittel, FWF Einzelprojekt-Forschungsförderung
7.22 Weitere Informationen (wenn erforderlich): -

5.3 Ethics applicant - Clinical Department of Transplant Surgery

8. Biometrie, Datenschutz:

(Hier nur Kurzinformationen in Stichworten, ausführlicher - wenn erforderlich - unter Punkt 7.15 und 7.16)

8.1 Studiendesign (z.B. doppelblind, randomisiert, kontrolliert, Placebo, Parallelgruppen, multizentrisch)

- 8.1.1 offen 8.1.2 randomisiert 8.1.3 Parallelgruppen 8.1.4 monozentrisch
 8.1.5 blind 8.1.6 kontrolliert 8.1.7 cross-over 8.1.8 multizentrisch
 8.1.9 doppelblind 8.1.10 Placebo 8.1.11 faktoriell 8.1.12 Pilotprojekt
 8.1.13 observer-blinded 8.1.14 Äquivalenzprüfung
 8.1.15 sonstiges:

8.1.16 Anzahl der Gruppen:

8.1.17 Stratifizierung: nein ja: Kriterien:

8.1.18 Messwiederholungen: nein ja: Zeitpunkte:

8.1.19 Hauptzielgröße:

8.1.20 Nullhypothese(n): -

8.1.21 Alternativhypothese(n): -

8.1.22 Nebenzielgrößen:

8.2 Studienplanung

Die Fallzahlberechnung basiert auf (Alpha = Fehler 1. Art, Power = 1 – Beta = 1 – Fehler 2. Art):

8.2.1 Alpha: 8.2.2 Power: 8.2.3 Stat.Verfahren:

8.2.4 Multiples Testen: nein ja: Korrekturverfahren.:

8.2.5 Erwartete Anzahl von Studienabbrecher/inne/n (Drop-out-Quote):

8.3 Geplante statistische Analyse

Population: 8.3.1 Intention-to-treat 8.3.2 Per protocol

8.3.3 Zwischenauswertung: nein ja: Abbruchkriterien:

8.3.4 Geplante statistische Verfahren: **deskriptive Statistik, Mittelwert, Standardabweichung, Korrelationstests (Korrelationskoeffizienten nach Pearson), stat. Auswertung werden mittels spezieller Software (OriginLab) durchgeführt, siehe auch Studienprotokoll.**

8.4 Dokumentationsbögen / Datenmanagement

8.4.1 Angaben zur Datenqualitätsprüfung

8.4.2 Angaben zum Datenmanagement

Patientenbezogene Daten werden nur in anonymisierter / codierter Form mit den Analyseergebnissen verglichen. (Eurotransplant Nummer) Die relevanten Daten werden unmittelbar nach der Explantation auf Dokumentationsbögen übertragen, so dass keine Beziehung zwischen den Daten einerseits und der Identität der Patienten andererseits hergestellt werden kann. Da die zu erwartenden Ergebnisse derzeit nicht unmittelbar für die Therapie (von Blutsverwandten) relevant sind, ist eine Weiterleitung der erzielten wissenschaftlichen Ergebnisse an die jeweiligen Angehörigen im Rahmen der Studie nicht vorgesehen. Die Sammlung der anonymisierten Daten und das Datenmanagement, sowie statistische Berechnungen erfolgen am Institut für Biomechanik, Technische Universität Graz.

8.5 Verantwortliche und Qualifikation

8.5.1 Wer führte die biometrische Planung durch (ggf. Nachweis der Qualifikation)?

DI Dr. Gerhard Sommer, Prof. Dr. Gerhard A. Holzapfel

8.5.2 Wer wird die statistische Auswertung durchführen (ggf. Nachweis der Qualifikation)?

Michael Kutschera (triaxiale Scherversuche), Roland Kresnik (biaxiale Zugversuche), Statistiker des Institutes für Biomechanik, TU Graz

5 Appendix

8.6 Datenschutz

8.6.1 Die Datenverarbeitung erfolgt a) personenbezogen b) indirekt personenbezogen
c) nicht personenbezogen

8.6.2 Wenn a): Begründung:

DVR-Nummer:

8.6.3 Wenn b): Wie erfolgt die Verschlüsselung?

Sämtliche Daten werden im Datenblatt anonym geführt.

5.3 Ethics applicant - Clinical Department of Transplant Surgery

9. Liste der eingereichten Unterlagen (wenn nicht gesondert dem Antrag beiliegend):

Dokument	Version/Identifikation	Datum
Protokoll	BiomechMyocard V2.0	14.12.11
Kurzfassung		
Patienteninformation / Einwilligungserklärung		
Prüfbogen (Case Report Form, CRF)		
Versicherungsbestätigung		
Amendment Nr.		
Amendment Nr.		
Amendment Nr.		
Lokales Amendment Nr.		

Name und Unterschrift der Antragstellerin/des Antragstellers

- 9.1 Name: **Dr. med.univ. Michaela Schwarz**
 9.2 Institution/ Firma: **Klinische Abteilung für Transplantationschirurgie**
 9.3 Position: **Assistenzärztin in Ausbildung**
 9.4 Antragsteller/in ist 9.4.1 koordinierende/r Prüfer/in (multizentrische Studie)
 (nur AMG-Studien) 9.4.2 Hauptprüfer/in (monozentrische Studie)
 9.4.3 Sponsor bzw. Vertreter/in des Sponsors
 9.4.4 vom Sponsor autorisierte Person/Organisation

Ich bestätige hiermit, dass die in diesem Antrag gemachten Angaben korrekt sind und dass ich der Meinung bin, dass die Durchführung der Studie in Übereinstimmung mit dem Protokoll, nationalen Regelungen und mit den Prinzipien der Guten Klinischen Praxis möglich sein wird.

Weiters stimme ich mit meiner Unterschrift zu, dass folgende Daten aus meinem Antrag ggf. durch die Ethikkommission veröffentlicht werden, um die Anträge nach Zahl und Inhalt transparent zu machen: EK-Nummer, Einreich-Datum, Projekttitel, Hauptprüfer, Sponsor/CRO, weitere Zentren.
 (Im Falle der Nicht-Zustimmung bitte diesen Absatz durchzustreichen)

.....
 Unterschrift der Antragstellerin/des Antragstellers

.....
 Datum

!!! Achtung: Diese Unterschrift ist in jedem Fall erforderlich !!!

Teil B

Studienkurzbezeichnung: Biomechanik des humanen Ventrikels

10. Angaben zur Prüferin/zum Prüfer

10.1 Name: **Dr. med.univ. Michaela Schwarz**

10.2 Krankenanstalt/Institut/Abteilung: **Klinische Abteilung für Transplantationschirurgie**

10.3 Telefon	10.4 „Pieps“/Mobil	10.5 Fax	10.6 e-mail-Adresse:
385 84444	385 80678	385 14446	michaela.schwarz@medunigraz.at

10.7 Jus practicandi: ja nein 10.8 Facharzt für:

10.9 Prüfärztekurs: ja nein

10.10 Sofern relevant: Präklinische Qualifikation (z.B. Labordiagnostik) bzw. Name der Verantwortlichen:

11. Geplante Anzahl der PatientInnen bzw. ProbandInnen an dieser Prüfstelle 30

12. Verantwortliche MitarbeiterInnen an der klinischen Studie (an Ihrer Prüfstelle)

Fr/Hr	Titel	Vorname	Name	Institution
Hr.	Dr.	Gerhard	Sommer	Inst. f. Biomechanik, TU Graz
Hr.	Prof. Dr.	Gerhard A.	Holzapfel	Inst. f. Biomechanik, TU Graz

13. Unterschrift der Prüferin/des Prüfers

Ich bestätige hiermit, dass die in diesem Antrag gemachten Angaben korrekt sind und dass ich der Meinung bin, dass die Durchführung der Studie in Übereinstimmung mit dem Protokoll, nationalen Regelungen und mit den Prinzipien der Guten Klinischen Praxis möglich sein wird.

.....
Unterschrift der Prüferin/des Prüfers
Datum

Bei multizentrischen AMG-Studien sind die Teile B von der Hauptprüferin/dem Hauptprüfer des jeweiligen Zentrums zu unterzeichnen. Alternativ zur Unterschrift auf den Teilen B können die Unterschriften der Hauptprüfer/innen auch auf den Unterschriftenseiten des Protokolls oder der Prüfärzterträge vorgelegt werden. Es muss jedenfalls eine eindeutige - durch Unterschrift dokumentierte - Zustimmung aller Hauptprüfer/innen zum Protokoll vorliegen.

14. Name und Unterschrift der Leiterin/des Leiters der Einrichtung* des Pflegedienstes*

14.1 Name: **Univ. Prof. Dr. Karlheinz Tscheliessnigg**

.....
Unterschrift der Leiterin/des Leiters
Datum

** Die Unterschrift der Leiterin/des Leiters des Pflegedienstes ist für Pflegeforschungsprojekte und die Anwendung neuer Pflegekonzepte und -methoden erforderlich, ansonsten die Unterschrift der Leiterin/des Leiters der jeweiligen Einrichtung. Einrichtung: die Klinik (wenn gegliedert: die klinische Abteilung), die Abteilung oder die gemeinsame Einrichtung*

!!! Achtung: Teil B ist in jedem Fall vollständig auszufüllen, bei multizentrischen klinischen Prüfungen nach AMG für jedes in Österreich teilnehmende Zentrum separat !!!

5.3 Ethics applicant - Clinical Department of Transplant Surgery

Ethikkommission



Medizinische Universität Graz

Auenbruggerplatz 2, A-8036 Graz
ethikkommission@medunigraz.at
Tel.: +43 / 316 / 385-13928, Fax: -14348

VOTUM gültig bis 16.12.2012

EK-Nummer: 24-107 ex 11/12
Studientitel: Biomechanik menschlicher ventrikulärer Myokarde (biaxialer Zugversuch, triaxialer Scherversuch)
Prüfer: *) Dr. Michaela Schwarz
Univ.Klinik für Chirurgie
Sponsor: (Prüfer)
CRO: -

*) Antragsteller

Die o.a. Studie wurde von der Ethikkommission erstmals in der Sitzung 03-11/12 am 12.12.2011 behandelt.

Die Ethikkommission ist zu folgendem Schluss gekommen:

Es besteht kein Einwand gegen die Durchführung der Studie in der vorliegenden Form.

Stimmberechtigte bzw. anwesende Mitglieder bei der Behandlung waren: Siehe beiliegende Liste vom 12.12.2011.

Kommissionsmitglieder, die für diesen Tagesordnungspunkt als befangen anzusehen waren und daher gemäß Geschäftsordnung an der Entscheidungsfindung und Abstimmung nicht teilgenommen haben: keine

Zur Beurteilung vorliegende Dokumente:

Dokumente eingegangen am 18.11.2011, begutachtet in der Sitzung 03-11/12 am 12.12.2011	
✓ Antragsformular	18.11.2011
Originalprotokoll November 2011	
Dokumente eingegangen am 30.11.2011, begutachtet in der Sitzung 03-11/12 am 12.12.2011	
Originalprotokoll November 2011	
Dokumente eingegangen am 05.12.2011, begutachtet in der Sitzung 03-11/12 am 12.12.2011	
✓ Sonstiges: Stellungnahme Prof. Pieske	01.12.2011
Dokumente eingegangen am 14.12.2011, begutachtet im 'expedited Review' am 16.12.2011	
✓ Originalprotokoll 2.0	14.12.2011

Es handelt sich um eine Studie im Rahmen einer Diplomarbeit.

Das Votum der Ethikkommission berührt in keiner Weise die alleinige Verantwortung der Prüferin / des Prüfers / der Prüfer für die ordnungsgemäße Durchführung der Studie unter Einhaltung aller einschlägiger gesetzlicher Bestimmungen und Richtlinien.

Weiters machen wir darauf aufmerksam, dass der Kommission unverzüglich zu melden sind:

- Abweichungen vom Protokoll aus Sicherheitsgründen oder Protokolländerungen
- Änderungen, die das Risiko der Teilnehmer/-innen erhöhen oder die Durchführung der Studie wesentlich beeinflussen
- Mutmaßliche unerwartete schwerwiegende Nebenwirkungen - SUSARs (AMG-Studien ab 1.5.2004)

EK-Nummer: 24-107 ex 11/12

Votum

Seite 1 von 2

Medizinische Universität Graz, Universitätsplatz 3, A-8010 Graz. www.medunigraz.at

Rechtsform: Juristische Person öffentlichen Rechts gem. Universitätsgesetz 2002. Information: Mitteilungsblatt der Universität und www.medunigraz.at. DVR-Nr. 210 9494.
UID: ATU 575 111 79. Bankverbindung: Bank Austria Creditanstalt BLZ 12000 Konto-Nr. 500 948 400 04, Raiffeisen Landesbank Steiermark BLZ 38000 Konto-Nr. 49510.


5 Appendix

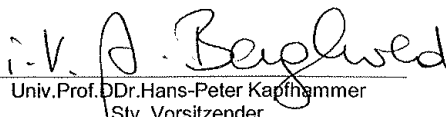
oder schwerwiegende unerwünschte Ereignisse - SAEs (andere Studien)

- Jegliche Information über sonstige Umstände, die die Sicherheit der Teilnehmer/-innen oder die Durchführung der Studie beeinträchtigen können

Dieses Votum gilt für ein Jahr ab dem Datum der Ausstellung. Bei längerer Studiendauer ist rechtzeitig vor Ablauf der Gültigkeit des Votums ein Zwischenbericht vorzulegen (Berichtsformular), um eine etwaige Verlängerung zu erlangen.

Graz, 16. Dezember 2011


Univ.-Prof. Dr. Peter H. Renak
Vorsitzender


Univ.-Prof. Dr. Hans-Peter Kapfhammer
Stv. Vorsitzender

Achtung: Bitte bei allen das Projekt betreffende Schreiben oder telefonischen Anfragen die EK-Nummer angeben!

5.3 Ethics applicant - Clinical Department of Transplant Surgery

Ethikkommission



Medizinische Universität Graz

Auenbruggerplatz 2, A-8036 Graz
ethikkommission@medunigraz.at
Tel.: +43 / 316 / 385-13928, Fax: -14348

Liste der stimmberechtigten bzw. anwesenden Mitglieder

am 12. Dezember 2011

Univ.Prof.DI Dr.Andrea Berghold
Univ.Prof.Dr.Josef Donnerer
Univ.Prof.Mag.Dr.H.Jesser-Huß
Univ.Prof.Dr.Elisabeth Mahla
Univ.Prof.Dr. Leopold Neuhold
Univ.Prof.DI Dr.Peter H. Rehak
Univ.Prof.Dr.Ekkehard Ring
OPfl. DGKP Thomas Schelischansky, MSc
Univ.Prof.Dr. Michael Speicher
Univ.Prof.Dr.Rudolf Stauber
Mag.Monika Steinwender
Univ.Prof.Dr.Hermann Toplak
Ursula Vennemann
Univ.Prof.Dr.Kurt Weber
Univ.Prof.Dr.Andreas Zimmer
Ing.Franz Deutschmann
Doz.Dr.Christian Fazekas
Univ.Prof.DI Dr.Josef Haas
Univ.Prof.DDr.Hans-Peter Kapfhammer

Beigezogene Fachärzte

PD Dr.Philipp Klaritsch

EK-Nummer: 24-107 ex 11/12

Mitgliederliste

Medizinische Universität Graz, Universitätsplatz 3, A-8010 Graz. www.medunigraz.at

Rechtsform: Juristische Person öffentlichen Rechts gem. Universitätsgesetz 2002. Information: Mitteilungsblatt der Universität und www.medunigraz.at. DVR-Nr. 210 9494.
UID: ATU 575 111 79. Bankverbindung: Bank Austria Creditanstalt BLZ 12000 Konto-Nr. 500 948 400 04, Raiffeisen Landesbank Steiermark BLZ 38000 Konto-Nr. 49510.

5 Appendix

Antrag	
Version 6.3 vom 25.03.2011	Bitte immer die <u>aktuelle</u> Version verwenden (http://ethikkommissionen.at)!

Dieses Formular soll für Einreichungen bei österreichischen Ethikkommissionen verwendet werden.
 Es setzt sich aus einem allgemeinen **Teil A** - Angaben zur Studie und zum Sponsor -
 und aus einem speziellen **Teil B** - Angaben zu der/den einzelnen Prüfstelle(n) - zusammen.
 Bei Einreichungen für mehrere Zentren (Prüfer/innen) muss nur der Teil B an das jeweilige Zentrum angepasst werden.

Adresse der Ethikkommission (optional) An die Ethikkommission der Medizinischen Universität Graz LKH Universitätsklinikum Auenbruggerplatz 2, 3. OG A-8036 Graz	Raum für Eingangsstempel, EK-Nummer, etc. Bitte Freilassen!
---	--

ANTRAG AUF BEURTEILUNG EINES KLINISCHEN FORSCHUNGSPROJEKTES

für folgende Prüfer/innen bei folgenden österreichischen Ethikkommissionen:

- ▶ Bitte **alle** Ethikkommissionen eintragen, an die der Antrag gesendet wird (**Kurzbezeichnung!**) ◀
- ▶ Im Falle einer **multizentrischen Arzneimittelstudie** ist die **Leitethikkommission** als erste anzuführen! ◀

Zuständige Ethikkommission	Prüferin/Prüfer (lokale Studienleitung)
Ethikkommission Graz	Prof. Dr. Peter Regitnig

Teil A

1. Allgemeines:

- 1.1 Projekttitel: **Biomechanik humaner ventrikulärer Myokardien (Fortsetzung)**
- 1.2 Protokollnummer/-bezeichnung: **BiomechMyocard V 1.1** 1.2.1 EudraCT-Nr.:
- 1.3 Datum des Protokolls: **15.08.2011** 1.3.1 ISRCTN-Nr.:
- 1.4 Daten der beiliegenden Amendments: 1.4.1 Nr. 1.4.2 Datum:
- 1.4.3 Nr. 1.4.4 Datum:
- 1.4.5 Nr. 1.4.6 Datum:

1.5 Sponsor / RechnungsempfängerIn (Kontaktperson in der Buchhaltung):

- | | | | |
|----------------------|----------------|--|-----------------------------|
| | <u>Sponsor</u> | | <u>RechnungsempfängerIn</u> |
| 1.5.1 Name: | keine | | |
| 1.5.2 Adresse: | | | |
| 1.5.3 Kontaktperson: | | | |
| 1.5.4 Telefon: | | | |
| 1.5.5 FAX: | | | |
| 1.5.6 e-mail: | | | |
| 1.5.7 UID-Nummer | | | |

(wenn nicht gleich wie „Sponsor“)

5.4 Ethics applicant - Clinical Department of Pathology

2. Eckdaten der Studie

- 2.1 Art des Projektes: 2.1.1 Klinische Prüfung eines nicht registrierten **Arzneimittels**
 2.1.2 Klinische Prüfung eines registrierten **Arzneimittels**
 2.1.2.1 gemäß der Indikation 2.1.2.2 nicht gemäß der Indikation
 2.1.3 Klinische Prüfung einer neuen **medizinischen Methode**
 2.1.4 Klinische Prüfung eines **Medizinproduktes**
 2.1.4.1 mit CE-Kennzeichnung 2.1.4.2 ohne CE-Kennzeichnung
 2.1.4.3 Leistungsbewertungsprüfung (In-vitro-Diagnostika)
 2.1.5 **Nicht-therapeutische biomedizinische Forschung** am Menschen
(Grundlagenforschung)
 2.1.6 **Genetische Untersuchung**
 2.1.10 **Register**
 2.1.11 **Biobank**
 2.1.12 **Retrospektive Datenauswertung**
 2.1.13 **Fragebogen Untersuchung**
 2.1.14 **Psychologische Studie**
 2.1.15 **Pflegewissenschaftliche Studie**
 2.1.16 **Nicht-interventionelle Studie (NIS)**
 2.1.7 **Sonstiges** (z.B. Diätetik, Epidemiologie, etc.), bitte spezifizieren:

Zusatzinformation: 2.1.8 **Dissertation** 2.1.9 **Diplomarbeit**

2.2 Fachgebiet: **Pathologie, Biomechanik**

2.3 Arzneimittelstudie (wenn zutreffend)

2.4 Medizinproduktstudie (wenn zutreffend)

2.3.1 Prüfsubstanz(en):

2.4.1 Prüfprodukt(e):

2.3.2 Referenzsubstanz:

2.4.2 Referenzprodukt:

2.5 Klinische Phase: _____ (unbedingt angeben, bei Medizinprodukten die am ehesten zutreffende Phase)

2.6 Nehmen andere Zentren an der Studie teil: ja nein. Wenn **ja**:

2.6.1 im Inland

2.6.2 im Ausland

2.7 Liste der Zentren: **Institut für Pathologie, Medizinische Universität Graz**
Institut für Biomechanik, Technische Universität Graz

2.8 Liegen bereits Voten anderer Ethikkommissionen vor?

ja nein. Wenn **ja**, **Voten beilegen!**

2.9 Geplante **Gesamtzahl** der **Prüfungsteilnehmer/innen** (in allen teilnehmenden Zentren):

30

2.10 Charakterisierung der Prüfungsteilnehmer/innen: 2.10.1 Mindestalter: 2.10.2 Höchstalter:

2.10.3 Sind auch nicht persönlich Einwilligungsfähige einschließbar? ja nein

2.10.4 Einschließbar sind weibliche (und/oder) männliche Teilnehmer/innen.

2.10.5 Sind gebärfähige Frauen einschließbar? ja nein. Wenn **nein**: Begründung unter 7.5

5 Appendix

2.11 Dauer der Teilnahme der einzelnen Prüfungsteilnehmer/innen an der Studie: **nicht zutreffend**

2.11.1 Aktive Phase:

2.11.2 Nachkontrollen:

2.12 Voraussichtliche Gesamtdauer der Studie: **2 Jahre**

3a. Betrifft nur Studien gemäß AMG: Angaben zur Prüfsubstanz (falls nicht in Österreich registriert):

3.1 Registrierung in anderen Staaten? ja nein. Wenn **ja**, geben Sie an, in welchen:

3.2 Liegen über das zu prüfende Arzneimittel bereits aussagekräftige Ergebnisse von klinischen Prüfungen vor? ja nein

Wenn **ja**, bitte geben Sie folgende Daten an:

3.2.1 In welchen Staaten wurden die Prüfungen durchgeführt:

3.2.2 Phase: _____ (Wenn Studien in mehreren Phasen angeführt sind, die höchste Phase angeben)

3.2.3 Zeitraum:

3.2.4 Anwendungsart(en):

3.2.5 Wurde(n) die klinische(n) Prüfung(en) gemäß GCP-Richtlinien durchgeführt? ja nein

3.2.6 Liegt ein Abschlußbericht vor? ja nein

Wenn **ja**, bitte legen Sie die **Investigator's Brochure, relevante Daten** oder ein **Gutachten des Arzneimittelbeirates** bei.

3b. Sonstige im Rahmen der Studie verabreichte Medikamente, deren Wirksamkeit und/oder Sicherheit nicht Gegenstand der Prüfung sind:

Generic Name	Darreichungsform	Dosis

4. Betrifft nur Studien gemäß MPG: Angaben zum Medizinprodukt:

4.1 Bezeichnung des Produktes:

4.2 Hersteller:

4.3 Zertifiziert für diese Indikation: ja nein

4.4 Zertifiziert, aber für eine andere Indikation: ja nein

4.5 Das Medizinprodukt trägt ein CE-Zeichen ja nein

4.6 Die Produktbroschüre liegt bei.

4.7 Welche Bestimmungen bzw. Normen sind für die Konstruktion und Prüfung des Medizinproduktes herangezogen worden (Technische Sicherheit):

4.8 Allfällige Abweichungen von den o.a. Bestimmungen (Normen):

5.4 Ethics applicant - Clinical Department of Pathology

5. Angaben zur Versicherung (gemäß §32 Abs.1 Z.11 und Z.12 und Abs.2 AMG; §§47 und 48 MPG)

5.1 Eine Versicherung ist erforderlich: ja nein. Wenn ja:

5.1.1 Versicherungsgesellschaft

5.1.2 Adresse:

5.1.3 Telefon:

5.1.4 Polizzenummer:

5.1.5 Gültigkeitsdauer:

Diese Angaben müssen in der Patienten- / Probandeninformation enthalten sein!

7. Strukturierte Kurzfassung des Projektes (*in deutscher Sprache, kein Verweis auf das Protokoll*)

<p>7.1 Wenn Original-Projekttitle nicht in Deutsch: Deutsche Übersetzung des Titels: Biomechanik humaner ventrikulärer Myokardien (Biaxiale und triaxiale mechanische Untersuchung)</p>
<p>7.2 Zusammenfassung des Projektes (Rechtfertigung, Relevanz, Design, Maßnahmen und Vorgehensweise):</p> <p>Das mechanische Verhalten der Ventrikel des menschlichen Myokards (linker Ventrikel, rechter Ventrikel und Septum), im Speziellen der Muskelzellen und der umliegenden kollagenen Faserkomponenten, ist bis dato noch sehr dürftig erforscht. Eine systematische, biomechanische, mikrostrukturelle und histologische Untersuchung des humanen Herzmuskels soll daher durchgeführt werden.</p> <p>Daten aus biaxialen Zugversuchen am menschlichen Myokardgewebe existieren bis heute nur in sehr geringem Ausmaß, Daten aus triaxialen Scherversuchen existieren de facto gar nicht.</p> <p>Insbesondere sind die Einflüsse der zu Verbänden von mehrlagig angeordneten Muskelfasern zusammengesetzten sogenannten Sheet-Strukturen zu erfassen. Dazu werden Gewebescheiben in Hauptmuskelfaserrichtung mittels biaxialen Zugversuchen unter verschiedenen Lastprotokollen biomechanisch getestet. Neben den biaxialen Zugversuchen sollen die Schereigenschaften des Myokards auch mit Hilfe eines triaxialen Kraftaufnehmers, entsprechend der Koordinatenachsen die sich aus der Muskelfaserrichtung und Sheets ergeben, gemessen werden. Die daraus resultierenden Ergebnisse, sollen vor allem auch einer späteren mathematischen Modellierung dienen, welche die Einhaltung der drei Dimensionen unbedingt voraussetzt.</p> <p>Anschließend werden die laminare Struktur und Komponenten der geprüften Bereiche histologisch untersucht. Die folglich erhaltene räumliche Mikrostruktur der mechanisch relevanten Komponenten soll Aufschluss über noch nicht verstandene Einflüsse der Sheet-Strukturen auf die Stabilität des Herzwandgewebes geben. Derartig kombinierte biomechanische Daten von humanen Herzmuskelgeweben existieren bis heute nur in sehr geringem Ausmaß.</p> <p>Das Projekt erstreckt sich weniger über eine geplante Dauer, als über ein Versuchskontingent von mindestens 30 menschlichen Herzen. Dabei sollen jeweils beide Ventrikel eines menschlichen Herzens post-mortem getestet werden. Für die biaxialen mechanischen Untersuchungen sind die Herzen so zu beschneiden, dass sich je 3 Proben aus der lateralen Wand des linken Ventrikels, sowie je 2 Proben aus dem Septum und der medialen Wand des rechten Ventrikels extrahieren lassen. Für Untersuchungen der triaxialen Schereigenschaften werden, jeweils 3 Würfel vom linken und rechten Ventrikel in einem Winkel von 45° zur Base entnommen.</p> <p>Es sind keine Atria, Herzohren, Klappen oder versorgende Gefäße zur Untersuchung nötig. Die Ventrikel werden nur im Rahmen von routinemäßigen, klinischen Obduktionen entnommen und in einer dem Blut gleichzusetzenden Flüssigkeit gelagert (gepufferte physiologische Kochsalzlösung). Selbige dient dazu, fortschreitende Autolyse zu minimieren. Die Tests an den Proben aus dem Herzgewebe finden aufgrund der Autolyse auch innerhalb der folgenden 24h statt. Nach Abschluss werden die Gewebeproben in Formalin fixiert, um die mikroskopischen Struktur-Untersuchungen durchführen zu können.</p> <p>Folgende Maßnahmen bzw. Voraussetzungen werden bei der Präparateentnahme berücksichtigt (die klinische Obduktion wird durch die Probenentnahme nicht beeinträchtigt - siehe auch 7.6.):</p> <ol style="list-style-type: none"> 1) Die Ventrikelproben werden nach der klinischen Obduktion in gepufferter physiologischer Kochsalzlösung gelagert. 2) Extraktion der quadratischen Proben für den biaxialen Zugversuch aus dem spezifizierten Herzgewebe der Ventrikel und zusätzliche Extraktion der würfelförmigen Proben aus den Ventrikel für den triaxialen Scherversuch. 3) Erfassung der Hauptfaserrichtungen der Gewebeer- und Gewebegrundflächen durch mikroskopische Untersuchung für die biaxialen Zugversuche. (biaxial) <p>Erfassung der Sheet-Strukturen und Muskelfaserrichtung durch eine mikroskopische Untersuchung bzw. mit Hilfe eines Vergrößerungsglases für die triaxialen Scherversuche. (triaxial)</p> <ol style="list-style-type: none"> 4) Zuschneiden der Proben in definierter Größe (25x25x2,5mm) (LxBxT) in der mittleren Hauptfaserrichtung. (biaxial) <p>Zuschneiden der Proben in definierter Größe (4x4x4mm) (LxBxH) entsprechend eines definierten Koordinatensystems. (triaxial)</p> <ol style="list-style-type: none"> 5) Biaxial: Proben mit quadratischem Grundriss für die biaxialen mechanischen Untersuchungen

5.4 Ethics applicant - Clinical Department of Pathology

<p>werden aus dem Herzgewebe präpariert. Biaxiale Zugversuche mit verschiedenen Lastprotokollen bezüglich der Axial- und Umfangsrichtung werden an den Proben durchgeführt, wobei die Deformation der Probe berührungsfrei mit einem Videoextensometer bestimmt wird.</p> <p>Triaxial: Die extrahierten würfelförmigen Proben werden mit Hilfe eines Videoextensometers nachgemessen und deren Spannungs-Dehnungs-Kurven durch die Scherversuchsanlage aufgezeichnet.</p> <p>6) Histologische Untersuchungen der getesteten Proben hinsichtlich der Verteilung und des Vorkommens besagter Herzfaserverbände (den sog. Sheets) mit Spezialfärbung der elastischen und kollagenen Fasern.</p>
<p>7.3 Ergebnisse der prä-klinischen Tests oder Begründung für den Verzicht auf prä-klinischen Tests: In einer Pilot-Studie konnte gezeigt werden, dass biaxiale und triaxiale Tests an 15 frischen Schweineherzen eine deutliche Relevanz der Sheet-Struktur auf die biomechanischen Eigenschaften des ventrikulären Myokards erkennen lassen. Da diese Eigenschaften bei verschiedenen Spezies deutliche Unterschiede aufweisen, soll diese Abhängigkeit nun auch am humanen Myokard überprüft bzw. nachgewiesen werden.</p>
<p>7.4 Primäre Hypothese der Studie (wenn relevant auch sekundäre Hypothesen): Die biaxiale und triaxiale Untersuchung der biomechanischen Eigenschaften und deren Variation in Zusammenhang mit den erhaltenen Sheet-Strukturen der Gewebeprobe, soll den wesentlichen Einfluss der Herzmuskelfaserverbände (Sheets) auf die Systemeigenschaften des Myokardiums nachweisen und beschreiben. Dadurch werden grundlegende, mechanische und bis dato nicht existente Daten der Mechanik des ventrikulären Herzmuskelgewebes gewonnen und diese für computerunterstützte Simulationen nutzbar gemacht.</p>
<p>7.5 Relevante Ein- und Ausschlusskriterien: Nur Ventrikel normaler Größe und Wanddicke und ohne frische oder alte ischämische Veränderungen können zur Entnahme und Extraktion der angegebenen Anzahl an Proben dienen.</p>
<p>7.6 Ethische Überlegungen (Identifizieren und beschreiben Sie alle möglicherweise auftretenden Probleme. Beschreiben Sie den möglichen Wissenszuwachs, der durch die Studie erzielt werden soll und seine Bedeutung, sowie mögliche Risiken für Schädigungen oder Belastungen der Prüfungsteilnehmer/innen. Legen Sie Ihre eigene Bewertung des Nutzen/Risiko-Verhältnisses dar):</p> <ol style="list-style-type: none"> 1. Die Manipulationen werden nur an Leichen durchgeführt, die auch zur pathologischen Obduktion vorgesehen sind. Das bedeutet, dass die Indikation zur Obduktion zuvor und unabhängig von eventuell geplanten zusätzlichen Manipulationen gestellt wird. 2. Die Manipulationen dürfen die Bestimmung der Todesursache und somit das Ziel der Obduktion nicht behindern oder unmöglich machen. Soweit möglich, soll die Manipulation nach der Obduktion durchgeführt werden. 3. Die Manipulationen müssen in den Räumen des Institutes für Pathologie, die auch zur Obduktion dienen erfolgen. 4. Die Freigabe der Leichen zur Bestattung darf nicht verzögert werden, d.h. Obduktion und Manipulation sollen am selben Tag durchgeführt werden. 5. Der für die Manipulation verantwortliche Arzt ist während der gesamten Dauer des Eingriffs anwesend. 6. Bei jeder Manipulation wird ein Protokoll geführt, das die Daten der Leiche sowie Art und Zweck der Manipulation beinhaltet. 7. Die Manipulationen erfolgen in pietätvoller Weise. 8. Die Manipulationen dienen keinem finanziellen Zweck. 9. Die Manipulationen dienen einer klaren Zielsetzung, die zukünftig der ärztlichen Betreuung von Patienten dient. 10. Die Manipulationen entstellen die sichtbaren Teile der Leiche nicht.
<p>7.7 Begründung für den Einschluss von Personen aus geschützten Gruppen (z.B. Minderjährige, temporär oder permanent nicht-einwilligungsfähige Personen; wenn zutreffend):</p>
<p>7.8 Beschreibung des Rekrutierungsverfahrens</p>

5 Appendix

(alle zur Verwendung bestimmte Materialien, z.B. Insetate inkl. Layout müssen beigelegt werden): Entnahme von Gewebe im Rahmen von routinemäßig durchgeführten klinischen Obduktionen am Institut für Pathologie der Medizinischen Universität Graz.
7.9 Vorgehensweise an der/den Prüfstelle(n) zur Information und Erlangung der informierten Einwilligung von Prüfungsteilnehmer/inne/n, bzw. Eltern oder gesetzlichen Vertreter/inne/n, wenn zutreffend (wer wird informieren und wann, Erfordernis für gesetzliche Vertretung, Zeugen, etc.):
7.10 Risikoabschätzung, vorhersehbare Risiken der Behandlung und sonstiger Verfahren, die verwendet werden sollen (inkl. Schmerzen, Unannehmlichkeiten, Verletzung der persönlichen Integrität und Maßnahmen zur Vermeidung und/oder Versorgung von unvorhergesehenen / unerwünschten Ereignissen):
7.11 Voraussichtliche Vorteile für die eingeschlossenen Prüfungsteilnehmer/innen:
7.12 Relation zwischen Prüfungsteilnehmer/in und Prüfer/in (z.B. Patient/in - Ärztin/Arzt, Student/in - Lehrer/in, Dienstnehmer/in - Dienstgeber/in, etc.):
7.13 Verfahren an der/den Prüfstelle(n) zur Feststellung, ob eine einzuschließende Person gleichzeitig an einer anderen Studie teilnimmt oder ob eine erforderliche Zeitspanne seit einer Teilnahme an einer anderen Studie verstrichen ist (von besonderer Bedeutung, wenn gesunde Proband/inn/en in pharmakologische Studien eingeschlossen werden):
7.14 Methoden, um unerwünschte Effekte ausfindig zu machen, sie aufzuzeichnen und zu berichten (Beschreiben Sie wann, von wem und wie, z.B. freies Befragen und/oder an Hand von Listen):
7.15 Optional: Statistische Überlegungen und Gründe für die Anzahl der Personen, die in die Studie eingeschlossen werden sollen (ergänzende Informationen zu Punkt 8, wenn erforderlich): In bekannter Literatur weisen Studien dieses Umfanges an tierischem Gewebe bereits gute Aussagekraft über die biomechanischen Zusammenhänge auf.
7.16 Optional: Verwendete Verfahren zum Schutz der Vertraulichkeit der erhobenen Daten, der Quelldokumente und von Proben (ergänzende Informationen zu Punkt 8, wenn erforderlich): Patientenbezogene Daten (Alter, Geschlecht, Grundkrankheit, Todesursache) werden nur in anonymisierter Form mit den Analyseergebnissen verglichen, so dass keine Beziehung zwischen den Daten einerseits und der Identität der Patienten andererseits hergestellt werden kann.
7.17 Plan zur Behandlung oder Versorgung nachdem die Personen ihre Teilnahme an der Studie beendet haben (wer wird verantwortlich sein und wo): -
7.18 Betrag und Verfahren der Entschädigung oder Vergütung an die Prüfungsteilnehmer/innen (Beschreibung des Betrages, der während der Prüfungsteilnahme bezahlt wird und wofür, z.B. Fahrtspesen, Einkommensverlust, Schmerzen und Unannehmlichkeiten, etc.): -
7.19 Regeln für das Aussetzen oder vorzeitige Beenden der Studie an der/den Prüfstelle(n) in diesem Mitgliedstaat oder der gesamten Studie: -
7.20 Vereinbarung über den Zugriff der Prüferin/des Prüfers/der Prüfer auf Daten, Publikationsrichtlinien, etc. (wenn nicht im Protokoll dargestellt): Daten die in Publikationen veröffentlicht werden unterliegen den strengen Kriterien der Journals und sind anonymisiert.
7.21 Finanzierung der Studie (wenn nicht im Protokoll dargestellt) und Informationen über finanzielle oder andere Interessen der Prüferin/des Prüfers/der Prüfer:

5.4 Ethics applicant - Clinical Department of Pathology

Institutseigene Mittel, FWF Einzelprojekt-Forschungsförderung
7.22 Weitere Informationen (wenn erforderlich): -

8. Biometrie, Datenschutz:

(Hier nur Kurzinformationen in Stichworten, ausführlicher - wenn erforderlich - unter Punkt 7.15 und 7.16)

8.1 Studiendesign (z.B. doppelblind, randomisiert, kontrolliert, Placebo, Parallelgruppen, multizentrisch)

- 8.1.1 offen 8.1.2 randomisiert 8.1.3 Parallelgruppen 8.1.4 monozentrisch
 8.1.5 blind 8.1.6 kontrolliert 8.1.7 cross-over 8.1.8 multizentrisch
 8.1.9 doppelblind 8.1.10 Placebo 8.1.11 faktoriell 8.1.12 Pilotprojekt
 8.1.13 observer-blinded 8.1.14 Äquivalenzprüfung
 8.1.15 sonstiges:

8.1.16 Anzahl der Gruppen:

8.1.17 Stratifizierung: nein ja: Kriterien:

8.1.18 Messwiederholungen: nein ja: Zeitpunkte:

8.1.19 Hauptzielgröße:

8.1.20 Nullhypothese(n): -

8.1.21 Alternativhypothese(n): -

8.1.22 Nebenzielgrößen:

8.2 Studienplanung

Die Fallzahlberechnung basiert auf (Alpha = Fehler 1. Art, Power = 1 – Beta = 1 – Fehler 2. Art):

8.2.1 Alpha: 8.2.2 Power: 8.2.3 Stat.Verfahren:

8.2.4 Multiples Testen: nein ja: Korrekturverfahren.:

8.2.5 Erwartete Anzahl von Studienabbrecher/inne/n (Drop-out-Quote):

8.3 Geplante statistische Analyse

Population: 8.3.1 Intention-to-treat 8.3.2 Per protocol

8.3.3 Zwischenauswertung: nein ja: Abbruchkriterien:

8.3.4 Geplante statistische Verfahren: **deskriptive Statistik, Mittelwert, Standardfehler, Konfidenzintervall, biomechanische Auswertung mittels spezieller Software (OriginLab).**

8.4 Dokumentationsbögen / Datenmanagement

8.4.1 Angaben zur Datenqualitätsprüfung

8.4.2 Angaben zum Datenmanagement

Patientenbezogene Daten werden nur in anonymisierter / codierter Form mit den Analyseergebnissen verglichen. Die relevanten Daten werden unmittelbar nach der Obduktion auf Dokumentationsbögen übertragen, so dass keine Beziehung zwischen den Daten einerseits und der Identität der Patienten andererseits hergestellt werden kann. Da die zu erwartenden Ergebnisse derzeit nicht unmittelbar für die Therapie (von Blutsverwandten) relevant sind, ist eine Weiterleitung der erzielten wissenschaftlichen Ergebnisse an die jeweiligen Angehörigen im Rahmen der Studie nicht vorgesehen. Die Sammlung der anonymisierten Daten und das Datenmanagement, sowie statistische Berechnungen erfolgen am Institut für Biomechanik, Technische Universität Graz.

8.5 Verantwortliche und Qualifikation

8.5.1 Wer führte die biometrische Planung durch (ggf. Nachweis der Qualifikation)?

Prof. Dr. Gerhard A. Holzapfel, Dr. Gerhard Sommer, Prof. Dr. Peter Regitnig

8.5.2 Wer wird die statistische Auswertung durchführen (ggf. Nachweis der Qualifikation)?

Michael Kutschera (triaxiale Scherversuche), Roland Kresnik (biaxiale Zugversuche), Statistiker des Institutes für Biomechanik, TU Graz

5.4 Ethics applicant - Clinical Department of Pathology

8.6 Datenschutz

8.6.1 Die Datenverarbeitung erfolgt a) personenbezogen b) indirekt personenbezogen
c) nicht personenbezogen

8.6.2 Wenn a): Begründung:

DVR-Nummer:

8.6.3 Wenn b): Wie erfolgt die Verschlüsselung?

Sämtliche Daten werden im Datenblatt anonym geführt.

5 Appendix

9. Liste der eingereichten Unterlagen (wenn nicht gesondert dem Antrag beiliegend):

Dokument	Version/Identifikation	Datum
Protokoll	BiomechMyocard V 1.1	15.08.11
Kurzfassung		
Patienteninformation / Einwilligungserklärung		
Prüfbogen (Case Report Form, CRF)		
Versicherungsbestätigung		
Amendment Nr.		
Amendment Nr.		
Amendment Nr.		
Lokales Amendment Nr.		

Name und Unterschrift der Antragstellerin/des Antragstellers

- 9.1 Name: **ao.Univ.Prof.Dr. Peter Regitnig**
- 9.2 Institution/ Firma: **Institut für Pathologie, MedUni Graz**
- 9.3 Position: **Facharzt für Pathologie**
- 9.4 Antragsteller/in ist 9.4.1 koordinierende/r Prüfer/in (multizentrische Studie)
 (nur AMG-Studien) 9.4.2 Hauptprüfer/in (monozentrische Studie)
 9.4.3 Sponsor bzw. Vertreter/in des Sponsors
 9.4.4 vom Sponsor autorisierte Person/Organisation

Ich bestätige hiermit, dass die in diesem Antrag gemachten Angaben korrekt sind und dass ich der Meinung bin, dass die Durchführung der Studie in Übereinstimmung mit dem Protokoll, nationalen Regelungen und mit den Prinzipien der Guten Klinischen Praxis möglich sein wird.

Weiters stimme ich mit meiner Unterschrift zu, dass folgende Daten aus meinem Antrag ggf. durch die Ethikkommission veröffentlicht werden, um die Anträge nach Zahl und Inhalt transparent zu machen: EK-Nummer, Einreich-Datum, Projekttitel, Hauptprüfer, Sponsor/CRO, weitere Zentren.
 (Im Falle der Nicht-Zustimmung bitte diesen Absatz durchzustreichen)

.....
 Unterschrift der Antragstellerin/des Antragstellers

.....
 Datum

!!! Achtung: Diese Unterschrift ist in jedem Fall erforderlich !!!

5.4 Ethics applicant - Clinical Department of Pathology

Teil B

Studienkurzbezeichnung: Biomechanik humaner Ventrikel

10. Angaben zur Prüferin/zum Prüfer

10.1 Name: **ao.Univ.Prof.Dr. Peter Regitnig**

10.2 Krankenanstalt/Institut/Abteilung: **Institut für Pathologie**

10.3 Telefon	10.4 „Pieps“/Mobil	10.5 Fax	10.6 e-mail-Adresse:
385-81629		385-13432	peter.regitnig@medunigraz.at;

10.7 Jus practicandi: ja nein 10.8 Facharzt für: **Pathologie**

10.9 Prüfärztekurs: ja nein

10.10 Sofern relevant: Präklinische Qualifikation (z.B. Labordiagnostik) bzw. Name der Verantwortlichen:

11. Geplante Anzahl der PatientInnen bzw. ProbandInnen an dieser Prüfstelle 30

12. Verantwortliche MitarbeiterInnen an der klinischen Studie (an Ihrer Prüfstelle)

Fr/Hr	Titel	Vorname	Name	Institution
Hr.	Dr.	Gerhard	Sommer	Inst. f. Biomechanik, TU Graz
Hr.	Prof. Dr.	Gerhard A.	Holzapfel	Inst. f. Biomechanik, TU Graz

13. Unterschrift der Prüferin/des Prüfers

Ich bestätige hiermit, dass die in diesem Antrag gemachten Angaben korrekt sind und dass ich der Meinung bin, dass die Durchführung der Studie in Übereinstimmung mit dem Protokoll, nationalen Regelungen und mit den Prinzipien der Guten Klinischen Praxis möglich sein wird.

.....
Unterschrift der Prüferin/des Prüfers

.....
Datum

Bei multizentrischen AMG-Studien sind die Teile B von der Hauptprüferin/dem Hauptprüfer des jeweiligen Zentrums zu unterzeichnen. Alternativ zur Unterschrift auf den Teilen B können die Unterschriften der Hauptprüfer/innen auch auf den Unterschriftenseiten des Protokolls oder der Prüfärzterträge vorgelegt werden. Es muss jedenfalls eine eindeutige - durch Unterschrift dokumentierte - Zustimmung aller Hauptprüfer/innen zum Protokoll vorliegen.

14. Name und Unterschrift der Leiterin/des Leiters der Einrichtung* des Pflegedienstes*

14.1 Name: **Univ.-Prof. Dr.med.univ. Gerald Hoefler**

.....
Unterschrift der Leiterin/des Leiters

.....
Datum

** Die Unterschrift der Leiterin/des Leiters des Pflegedienstes ist für Pflegeforschungsprojekte und die Anwendung neuer Pflegekonzepte und -methoden erforderlich, ansonsten die Unterschrift der Leiterin/des Leiters der jeweiligen Einrichtung. Einrichtung: die Klinik (wenn gegliedert: die klinische Abteilung), die Abteilung oder die gemeinsame Einrichtung*

!!! Achtung: Teil B ist in jedem Fall vollständig auszufüllen, bei multizentrischen klinischen Prüfungen nach AMG für jedes in Österreich teilnehmende Zentrum separat !!!

Ethikkommission



Medizinische Universität Graz

Auenbruggerplatz 2, A-8036 Graz
ethikkommission@medunigraz.at
Tel.: +43 / 316 / 385-13928, Fax: -14348

VOTUM gültig bis 18.10.2012

EK-Nummer: 24-003 ex 11/12
Studientitel: Biomechanik der ventrikulären Myokarde - biaxialer Zugversuch, triaxialer Scherversuch
Prüfer: *) Univ.Prof.Dr. Peter Regitnig
Inst. für Pathologie
Sponsor: (Prüfer)
CRO: -

*) Antragsteller

Die o.a. Studie wurde von der Ethikkommission erstmals in der Sitzung 01-11/12 am 17.10.2011 behandelt.

Die Ethikkommission ist zu folgendem Schluss gekommen:

Es besteht kein Einwand gegen die Durchführung der Studie in der vorliegenden Form.

Stimmberechtigte bzw. anwesende Mitglieder bei der Behandlung waren: Siehe beiliegende Liste vom 17.10.2011.

Kommissionsmitglieder, die für diesen Tagesordnungspunkt als befangen anzusehen waren und daher gemäß Geschäftsordnung an der Entscheidungsfindung und Abstimmung nicht teilgenommen haben: keine

Zur Beurteilung vorliegende Dokumente:

Dokumente eingegangen am 16.09.2011, begutachtet in der Sitzung 01-11/12 am 17.10.2011

✓ Antragsformular	14.09.2011
✓ Originalprotokoll 1.1	15.08.2011

Es handelt sich um eine Studie im Rahmen einer Diplomarbeit.

Das Votum der Ethikkommission berührt in keiner Weise die alleinige Verantwortung der Prüferin / des Prüfers / der Prüfer für die ordnungsgemäße Durchführung der Studie unter Einhaltung aller einschlägiger gesetzlicher Bestimmungen und Richtlinien.

Weiters machen wir darauf aufmerksam, dass der Kommission unverzüglich zu melden sind:

- Abweichungen vom Protokoll aus Sicherheitsgründen oder Protokolländerungen
- Änderungen, die das Risiko der Teilnehmer/-innen erhöhen oder die Durchführung der Studie wesentlich beeinflussen
- Mutmaßliche unerwartete schwerwiegende Nebenwirkungen - SUSARs (AMG-Studien ab 1.5.2004) oder schwerwiegende unerwünschte Ereignisse - SAEs (andere Studien)
- Jegliche Information über sonstige Umstände, die die Sicherheit der Teilnehmer/-innen oder die Durchführung der Studie beeinträchtigen können

EK-Nummer: **24-003 ex 11/12**

Votum

Seite 1 von 2

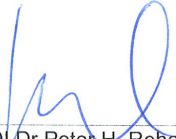
Medizinische Universität Graz, Universitätsplatz 3, A-8010 Graz. www.medunigraz.at

Rechtsform: Juristische Person öffentlichen Rechts gem. Universitätsgesetz 2002. Information: Mitteilungsblatt der Universität und www.medunigraz.at. DVR-Nr. 210 9494.
UID: ATU 575 111 79. Bankverbindung: Bank Austria Creditanstalt BLZ 12000 Konto-Nr. 500 948 400 04, Raiffeisen Landesbank Steiermark BLZ 38000 Konto-Nr. 49510.

5.4 Ethics applicant - Clinical Department of Pathology

Dieses Votum gilt für ein Jahr ab dem Datum der Ausstellung. Bei längerer Studiendauer ist rechtzeitig vor Ablauf der Gültigkeit des Votums ein Zwischenbericht vorzulegen (Berichtsformular), um eine etwaige Verlängerung zu erlangen.

Graz, 18. Oktober 2011



Univ.Prof.Dr.Peter H. Rehak
Vorsitzender



Univ.Prof.DDr.Hans-Peter Kapfhammer
Stv. Vorsitzender

Achtung: Bitte bei allen das Projekt betreffende Schreiben oder telefonischen Anfragen die EK-Nummer angeben!

Ethikkommission



Medizinische Universität Graz

Auenbruggerplatz 2, A-8036 Graz
ethikkommission@medunigraz.at
Tel.: +43 / 316 / 385-13928, Fax: -14348

Liste der stimmberechtigten bzw. anwesenden Mitglieder

am 17. Oktober 2011

Univ.Prof.DI Dr.Andrea Berghold
Univ.Prof.Dr.Josef Donnerer
Univ.Prof.DI Dr.Josef Haas
Univ.Prof.Mag.Dr.H.Jesser-Huß
Univ.Prof.DDr.Hans-Peter Kapfhammer
Univ.Prof.Dr. Leopold Neuhold
Univ.Prof.Dr.Barbara Plecko-Startinig
Univ.Prof.DI Dr.Peter H. Rehak
Univ.Prof.Dr.Ekkehard Ring
OPfl. DGKP Thomas Schelischansky, MSc
Univ.Prof.Dr.Rudolf Stauber
Univ.Prof.Dr.Hermann Toplak
Ursula Vennemann
Univ.Prof.Dr.Kurt Weber
Univ.Prof.Dr.Ursula Viktoria Wisiak
Ing.Franz Deutschmann
Univ.Prof.Dr.Wolfgang Kröll
Mag.Renate Skledar
Univ.Prof.Dr. Michael Speicher

Beigezogene Fachärzte

Univ.Prof.Dr.Herwig Cerwenka
Univ.Prof.Dr.Helmut Schöllnast
Univ.Prof.Dr.Gerhard Schuhmann

Statutory Declaration

I declare that I have authored this Thesis independently, that I have not used other than the declared sources/resources, and that I have explicitly marked all material, which has been quoted by the relevant reference.

date

signature